

# JPTM

Journal of Pathology  
and Translational Medicine

March 2025  
Vol. 59 / No.2  
jpatholtm.org  
pISSN: 2383-7837  
eISSN: 2383-7845



*Clinically Relevant*  
*Categorization of High-Grade*  
*Serous Ovarian Carcinoma*



### Aims & Scope

The *Journal of Pathology and Translational Medicine* is an open venue for the rapid publication of major achievements in various fields of pathology, cytopathology, and biomedical and translational research. The Journal aims to share new insights into the molecular and cellular mechanisms of human diseases and to report major advances in both experimental and clinical medicine, with a particular emphasis on translational research. The investigations of human cells and tissues using high-dimensional biology techniques such as genomics and proteomics will be given a high priority. Articles on stem cell biology are also welcome. The categories of manuscript include original articles, review and perspective articles, case studies, brief case reports, and letters to the editor.

### Subscription Information

To subscribe to this journal, please contact the Korean Society of Pathologists/the Korean Society for Cytopathology. Full text PDF files are also available at the official website (<https://jpatholm.org>). *Journal of Pathology and Translational Medicine* is indexed by Emerging Sources Citation Index (ESCI), PubMed, PubMed Central, Scopus, KoreaMed, KoMCI, WPRIM, Directory of Open Access Journals (DOAJ), and CrossRef. Circulation number per issue is 50.

### Contact the Korean Society of Pathologists/the Korean Society for Cytopathology

**Publishers:** Kang, Gyeong Hoon, MD; Choi, Yoon Jung, MD, PhD

**Editors-in-Chief:** Jung, Chan Kwon, MD; Park, So Yeon, MD

**Published by** the Korean Society of Pathologists/the Korean Society for Cytopathology

### Editorial Office

Room 1209 Gwanghwamun Officia, 92 Saemunan-ro, Jongno-gu, Seoul 03186, Korea

Tel: +82-2-795-3094 Fax: +82-2-790-6635 E-mail: [office@jpatholm.org](mailto:office@jpatholm.org)

#1508 Renaissancetower, 14 Mallijae-ro, Mapo-gu, Seoul 04195, Korea

Tel: +82-2-593-6943 Fax: +82-2-593-6944 E-mail: [office@jpatholm.org](mailto:office@jpatholm.org)

### Printed by M2PI

#805, 26 Sangwon 1-gil, Seongdong-gu, Seoul 04779, Korea

Tel: +82-2-6966-4930 Fax: +82-2-6966-4945 E-mail: [support@m2-pi.com](mailto:support@m2-pi.com)

### Manuscript Editing by InfoLumi Co.

210-202, 421 Pangyo-ro, Bundang-gu, Seongnam 13522, Korea

Tel: +82-70-8839-8800 E-mail: [infolumi.chang@gmail.com](mailto:infolumi.chang@gmail.com)

Front cover image: Histologic images of common histomic clusters in ovarian cancer (p. 96)

© 2025 The Korean Society of Pathologists/The Korean Society for Cytopathology

© Journal of Pathology and Translational Medicine is an Open Access journal under the terms of the Creative Commons Attribution Non-Commercial License (<https://creativecommons.org/licenses/by-nc/4.0>).

© This paper meets the requirements of KS X ISO 9706, ISO 9706-1994 and ANSI/NISO Z.39.48-1992 (Permanence of Paper).



## All-in-One VENTANA DP Subscription

### Roche만의 새로운 구독 서비스 플랫폼

Experience Roche Digital Pathology by all-in-one Subscription

Roche  
subscription is...

- R** easonable offer
- O** pportunity to experience Roche
- C** ost-effective system
- H** igh quality of supporting
- E** ligible solution to optimize your work

# Editorial Board

---

## Editors-in-Chief

Jung, Chan Kwon, MD (*The Catholic University of Korea, Korea*) <https://orcid.org/0000-0001-6843-3708>

Park, So Yeon, MD (*Seoul National University, Korea*) <https://orcid.org/0000-0002-0299-7268>

## Associate Editors

Bychkov, Andrey, MD (*Kameda Medical Center, Japan; Nagasaki University Hospital, Japan*) <https://orcid.org/0000-0002-4203-5696>

Kim, Haeryoung, MD (*Seoul National University, Korea*) <https://orcid.org/0000-0002-4205-9081>

Lee, Hee Eun, MD (*Mayo Clinic, USA*) <https://orcid.org/0000-0001-6335-7312>

Shin, Eunah, MD (*Yongin Severance Hospital, Yonsei University, Korea*) <https://orcid.org/0000-0001-5961-3563>

## Editorial Board

Avila-Casado, Maria del Carmen, MD (*University of Toronto, Toronto General Hospital UHN, Canada*)

Bae, Jeong Mo, MD (*Seoul National University, Korea*)

Bae, Young Kyung, MD (*Yeungnam University, Korea*)

Bongiovanni, Massimo, MD (*Lausanne University Hospital, Switzerland*)

Bova, G. Steven, MD (*University of Tampere, Finland*)

Choi, Joon Hyuk (*Yeungnam University, Korea*)

Chong, Yo Sep, MD (*The Catholic University of Korea, Korea*)

Chung, Jin-Haeng, MD (*Seoul National University, Korea*)

Fadda, Guido, MD (*Catholic University of Rome-Foundation Agostino Gemelli University Hospital, Italy*)

Fukushima, Noriyoshi, MD (*Jichi Medical University, Japan*)

Go, Heounjeong (*University of Ulsan, Korea*)

Hong, Soon Won, MD (*Yonsei University, Korea*)

Jain, Deepali, MD (*All India Institute of Medical Sciences, India*)

Kakudo, Kennichi, MD (*Izumi City General Hospital, Japan*)

Kim, Jang-Hee, MD (*Ajou University, Korea*)

Kim, Jung Ho, MD (*Seoul National University, Korea*)

Kim, Se Hoon, MD (*Yonsei University, Korea*)

Komuta, Mina, MD (*Keio University, Tokyo, Japan*)

Lai, Chiung-Ru, MD (*Taipei Veterans General Hospital, Taiwan*)

Lee, C. Soon, MD (*University of Western Sydney, Australia*)

Lee, Hwajeong, MD (*Albany Medical College, USA*)

Lee, Sung Hak, MD (*The Catholic University of Korea, Korea*)

Liu, Zhiyan, MD (*Shanghai Jiao Tong University, China*)

Lkhagvadorj, Sayamaa, MD (*Mongolian National University of Medical Sciences, Mongolia*)

Lo, Regina, MD (*The University of Hong Kong, Hong Kong*)

Moran, Cesar, MD (*MD Anderson Cancer Center, U.S.A.*)

Paik, Jin Ho, MD (*Seoul National University, Korea*)

Park, Jeong Hwan (*Seoul National University, Korea*)

Sakhuja, Puja, MD (*Govind Ballabh Pant Hospital, India*)

Shahid, Pervez, MD (*Aga Khan University, Pakistan*)

Song, Joon Seon, MD (*University of Ulsan, Korea*)

Tan, Puay Hoon, MD (*National University of Singapore, Singapore*)

Than, Nandor Gabor, MD (*Semmelweis University, Hungary*)

Tse, Gary M., MD (*The Chinese University of Hong Kong, Hong Kong*)

Yatabe, Yasushi, MD (*Aichi Cancer Center, Japan*)

Zhu, Yun, MD (*Jiangsu Institution of Nuclear Medicine, China*)

## Ethic Editor

Choi, In-Hong, MD (*Yonsei University, Korea*)

Huh, Sun, MD (*Hallym University, Korea*)

## Statistics Editors

Kim, Dong Wook (*National Health Insurance Service Ilsan Hospital, Korea*)

Lee, Hye Sun (*Yonsei University, Korea*)

## Manuscript Editor

Chang, Soo-Hee (*InfoLumi Co., Korea*)

## Layout Editor

Jeong, Eun Mi (*M2PI, Korea*)

## Website and JATS XML File Producers

Choi, Min Young (*M2PI, Korea*)

## Administrative Assistants

Lee, Hye jin (*The Korean Society of Pathologists*)

Kim, Song Yeun (*The Korean Society for Cytopathology*)

## Contents

---

Vol. 59, No.2, March 2025

### ORIGINAL ARTICLES

- 91      Categorizing high-grade serous ovarian carcinoma into clinically relevant subgroups using deep learning–based histomic clusters  
Byungsoo Ahn, Eunhyang Park
- 105     Association study of *TYMS* gene expression with *TYMS* and *ENOSF1* genetic variants in neoadjuvant chemotherapy response of gastric cancer  
Khadijeh Arjmandi, Iman Salahshourifar, Shiva Irani, Fereshteh Ameli, Mohsen Esfandbod
- 115     Low Ki-67 labeling index is a clinically useful predictive factor for recurrence-free survival in patients with papillary thyroid carcinoma  
Takashi Masui, Katsunari Yane, Ichiro Ota, Kennichi Kakudo, Tomoko Wakasa, Satoru Koike, Hiroataka Kinugawa, Ryuji Yasumatsu, Tadashi Kitahara
- 125     Characteristics of *RET* gene mutations in Vietnamese medullary thyroid carcinoma patients: a single-center analysis  
Van Hung Pham, Quoc Thang Pham, Minh Nguyen, Hoa Nhat Ngo, Thao Thi Thu Luu, Nha Dao Thi Minh, Trâm Đặng, Anh Tu Thai, Hoang Anh Vu, Dat Quoc Ngo

### CASE STUDIES

- 133     Uncommon granulomatous manifestation in Epstein-Barr virus–positive follicular dendritic cell sarcoma: a case report  
Henry Goh Di Shen, Yue Zhang, Wei Qiang Leow
- 139     Mucocele of the rectal stump: mucinous cystic neoplasm with low-grade dysplasia simulating low-grade appendiceal mucinous neoplasm  
Hasan Basri Aydin, Maria Faraz, A. David Chismark, Haiyan Qiu, Hwajeong Lee

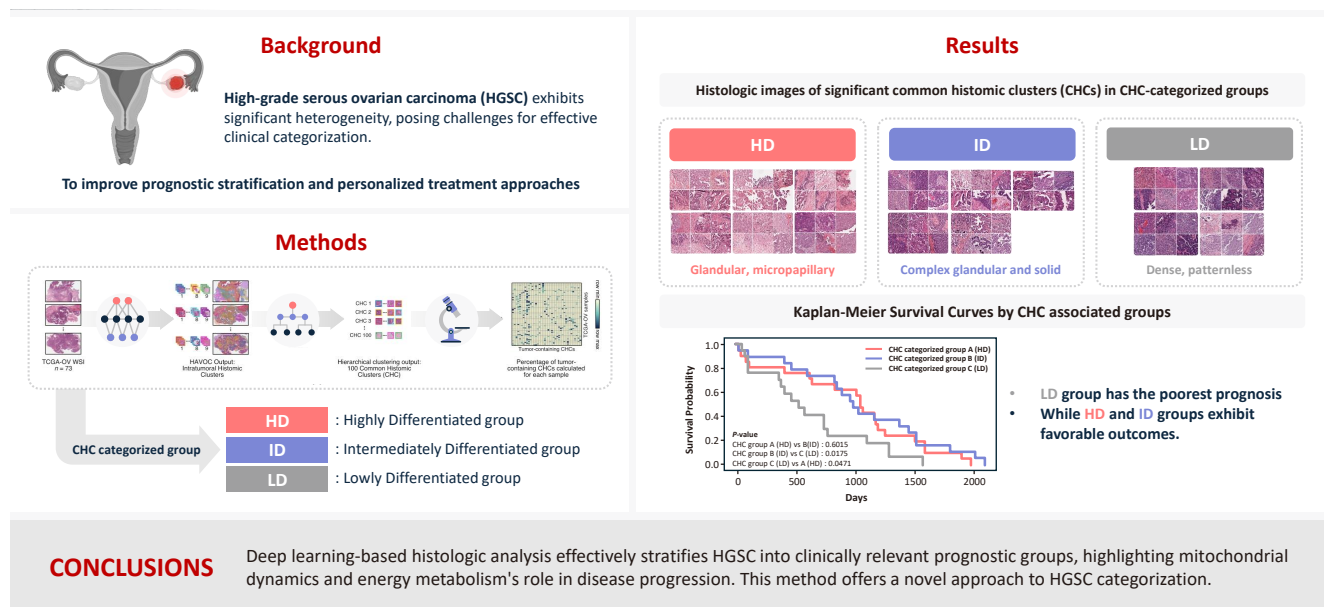
### CORRESPONDENCE

- 147     Erratum: Breast fine-needle aspiration cytology in the era of core-needle biopsy: what is its role?  
Ahrong Kim, Hyun Jung Lee, Jee Yeon Kim

# Categorizing high-grade serous ovarian carcinoma into clinically relevant subgroups using deep learning-based histomic clusters

Byungsoo Ahn, Eunhyang Park

## Graphical abstract



# Categorizing high-grade serous ovarian carcinoma into clinically relevant subgroups using deep learning-based histomic clusters

Byungsoo Ahn, Eunhyang Park

Department of Pathology, Severance Hospital, Yonsei University College of Medicine, Seoul, Korea

**Background:** High-grade serous ovarian carcinoma (HGSC) exhibits significant heterogeneity, posing challenges for effective clinical categorization. Understanding the histomorphological diversity within HGSC could lead to improved prognostic stratification and personalized treatment approaches. **Methods:** We applied the Histomic Atlases of Variation Of Cancers model to whole slide images from The Cancer Genome Atlas dataset for ovarian cancer. Histologically distinct tumor clones were grouped into common histomic clusters. Principal component analysis and K-means clustering classified HGSC samples into three groups: highly differentiated (HD), intermediately differentiated (ID), and lowly differentiated (LD). **Results:** HD tumors showed diverse patterns, lower densities, and stronger eosin staining. ID tumors had intermediate densities and balanced staining, while LD tumors were dense, patternless, and strongly hematoxylin-stained. RNA sequencing revealed distinct patterns in mitochondrial oxidative phosphorylation and energy metabolism, with upregulation in the HD, downregulation in the LD, and the ID positioned in between. Survival analysis showed significantly lower overall survival for the LD compared to the HD and ID, underscoring the critical role of mitochondrial dynamics and energy metabolism in HGSC progression. **Conclusions:** Deep learning-based histologic analysis effectively stratifies HGSC into clinically relevant prognostic groups, highlighting the role of mitochondrial dynamics and energy metabolism in disease progression. This method offers a novel approach to HGSC categorization.

**Keywords:** Carcinoma, ovarian epithelial; Oxidative phosphorylation; Energy metabolism; Deep learning

## INTRODUCTION

High-grade serous ovarian carcinoma (HGSC) is the most aggressive and prevalent form of ovarian cancer, accounting for approximately 70%–80% of ovarian cancer deaths worldwide [1]. Despite intensive treatment including cytoreduction surgery, platinum-based chemotherapy and emerging targeted therapies, most patients experience recurrence, with a median progression-free survival of 13.8 months for those at stage III–IV [2]. Although numerous genomic, transcriptomic, and proteomic biomarkers have been proposed, none have been adopted into standard clinical practice. Determining treatment sensitivity or resistance requires several treatment cycles, which

expose patients to potentially unnecessary adverse events [3,4]. The challenge arises from the significant inter- and intratumoral heterogeneity of HGSC, which poses a major obstacle to stratifying and classifying HGSC patients [5]. Currently, there is no World Health Organization recommended effective histological subclassification for HGSC.

While several tools exist to categorize HGSC, the most widely accepted classification is based on four molecular subtypes derived from The Cancer Genome Atlas (TCGA): immunoreactive, differentiated, proliferative, and mesenchymal [6]. Previous studies reported that the mesenchymal or proliferative subtypes tend to have worse overall survival, whereas the immunoreactive patterns often have a more favorable prognosis

**Received:** September 3, 2024 **Revised:** October 22, 2024 **Accepted:** October 22, 2024

**Corresponding Author:** Eunhyang Park, MD, PhD

Department of Pathology, Severance Hospital, Yonsei University College of Medicine, 50-1 Yonsei-ro, Seodaemun-gu, Seoul 03722, Korea  
Tel: +82-2-2228-1793, Fax: +82-2-362-0860, E-mail: epark54@yuhs.ac

This is an Open Access article distributed under the terms of the Creative Commons Attribution Non-Commercial License (<https://creativecommons.org/licenses/by-nc/4.0/>) which permits unrestricted non-commercial use, distribution, and reproduction in any medium, provided the original work is properly cited.

© 2025 The Korean Society of Pathologists/The Korean Society for Cytopathology

[7,8]. However, molecular genetic testing is expensive and time-consuming, limiting its application to clinical practice.

Additionally, attempts to categorize HGSC into histological subtypes based on the molecular classifications have been hindered by poor interobserver agreement, limiting the clinical applicability [9,10]. However, recent advances in digital pathology have enabled new efforts to stratify HGSC based on histological findings using deep learning techniques, which can extract clinically relevant histological patterns that are not apparent to the human eye. For instance, our team developed PathoRiCH, a deep learning classifier designed to predict platinum resistance based solely on hematoxylin and eosin (H&E) staining images [11]. Despite this progress, previous histologic image-based deep learning studies have analyzed pre-categorized HGSC samples in a simplistic binary classification of HGSC as either having a favorable or poor prognosis [12-14]. This oversimplifies the complex heterogeneous nature of HGSC.

To address the limitations of these approaches and better capture the complex intratumoral heterogeneity of HGSC, our approach introduces a novel bottom-up classification method grounded in classical pathology. Instead of relying on predefined molecular data or survival prognosis information, we focus on grouping tumor clusters with similar histopathological patterns across different HGSC tumors. We hypothesize that different clonal expansions within HGSC may have varying effects on clinical prognosis, with certain clonal combinations leading to poor survival and others to a more favorable prognosis. To achieve this, we utilized the Histomic Atlases of Variation Of Cancers (HAVOC) model pipeline to HGSC [15]. Unlike other deep learning tools trained on histopathological patterns labeled with predefined molecular data, which may limit the generalization of intratumoral heterogeneity, HAVOC partitions histological patterns observed in whole slide images (WSIs) in an unsupervised manner. This allows for a more comprehensive exploration of intratumoral heterogeneity.

In this study, we identified various tumor clones present within The Cancer Genome Atlas dataset for ovarian cancer (TCGA-OV) using the HAVOC model. The detected clones were then grouped by similar histopathological patterns into common histomic clusters (CHCs). We then categorized HGSCs into three different groups based on different CHC combinations. Each group's histomorphologic and molecular characteristics were evaluated, and their clinical relevance was investigated.

## MATERIALS AND METHODS

### Study cohort

The TCGA-OV dataset from the Genomic Data Commons data portal (<https://portal.gdc.cancer.gov/>) was used. A total of 73 cases were selected based on the availability of H&E-stained WSI from formalin-fixed paraffin-embedded tissue during the primary debulking surgery, along with RNA sequencing data. WSI from frozen sections were excluded due to severe freezing and ice-crystal artifacts that hinder histomorphological analysis. No additional exclusion criteria were applied. Homologous recombination deficiency (HRD) information was obtained from Zhang et al. [16], based on the representative HRD algorithm using loss of heterozygosity, telomeric allelic imbalance, and large-scale state transitions. The TCGA molecular classifications were sourced from Verhaak et al. [8].

### Histologic clustering to find inter-tumoral CHCs

The 73 HGSC WSIs from the TCGA-OV dataset were processed through the HAVOC pipeline. Patch images ( $258 \mu\text{m}^2$ ,  $512 \times 512$  pixels) were extracted from the WSIs, which were then grouped into intratumoral heterogenic tumor clusters using the default setting of  $K = 9$  (Fig. 1A) [15]. Subsequently, these HAVOC-generated histomic variation clusters were grouped by hierarchical clustering to identify CHCs across all samples, where the elbow method was used for finding the optimal number of cluster ( $k = 100$ ) (Supplementary Fig. S1). The patch counts for clusters belonging to each TCGA sample are provided in Supplementary Data S1.

### Principal component analysis and K-means clustering analysis

Two pathologists (B.A. and E.P.) reviewed all CHCs, selecting those with more than 10% tumor cells as tumor-containing CHCs for further analysis. The percentages of tumor-containing CHCs within each sample were calculated based on the total number of tumor cluster patches present (Supplementary Data S1). Principal component analysis (PCA) analysis was performed on this percentage data, followed by K-means clustering to categorize the samples into three CHC-categorized groups (Fig. 1B). The optimal number of clusters was determined by the highest silhouette score (Supplementary Fig. S2).

### Histologic analysis

The distribution of each tumor-containing CHC across the

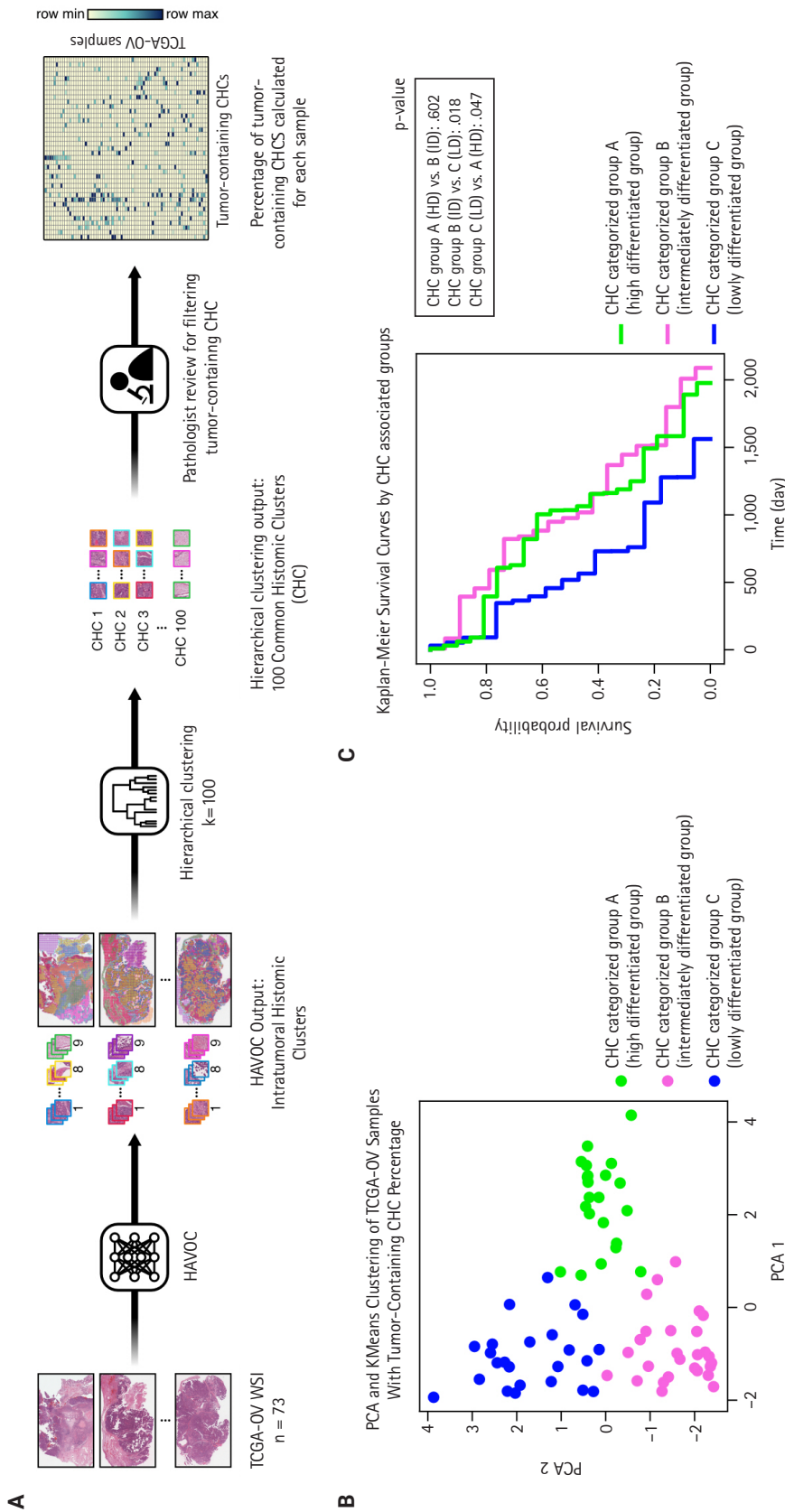


**Fig. 1.** Histomic analysis workflow and survival analysis of The Cancer Genome Atlas (TCGA) dataset for ovarian cancer. (A) Seventy-three whole slide images (WSI) of TCGA dataset for ovarian cancer (TCGA-OV) are processed using the Histomic Atlases of Variation Of Cancers (HAVOC) pipeline to extract patch images, which are then grouped into intratumoral histomic clusters. Hierarchical clustering identifies 100 common histomic clusters (CHCs), which are reviewed by pathologists to include only those with  $\geq 10\%$  tumor content. The percentage of tumor-containing CHCs in each sample is calculated. The top right heatmap visualizes these percentages across TCGA-OV samples, with a color scale ranging from blue (low), to green (intermediate), to white (high). (B) Principal component analysis (PCA) and K-means clustering are performed on the TCGA-OV samples based on the percentage of tumor-containing CHCs. The samples are categorized into three groups: CHC-associated group A (highly differentiated [HD] group), group B (intermediately differentiated [ID] group), and group C (lowly differentiated [LD] group). (C) The Kaplan-Meier survival curves for the three CHC-associated groups reveal significantly lower survival for group C (LD group) compared to group A (HD group) ( $p = .047$ ) and group B (ID group) ( $p = .018$ ).

three CHC-categorized groups was compared using pairwise t-tests. Histologic features of the CHCs were analyzed by two pathologists (B.A. and E.P.). For quantitative analysis, Hover-Net with pretrained official fast-PanNuke checkpoint (panoptic quality score of 0.4863 for multi-class segmentation on TCGA ovary tissues) was used to segment nuclei present in all patches generated by the HAVOC pipeline into three cell types: tumor cells, stromal cells, and inflammatory cells [17]. Six nucleus shape features (area, circularity, length, maximum diameter, minimum diameter, and solidity) and eight nucleus color features (maximum, minimum, mean, and median values for both H&E staining) were extracted using QuPath ver. 0.5.1 with the default resolution setting of 2 μm per pixel [18]. Descriptive statistical analyses for all histologic features were performed using KNIME ver. 5.2.3 [19]. The Welch ANOVA test and the Games-Howell test were used to determine if each CHC had unique histologic features. Immune cell analysis was conducted using CIBERSROT<sub>x</sub> [20].

**RNA sequencing analysis**

Differential gene expression (DEG) analysis was performed

using edgeR [21] with a cutoff of  $p \leq 0.01$  and  $\log(\text{fold change}) \geq 1.0$ . Enrichment analysis was conducted using fgsea [22] and Gene Ontology Biological Process (GO:BP) terms with a cutoff of false discovery rate (FDR)  $\leq 0.01$  and  $\log(\text{fold change}) \geq 0.2$ .

**Statistical analysis**

Chi-squared test was used to evaluate correlations between categorical variables. Kaplan-Meier survival curves and multivariable Cox proportional hazards regression analyses were used for survival analyses. Two-tailed p-values  $< 0.05$  were considered statistically significant for all analyses. All data were analyzed using Python (ver. 3.10).

**RESULTS**

**Cohort characteristics**

The clinicopathologic characteristics of the 73 TCGA samples are shown in Table 1. Most samples (77%) were in International Federation of Gynecology and Obstetrics (FIGO) stage IIIC, followed by stage IV (21%) and stage IIC (1.4%). The molecular classifications were 25% differentiated, 14% immunoreactive,

**Table 1.** Clinicopathologic information of all samples and three histologic subgroups in high-grade serous ovarian carcinoma from the TCGA-OV dataset

Characteristic	All samples (n = 73)	Group A	Group B	Group C	p-value <sup>a</sup>
		HD group (n = 22)	ID group (n = 27)	LD group (n = 24)	
Age (yr)					.471
<63	34 (46.6)	8 (36.4)	13 (48.1)	13 (54.2)	
≥63	39 (53.4)	14 (63.6)	14 (51.9)	11 (45.8)	
FIGO stage					.651
IIC	1 (1.4)	0	1 (3.7)	0	
IIIC	56 (76.7)	18 (81.8)	19 (70.4)	19 (79.2)	
IV	15 (20.5)	4 (18.2)	7 (25.9)	4 (16.7)	
Unknown	1 (1.4)	0	0	1 (4.2)	
Molecular classification					.523
Differentiated	18 (24.7)	5 (22.7)	9 (33.3)	4 (16.7)	
Immunoreactive	10 (13.7)	4 (18.2)	3 (11.1)	3 (12.5)	
Mesenchymal	16 (21.9)	6 (27.3)	4 (14.8)	6 (25.0)	
Proliferative	29 (39.7)	7 (31.8)	11 (40.7)	11 (45.8)	
HRD status					.471
HRD	34 (46.6)	9 (40.9)	15 (55.6)	10 (41.7)	
Non-HRD	34 (46.6)	10 (45.5)	10 (37.0)	14 (58.3)	
Unknown	5 (6.8)	3 (13.6)	2 (7.4)	0	

Values are presented as number (%).

TCGA-OV, The Cancer Genome Atlas dataset for ovarian cancer; HD, highly differentiated; ID, intermediately differentiated; LD, lowly differentiated; FIGO, International Federation of Gynecology and Obstetrics; HRD, homologous recombination deficiency.

<sup>a</sup>Chi-squared test of independence was used to compare the three common histomic cluster-categorized groups.

22% mesenchymal, and 40% proliferative. HRD status showed 47% as HRD-positive, 47% as non-HRD, and 6.8% as unknown.

### Finding CHC-categorized groups

As illustrated in Fig. 1A, we identified various histologically distinct tumor clones within HGSC samples in the TCGA-OV datasets using the HAVOC pipeline. Hierarchical clustering of the mean feature values for each tumor clone was then employed to group them into 100 unique CHCs, of which 40 CHCs contained more than 10% tumor cells. Using the percentage of tumor-containing CHCs for each sample, we applied PCA and K-means clustering to categorize the TCGA samples into three distinct groups: temporarily named groups A, B, and C (Fig. 1B). In terms of clinicopathologic characteristics, no significant differences in patient age, FIGO stage, molecular classification, or HRD status were observed across the three CHC-categorized groups (Table 1).

### Histologic analysis by pathologists reveals unique morphological differences in highly differentiated, intermediately differentiated, and lowly differentiated groups

Using a pairwise t-test, we compared the percentage of the 40 tumor-containing CHCs across the three CHC-categorized groups (Supplementary Fig. S3) and identified significantly present CHCs for each group: six in group A, five in group B, and four in group C (Fig. 2).

All three groups exhibited poorly differentiated histologic features, characterized by high-grade cytologic atypia, nuclear pleomorphism, prominent nucleoli, and at least focal patternless sheet-like solid morphologies. However, some CHCs exhibited unique histomorphological characteristics that distinguished the groups. Group A included CHCs with high histomorphological variability, predominantly featuring more differentiated patterns, such as glandular (CHC36) and micropapillary patterns (CHC37), with a relatively low tumor-to-stromal ratio. It also included small islands or cord-like patterns within fibrotic stroma (CHC23). Group B exhibited more poorly differentiated morphology than the group A, with complex glandular to solid cluster patterns of hyperchromatic monotonous tumor cells (CHC1, CHC4, and CHC5). In contrast, group C consisted entirely of patternless sheet-like hyperchromatic monotonous tumor cells with sieve-like spaces and a high tumor-to-stromal ratio. Based on these histologic features, we named our CHC-categorized groups A–C as highly differ-

entiated (HD), intermediately differentiated (ID), and lowly differentiated (LD), respectively.

### Quantitative histologic analysis using Hover-Net and QuPath confirms unique histomorphologic traits in HD, ID, and LD groups

To objectively evaluate the histologic features of CHCs, we detected nuclei present in all tumor-containing patches via Hover-Net and extracted their histologic features using QuPath (Supplementary Fig. S4). A total of 50,050,242 nuclei were segmented and categorized into three cell types: tumor (39,477,010 cells, 78.9%), stromal (7,857,234 cells, 15.7%), and inflammatory (2,715,998 cells, 5.4%) (Supplementary Data S2). The Welch ANOVA and Games-Howell tests showed that 95%–100% of the pairwise comparisons of tumor and stromal nuclei features between different CHCs were statistically significant ( $p < .05$ ) (Supplementary Data S3, S4). The overall mean values of six nucleus shape features and eight color features for tumor-containing CHCs are illustrated in Supplementary Fig. S5.

First, cell densities and cell counts per WSI patches were compared in the significant CHCs among the HD, ID, and LD groups (Fig. 3A). The HD group was characterized by CHCs with low-density tumor nuclei patches (CHC 23, 28, and 31), while the LD group included CHCs with high-density tumor nuclei (CHC 11 and 14). The ID group's nuclei density fell between those of the other two groups. For stromal cells, all three CHC groups showed low stromal cell density, except for certain CHCs, such as CHC 23 in the HD group. Regarding inflammatory cell count comparisons, there was no difference in inflammatory cell density across all three groups, which was further confirmed by CIBERSORTx analysis ( $FDR > 0.05$ ) (Supplementary Fig. S6).

Quantitative histologic features of tumor and stromal nuclei revealed distinctive patterns among the three CHC groups (Fig. 3B, C). The HD group displayed variation in size across its CHCs, with some (CHC31 and CHC8) exhibiting larger tumor and stromal nuclei, while others (CHC23) showed smaller nuclei. The HD group CHCs were overall irregular in shape, exhibiting low circularity and solidity. In contrast, CHCs in the ID and LD groups were characterized by larger tumor and stromal nuclei with more regular, circular, and solid shapes, with less size variation across CHCs compared to the HD group.

The most striking differences among the groups were in their nucleus color features. The HD group was characterized by low hematoxylin and high eosin staining for both tumor and stro-

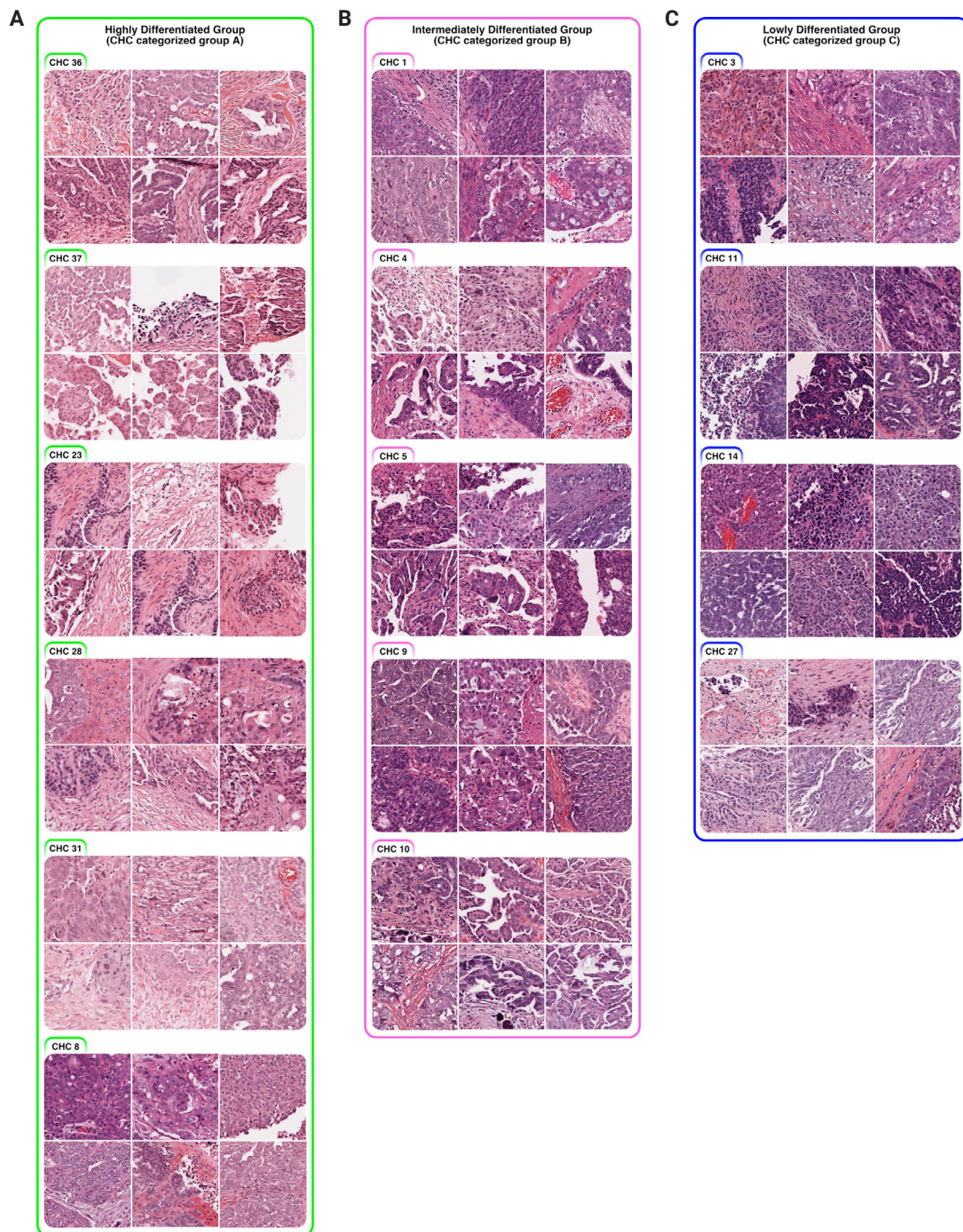


**Fig. 2.** Histologic images of significant common histomic clusters (CHCs) in CHC-categorized groups. (A) CHC-categorized group A (highly differentiated group) includes CHCs with more differentiated patterns, such as glandular (CHC36) and micropapillary patterns (CHC37) with a relatively low tumor-to-stromal ratio. It also included small islands or cord-like patterns within fibrotic stroma (CHC23). The rest (CHC8, 28, 31) shows sheet-like patterns of pleomorphic tumor cells with vesicular spaces. (B) CHC-categorized group B (intermediately differentiated group) exhibits CHCs with more poorly differentiated morphology compared to group A (highly differentiated group) with complex glandular to solid cluster patterns of hyperchromatic monotonous tumor cells (CHC1, CHC4, and CHC5). There is also CHC with micropapillary pattern (CHC10) and sheet-like pattern with sieve-like spaces (CHC9). (C) All CHCs in the CHC-categorized group C (lowly differentiated group) shows poorly differentiated, patternless, sheet-like pattern of hyperchromatic, monotonous tumor cells with sieve-like spaces (CHC3, CHC11, CHC14, and CHC27).

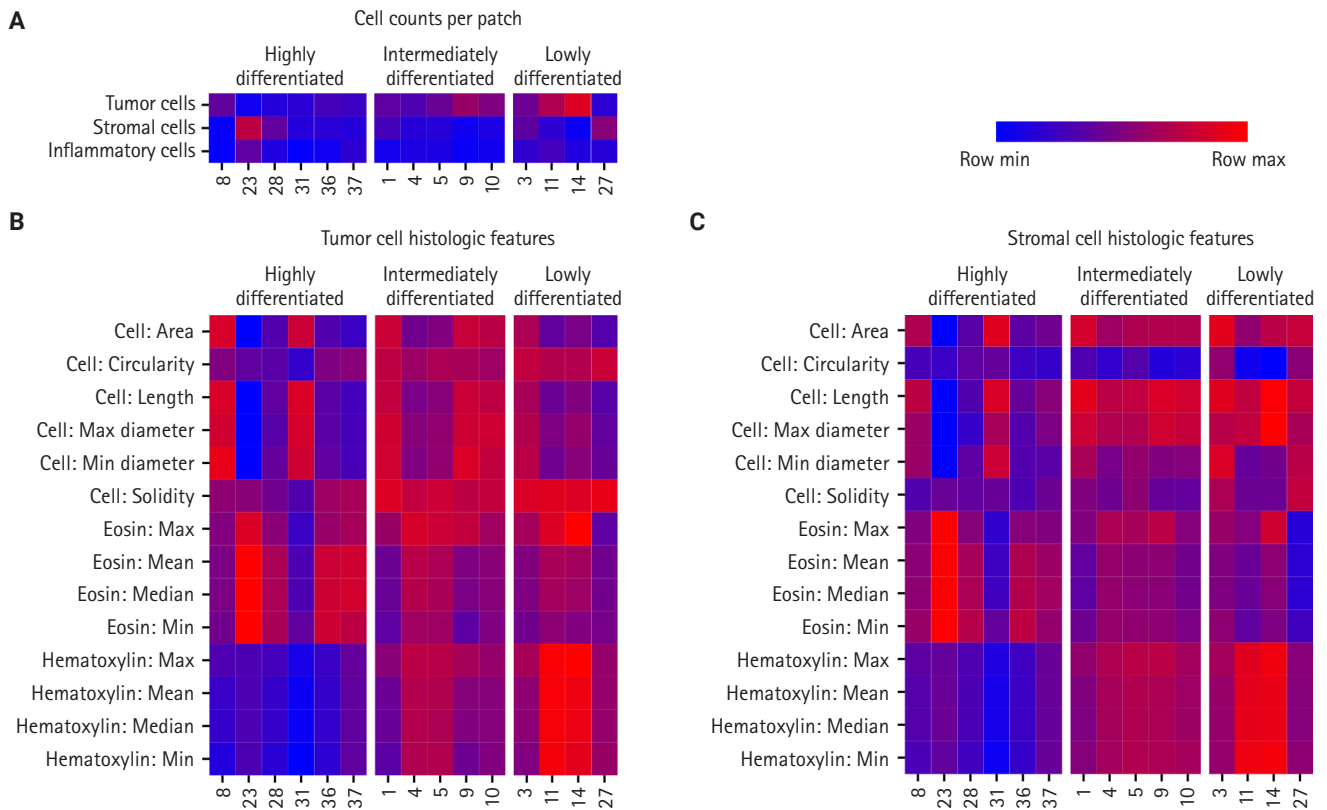


**Fig. 3.** Heatmap of quantitative histologic analysis using nuclei detection from Hover-Net across the three common histomic cluster-associated groups. (A) The heatmap shows mean tumor, stromal, and inflammatory cell counts per patch image across the three common histomic cluster (CHC)-associated groups. (B) The heatmap shows mean values of six nucleus shape features and eight nucleus color features extracted using QuPath for tumor cells across the three CHC-associated groups. (C) The heatmap shows mean values of six nucleus shape features and eight nucleus color features extracted using QuPath for stromal cells across the three CHC-associated groups.

mal nuclei. The LD group exhibited strong hematoxylin staining and low eosin staining. Meanwhile, the ID group exhibited more balanced staining levels, positioning itself between HD and LD groups.

The quantitative histologic analysis complements the qualitative assessments by pathologists. In the HD group, differentiated patterns such as glandular (CHC36) and micropapillary (CHC37) corresponded with a low tumor-to-stromal ratio. Additionally, CHC23, marked by fibrotic stroma, was validated by its high stromal density. Conversely, most CHCs from the ID and LD groups, characterized by patternless hyperchromatic sheet-like patterns (CHC3, 4, 5, 11, 14), were supported by quantitative findings of a high tumor-to-stromal ratio and increased hematoxylin staining.

### DEG and gene enrichment analysis reveal distinctive molecular characteristics in HD, ID, and LD groups

The RNA sequencing analysis compared the three CHC groups in a pairwise manner, highlighting significant DEGs with a log<sub>2</sub> (fold change) greater than 1 (Fig. 4A). The HD group showed increased expression of genes involved in genome stability and calcium signaling, such as TDRD12 and CALML5, compared to the ID group, suggesting enhanced genomic maintenance and cellular regulation. It also exhibited upregulation of oxidative phosphorylation (OXPHOS) and mitochondrial-related genes, such as *NDUFC2* and *UQCRHL*, compared to the LD group, indicating higher metabolic activity in the HD group.

In contrast, the ID group showed upregulation of genes related to vesicle trafficking, cellular communication, and RNA processing, including *DENND2A*, *RAB3B*, and *SRRM3*, in comparison to the HD group. Additionally, the ID group demonstrated

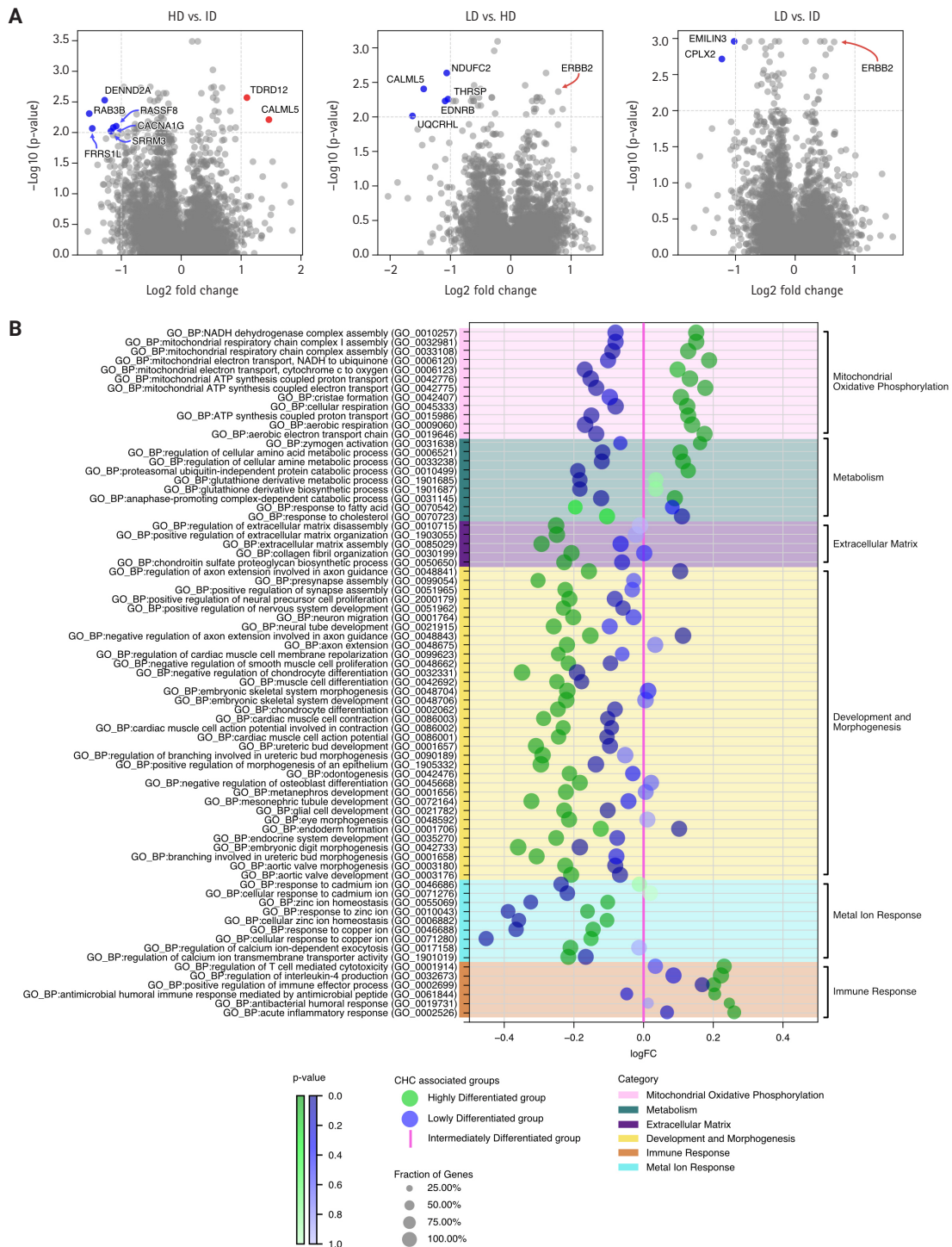


**Fig. 4.** Differentially expressed genes (DEG) and gene enrichment analysis comparing the three common histomic cluster-associated groups. (A) Pairwise DEG analysis between the three groups is shown as three volcano plots. Using a cutoff of  $p \leq .01$  and  $\log(\text{fold change}) \geq 1.0$ , upregulated genes are highlighted in red, and downregulated genes in blue. In the lowly differentiated (LD) group, no genes were significantly upregulated, but *ERBB2*, marked with an arrow, is noted for its potential clinical significance. (B) Gene enrichment analysis using gene ontology biological process (GO:BP) terms compared the three CHC-categorized groups, with the intermediately differentiated (ID) group as a pivot (pink line in the middle) to compare the highly differentiated (HD) (green dots) and LD groups (blue dots). The GO terms were divided into six categories, many of which showed significant differences between the three CHC-associated groups.

higher expression of the tumor suppressor gene *CPLX2* and the cancer-associated fibroblast (CAF) protein *EMILIN3* compared to the LD group. These DEGs suggest that interactions and modulations of the tumor are key mechanisms in the ID group.

Lastly, the LD group did not show any significantly upregulated genes with a  $\log_2$  (fold change) greater than 1 compared to the ID and HD groups. However, the upregulation of the oncogene *ERBB2*, despite a lower fold change, hints at its involvement in oncogenic signaling within the LD group.

The enrichment analysis using GO:BP terms was conducted between all three CHC-categorized groups in pairs, with fold change differences illustrated in [Supplementary Fig. S7](#). To simplify these complex three-way comparisons, which are difficult to grasp ([Fig. 4B](#)) was created: using the LD group as a pivot, gene enrichments of the HD and ID groups were plotted for a clearer comparison.

Overall, the HD group deviated the most from the ID group, particularly in processes related to mitochondrial oxidative phosphorylation. GO terms, such as mitochondrial ATP synthesis coupled proton transport and mitochondrial respiratory chain complex assembly, were markedly upregulated, aligning with DEG analysis. Additionally, the HD group showed upregulation of metabolic process, such as glutathione derivative metabolic process, highlighting heightened metabolic activities alongside active mitochondrial energy production. Beyond energy metabolism, the HD group showed significant upregulation of immune processes, as indicated by GO terms such as positive regulation of immune effector process and regulation of T cell-mediated cytotoxicity. However, the number of significant immune terms was limited to six, many of which were associated with acute immune responses, such as antibacterial humoral response and acute inflammatory response.

In contrast, the HD group had significant downregulation in development and morphogenesis processes, as well as extracellular matrix, compared to the LD and ID groups. Specifically, for development and morphogenesis, there was marked downregulation in GO terms associated with skeletal development (e.g., embryonic skeletal system morphogenesis, muscle cell differentiation) and nervous system development (e.g., presynapse assembly, neuron migration). Additionally, GO terms related to the extracellular matrix, such as collagen fibril organization and extracellular matrix assembly, were also significantly downregulated.

The ID group consistently positioned at a midpoint between the HD and LD groups regarding all GO terms related to mi-

tochondrial and metabolic processes. In terms of extracellular matrix, development, and morphogenesis, the ID group showed significant downregulation for all associated GO terms compared to the HD group. Against the LD group, the ID group showed either no significant difference or slight upregulation. For immune response, the ID group demonstrated the lowest enrichment among the three groups. The most striking characteristics for the ID group was the significant upregulation of metal ion responses related to cadmium, zinc, and copper, as indicated by GO terms such as response to zinc ion, response to cadmium ion, and response to copper ion.

Lastly, the LD group exhibited the lowest regulation in mitochondrial oxidative phosphorylation, metabolic processes, and metal ion responses among the three CHC-associated groups, highlighting the molecular spectrum across them. The most notable differences were observed in mitochondrial OXPHOS and metabolism, with biological activity progressively increasing from LD to ID to HD.

### Survival analysis reveals clinically significant survival difference between CHC-categorized groups

The Kaplan-Meier survival curves for the CHC-categorized groups demonstrated significant differences in overall survival probabilities ([Fig. 1C](#)). The LD group had the lowest survival probability over time compared to the HD ( $p = .047$ ) and ID groups ( $p = .018$ ). There was no significant survival difference between the HD and ID groups ( $p = .602$ ). [Table 2](#) shows survival, histology, and RNA molecular analysis results for the three CHC-categorized groups. Additionally, a multivariable Cox proportional hazards regression analysis was performed to evaluate the association of various clinicopathologic factors with survival. The CHC-categorized group was identified as the only independent prognostic factor ([Fig. 5](#)).

## DISCUSSION

In this study, we performed histomorphologic clustering of HGSC, deriving three distinct subgroups based on 40 tumor-containing CHCs. Given HAVOC's success in detecting intratumoral heterogeneity in high-grade gliomas, a similarly poorly differentiated tumor, we anticipated its capability to identify histologically distinct patterns in HGSC. With the identified CHCs, we categorized tumors in a manner relevant to clinical prognosis. Through PCA and K-means clustering analysis of CHCs in 73 TCGA-OV samples, we identified three

**Table 2.** Overview of the three CHC-categorized groups in terms of survival, histology, and RNA sequencing analysis

Overall survival	Quantitative histologic analysis		RNA sequencing <sup>a</sup>				
	Qualitative histologic analysis	Color features	Mt & Metab	ECM	Dev & Morph	Metal ion response	Immune response
Highly differentiated (HD) group	Favorable Low tumor-to-stromal ratio High variability among CHCs High pleomorphism of tumor cells Includes glandular and micropapillary patterns	High eosin with low hematoxylin staining High eosin with low hematoxylin staining	+++	+	+	++	+++
Intermediately differentiated (ID) group	Favorable Intermediate tumor-to-stromal ratio Peritumoral cleft-like spaces Includes complex glandular to solid patterns	Balanced hematoxylin and eosin staining	++	+++	+++	+++	++
Lowly differentiated (LD) group	Poor High tumor-to-stromal ratio Complete patternless sheet-like structure Peritumoral cleft-like spaces	High hematoxylin and low eosin staining	+	+++	+++	+/+++	+

CHC, common histologic cluster; Mt & Metab, mitochondria and metabolism; ECM, extracellular matrix; Dev & Morph, development and morphogenesis.

<sup>a</sup>Legend for RNA sequencing symbols: "+" indicates low expression, "++" represents moderate expression, and "+++" signifies high expression levels across the various categories.

histomorphologically unique groups with significant survival differences (Table 2). The HD and ID groups were associated with favorable overall survival. The HD group featured low tumor density, highly pleomorphic nucleoli, and focal glandular and micropapillary patterns with high eosinophilic staining. The ID group exhibited intermediate tumor density and focal complex glandular and solid patterns with a balanced H&E staining. In contrast, the LD group demonstrated significantly lower overall survival and was characterized by high tumor density, large monotonous nuclei, and a completely patternless structure with high hematoxylin staining.

Our new categorization of HGSC differs from the well-known TCGA molecular classification. The stromal-rich characteristics typical of the mesenchymal subtype (TCGA's poor prognosis group) were not present in the LD group. Similarly, the abundant lymphocyte features associated with the immunoreactive subtype (favorable prognosis group) were absent in both the HD and ID groups. Unlike molecular subtypes, our categorization emphasizes tumor cell density and H&E staining intensities of nuclei, as revealed by histology analysis. Both cell density and hematoxylin staining intensity increased progressively from the HD to ID to LD groups, a trend confirmed by both pathologist interpretations and quantitative analysis. Notably, the LD group exhibited the poorest overall survival, suggesting that higher tumor cell density and strong hematoxylin staining intensity are correlated with adverse prognosis in HGSC.

Our results suggest that H&E staining intensities provide valuable biological information, as varying nucleus intensities correlate with different prognostics groups in HGSC. To preserve the biological information integrated in the image, we opted to not use color normalization in this experiment. Currently, there is no universally accepted standard for normalization, and different techniques can yield varying results [23]. Additionally, normalization can introduce color artifacts that can potentially compromise the integrity of the image [24].

Gene enrichment analysis offers a new perspective on HGSC compared to the TCGA classifications, linking CHC-associated groups to energy metabolism, particularly mitochondrial dynamics, and OXPHOS. The LD group, associated with poor prognosis, showed significant downregulation of genes associated with mitochondria and OXPHOS compared to those in the ID and HD groups, with

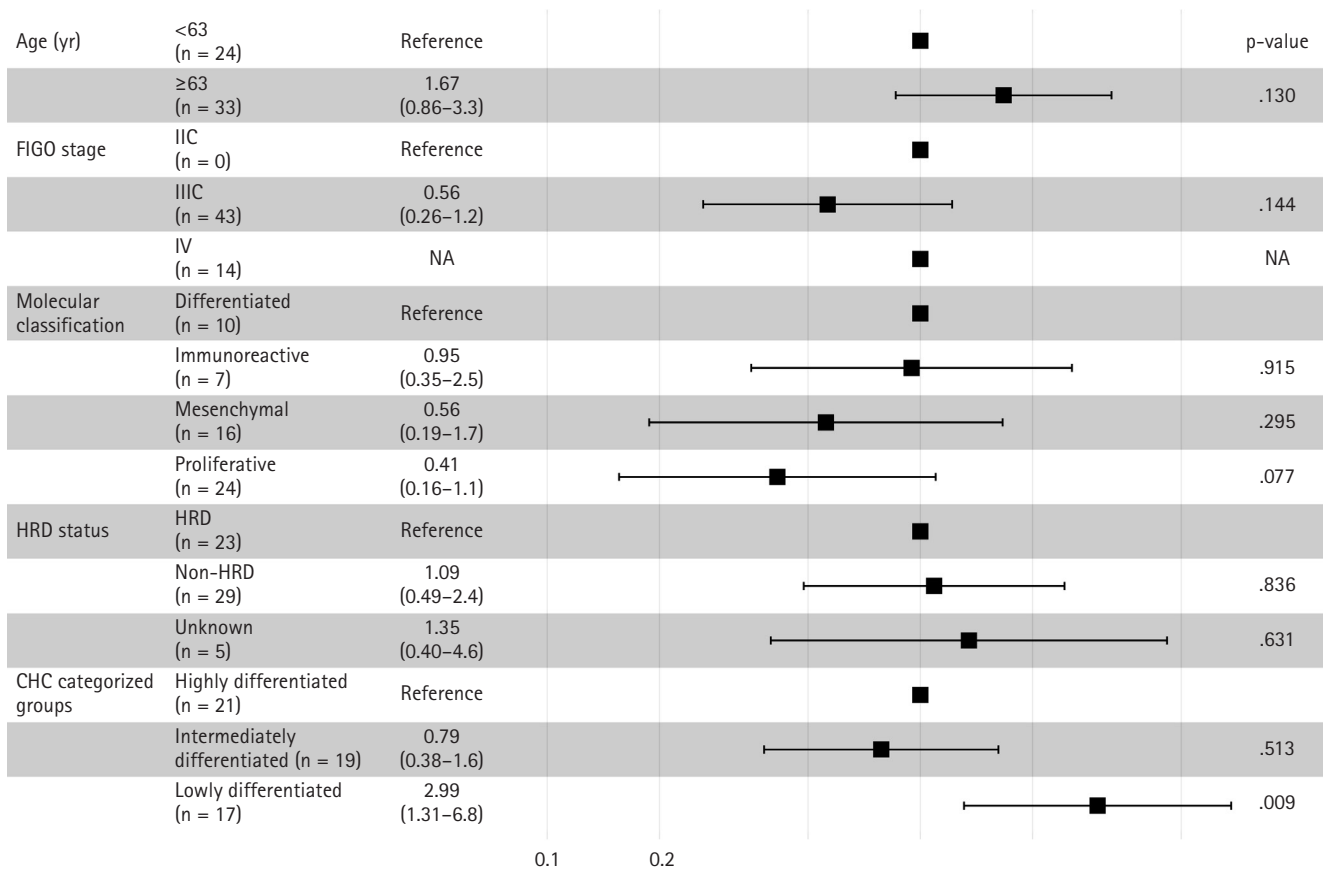


**Fig. 5.** Multivariable Cox proportional hazards regression analysis. The multivariable Cox proportional hazards regression analysis identifies the common histomic cluster (CHC)-categorized group as the sole independent prognostic factor, while other factors, including median age, International Federation of Gynecology and Obstetrics (FIGO) stage, clinicopathological characteristics, The Cancer Genome Atlas molecular classification, and homologous recombination deficiency (HRD) status, showed no significance. NA, not available.

the ID group positioned in between the other two groups. This finding aligns with studies indicating that increased OXPHOS generates reactive oxygen species, enhancing platinum-based chemotherapy sensitivity and favorable prognosis [25,26]. Additionally, a shift from OXPHOS to glycolytic metabolism is tied to higher invasiveness and poorer survival, as seen in the LD group [27]. This metabolic shift, causing mitochondrial fission and repositioning of mitochondria to the cell periphery leading to lamellipodia formation, may explain the nuclear shape changes observed in histologic analysis [28,29].

The DEG analysis revealed significant *ERBB2/HER2* upregulation in the LD group. A recent study suggested a potential link between HER2 and OXPHOS, as HER2 can translocate to mitochondria, stimulating OXPHOS and promoting tumorigenicity in breast cancer cells [30]. To identify HER2's role in HGSC, further investigation is needed on the HER2 localization and its association with OXPHOS in HGSC tumor cells.

Gene enrichment analysis revealed significant upregulation of extracellular matrix-related processes in the LD group compared to the favorable HD group. Despite no difference in stromal cell counts from the quantitative analysis, the LD group, associated with poor prognosis, exhibited larger and longer stromal nuclei with more intense hematoxylin staining, suggesting the presence of activated CAF [31].

Gene enrichment showed upregulation of a few immune terms in the HD group, primarily related to antibacterial and acute inflammatory responses rather than cancer-related immunity. Immune cell counts were comparable across the three CHC-associated groups, confirmed by CIBERSORT analysis, suggesting minor immune implications across the three groups.

Based on the overall analysis, we hypothesize that the three CHC-associated groups represent a spectrum of tumor progression: HD is the least progressed, LD is the most progressed, and ID is intermediate. Histomorphologic analysis shows a

progression from less dense differentiated tumors to solid, high-density cell tumors. Gene analysis supports this, with the ID group showing intermediate mitochondrial activity and metabolism. Interestingly, the ID group had survival rates similar to those of the HD group, suggesting that a shift from ID to LD may be key to poor prognosis in HGSC. Notably, the ID group exhibited significant upregulation of metal ion response genes, particularly those related to zinc, copper, and cadmium, compared to the other clusters. Both cadmium and zinc are associated with HGSC and could potentially play unique roles in its progression [32,33], warranting further investigation.

Our findings offer valuable prognostic insights and could guide treatment decisions by identifying CHCs linked to poor prognosis and potential resistance to standard therapies, such as platinum-based chemotherapy and radiation therapy. Additionally, they could lay the groundwork for developing digital biomarkers and targeted therapies, including mitochondria-targeted treatments for the OXPHOS-enhanced HD group and HER2-targeted therapies for the LD group.

The limitations of this study include a small sample size of 73, which may not adequately represent the extensive inter- and intra-tumoral heterogeneity present in HGSC. A larger sample size and multiple WSIs per patient are needed for future studies. Additionally, the genetic analysis relied on bulk sequencing. A more detailed analysis of the tumor microenvironment, particularly stromal and immune cell activities, would benefit from single-cell or spatial sequencing. Additionally, the TCGA-OV datasets lack comprehensive clinical information regarding specific treatments and chemotherapy regimens received by the patients, which could potentially serve as confounding factors influencing survival outcomes. Since this was a pilot study, further research is planned with larger in-house dataset, including more in-depth clinical information to better address the histologically distinct entities and their association with mitochondrial activity to a broader HGSC population.

In this study, we used HAVOC to examine intratumoral heterogeneity in HGSC with the TCGA-OV dataset, categorizing three histologically distinct groups with varying survival outcomes. Our findings illustrate a progression from well-differentiated histological patterns with high OXPHOS activity in HD, through the ID group, to poorly differentiated patterns with low OXPHOS in the LD group, indicating

a potential tumor progression from HD to LD. Despite the limited sample size, this pilot study lays the groundwork for future research to validate these histological entities and their link to mitochondrial activity.

### Supplementary Information

The Data Supplement is available with this article at <https://doi.org/10.4132/jptm.2024.10.23>.

### Ethics Statement

This study was conducted using only public data that Institutional Review Board was not required.

### Availability of Data and Material

The TCGA dataset is publicly available via the TCGA portal (<https://portal.gdc.cancer.gov>).

### Code Availability

Not applicable.

### ORCID

Byungsoo Ahn <https://orcid.org/0009-0007-3641-9590>  
Eunhyang Park <https://orcid.org/0000-0003-2658-5054>

### Author Contributions

Conceptualization: BA. Data curation: BA. Formal analysis: BA. Funding acquisition: EP. Investigation: EP. Methodology: BA. Project administration: EP. Resources: BA. Software: BA. Supervision: EP. Validation: BA. Visualization: BA. Writing—original draft: BA, EP. Writing—review & editing: BA, EP. Approval of final manuscript: BA, EP.

### Conflicts of Interest

The authors declare that they have no potential conflicts of interest.

### Funding Statement

This research was supported by a grant of the Korea Health Technology R&D Project through the Korea Health Industry Development Institute (KHIDI), funded by the Ministry of Health & Welfare, Republic of Korea (grant number: HI19C0481, HC21C0012, RS-2024-00438923) and a faculty research grant from Yonsei University College of Medicine (6-2021-0244 and 6-2022-0179) to E.P.

## REFERENCES

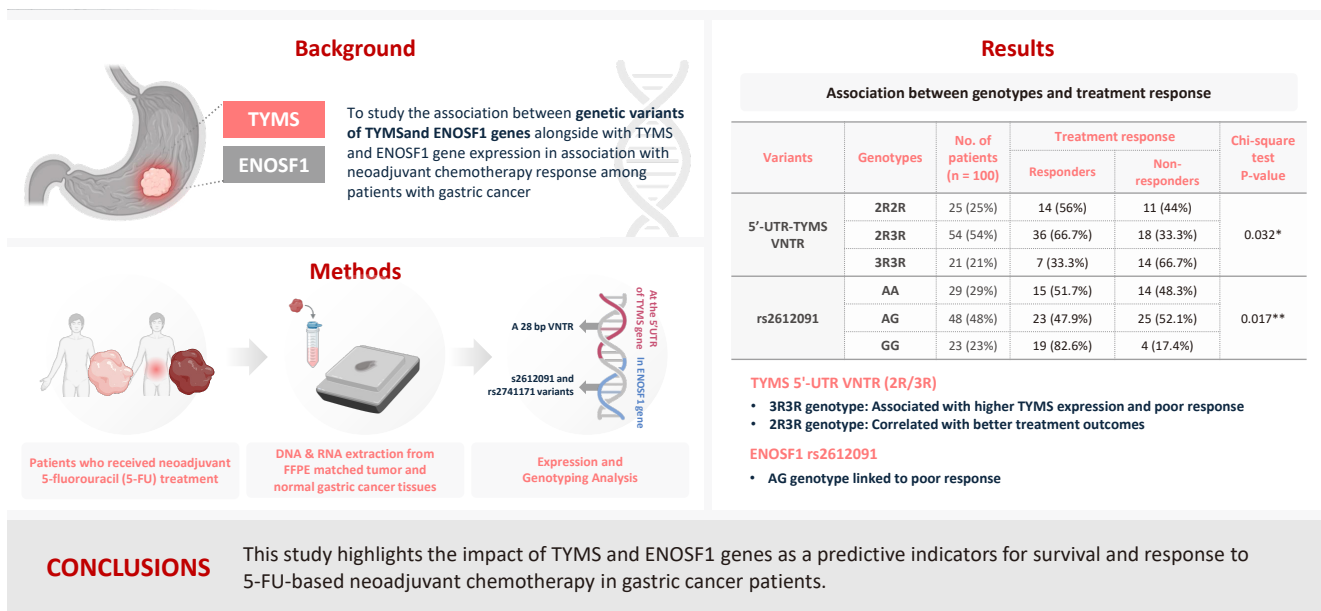
1. Ferlay J, Shin HR, Bray F, Forman D, Mathers C, Parkin DM. Estimates of worldwide burden of cancer in 2008: GLOBOCAN 2008. *Int J Cancer* 2010; 127: 2893-917.
2. Gonzalez-Martin A, Pothuri B, Vergote I, et al. Niraparib in patients with newly diagnosed advanced ovarian cancer. *N Engl J Med* 2019; 381: 2391-402.
3. Yu KH, Levine DA, Zhang H, Chan DW, Zhang Z, Snyder M. Predicting ovarian cancer patients' clinical response to platinum-based chemotherapy by their tumor proteomic signatures. *J Proteome Res* 2016; 15: 2455-65.
4. Dao F, Schlappé BA, Tseng J, et al. Characteristics of 10-year survivors of high-grade serous ovarian carcinoma. *Gynecol Oncol* 2016; 141: 260-3.
5. Hayashi T, Konishi I. Molecular histopathology for establishing diagnostic method and clinical therapy for ovarian carcinoma. *J Clin Med Res* 2023; 15: 68-75.
6. Cancer Genome Atlas Research Network. Integrated genomic analyses of ovarian carcinoma. *Nature* 2011; 474: 609-15.
7. Konecny GE, Wang C, Hamidi H, et al. Prognostic and therapeutic relevance of molecular subtypes in high-grade serous ovarian cancer. *J Natl Cancer Inst* 2014; 106: dju249.
8. Verhaak RG, Tamayo P, Yang JY, et al. Prognostically relevant gene signatures of high-grade serous ovarian carcinoma. *J Clin Invest* 2013; 123: 517-25.
9. Khashaba M, Fawzy M, Abdel-Aziz A, Eladawei G, Nagib R. Subtyping of high grade serous ovarian carcinoma: histopathological and immunohistochemical approach. *J Egypt Natl Canc Inst* 2022; 34: 6.
10. Miyagawa C, Nakai H, Otani T, et al. Histopathological subtyping of high-grade serous ovarian cancer using whole slide imaging. *J Gynecol Oncol* 2023; 34: e47.
11. Ahn B, Moon D, Kim HS, et al. Histopathologic image-based deep learning classifier for predicting platinum-based treatment responses in high-grade serous ovarian cancer. *Nat Commun* 2024; 15: 4253.
12. Laury AR, Blom S, Ropponen T, Virtanen A, Carpen OM. Artificial intelligence-based image analysis can predict outcome in high-grade serous carcinoma via histology alone. *Sci Rep* 2021; 11: 19165.
13. Zeng H, Chen L, Zhang M, Luo Y, Ma X. Integration of histopathological images and multi-dimensional omics analyses predicts molecular features and prognosis in high-grade serous ovarian cancer. *Gynecol Oncol* 2021; 163: 171-80.
14. Wang CW, Chang CC, Lee YC, et al. Weakly supervised deep learning for prediction of treatment effectiveness on ovarian cancer from histopathology images. *Comput Med Imaging Graph* 2022; 99: 102093.
15. Dent A, Faust K, Lam KH, et al. HAVOC: small-scale histomic mapping of cancer biodiversity across large tissue distances using deep neural networks. *Sci Adv* 2023; 9: eadg1894.
16. Zhang M, Ma SC, Tan JL, et al. Inferring homologous recombination deficiency of ovarian cancer from the landscape of copy number variation at subchromosomal and genetic resolutions. *Front Oncol* 2021; 11: 772604.
17. Graham S, Vu QD, Raza SE, et al. Hover-Net: simultaneous segmentation and classification of nuclei in multi-tissue histology images. *Med Image Anal* 2019; 58: 101563.
18. Bankhead P, Loughrey MB, Fernandez JA, et al. QuPath: open source software for digital pathology image analysis. *Sci Rep* 2017; 7: 16878.
19. Berthold MR, Cebron N, Dill F, et al. KNIME: the Konstanz information miner: version 2.0 and beyond. *ACM SIGKDD Explor Newsl* 2009; 11: 26-31.
20. Chen B, Khodadoust MS, Liu CL, Newman AM, Alizadeh AA. Profiling tumor infiltrating immune cells with CIBERSORT. *Methods Mol Biol* 2018; 1711: 243-59.
21. Robinson MD, McCarthy DJ, Smyth GK. edgeR: a Bioconductor package for differential expression analysis of digital gene expression data. *Bioinformatics* 2010; 26: 139-40.
22. Korotkevich G, Sukhov V, Budin N, Shpak B, Artyomov MN, Sergushichev A. Fast gene set enrichment analysis. Preprint bioRxiv at: <https://doi.org/10.1101/060012> (2021).
23. Hoque MZ, Keskinarkaus A, Nyberg P, Seppanen T. Stain normalization methods for histopathology image analysis: a comprehensive review and experimental comparison. *Inf Fusion* 2024; 102: 101997.
24. Khan AM, Rajpoot N, Treanor D, Magee D. A nonlinear mapping approach to stain normalization in digital histopathology images using image-specific color deconvolution. *IEEE Trans Biomed Eng* 2014; 61: 1729-38.
25. Gentric G, Kieffer Y, Mieulet V, et al. PML-regulated mitochondrial metabolism enhances chemosensitivity in human ovarian cancers. *Cell Metab* 2019; 29: 156-73.
26. Berndtsson M, Hagg M, Panaretakis T, Havelka AM, Shoshan MC, Linder S. Acute apoptosis by cisplatin requires induction of reactive oxygen species but is not associated with damage to nuclear DNA. *Int J Cancer* 2007; 120: 175-80.
27. Kleih M, Bopple K, Dong M, et al. Direct impact of cisplatin on

- mitochondria induces ROS production that dictates cell fate of ovarian cancer cells. *Cell Death Dis* 2019; 10: 851.
28. Cunniff B, McKenzie AJ, Heintz NH, Howe AK. AMPK activity regulates trafficking of mitochondria to the leading edge during cell migration and matrix invasion. *Mol Biol Cell* 2016; 27: 2662-74.
  29. Gao T, Zhang X, Zhao J, et al. SIK2 promotes reprogramming of glucose metabolism through PI3K/AKT/HIF-1alpha pathway and Drp1-mediated mitochondrial fission in ovarian cancer. *Cancer Lett* 2020; 469: 89-101.
  30. Novotna E, Milosevic M, Prukova D, et al. Mitochondrial HER2 stimulates respiration and promotes tumorigenicity. *Eur J Clin Invest* 2024; 54: e14174.
  31. Xing F, Saidou J, Watabe K. Cancer associated fibroblasts (CAFs) in tumor microenvironment. *Front Biosci (Landmark Ed)* 2010; 15: 166-79.
  32. Furtak G, Kozlowski M, Kwiatkowski S, Cymbaluk-Ploska A. The role of lead and cadmium in gynecological malignancies. *Antioxidants (Basel)* 2022; 11: 2468.
  33. Lin S, Yang H. Ovarian cancer risk according to circulating zinc and copper concentrations: a meta-analysis and Mendelian randomization study. *Clin Nutr* 2021; 40: 2464-8.

# Association study of *TYMS* gene expression with *TYMS* and *ENOSF1* genetic variants in neoadjuvant chemotherapy response of gastric cancer

Khadijeh Arjmandi<sup>1</sup>, Iman Salahshourifar<sup>1</sup>, Shiva Irani<sup>1</sup>, Fereshteh Ameli<sup>2</sup>, Mohsen Esfandbod<sup>3</sup>

## Graphical abstract



# Association study of *TYMS* gene expression with *TYMS* and *ENOSF1* genetic variants in neoadjuvant chemotherapy response of gastric cancer

Khadijeh Arjmandi<sup>1</sup>, Iman Salahshourifar<sup>1</sup>, Shiva Irani<sup>1</sup>, Fereshteh Ameli<sup>2</sup>, Mohsen Esfandbod<sup>3</sup>

<sup>1</sup>Department of Biology, Science and Research Branch, Islamic Azad University, Tehran, Iran

<sup>2</sup>Pathology Department, Cancer Institute, Imam Khomeini Hospital Complex, Tehran University of Medical Sciences, Tehran, Iran

<sup>3</sup>Department of Hematology and Oncology, Imam Khomeini Hospital Complex, Tehran University of Medical Sciences, Tehran, Iran

**Background:** The present research was designed to study the associations between genetic variants of *TYMS* and *ENOSF1* genes with *TYMS* and *ENOSF1* gene expression in neoadjuvant chemotherapy response among patients with gastric cancer. **Methods:** Formalin-embedded and paraffin-fixed matched tumor and normal gastric cancer tissue samples from patients who received neoadjuvant 5-fluorouracil (5-FU) treatment were obtained. DNA and RNA were extracted for all samples. A 28-bp variable number tandem repeat (VNTR) at the 5' untranslated region of *TYMS* gene and rs2612091 and rs2741171 variants in the *ENOSF1* gene were genotyped for normal tissue samples. The real-time polymerase chain reaction method was used to study the expression of *ENOSF1* and *TYMS* genes in both normal and tumor tissues. Data were analyzed using REST 2000 and SPSS ver. 26.0 software programs. **Results:** A significant association between *TYMS* 2R3R VNTR genotypes and 5-FU therapy was found ( $p = .032$ ). The 3R3R and 2R2R genotypes were significantly associated with increased and decreased survival time, respectively ( $p = .003$ ). The 3R3R genotype was significantly associated with *TYMS* overexpression ( $p < .001$ ). Moreover, a significant association was found between the rs2612091 genotype and treatment outcome ( $p = .017$ ). **Conclusions:** This study highlights the impact of *TYMS* and *ENOSF1* genes as predictive indicators for survival and response to 5-FU-based neoadjuvant chemotherapy in gastric cancer patients.

**Keywords:** Chemoresistance; Pharmacogenetics; Precision medicine; Stomach neoplasms; Genetic variants

## INTRODUCTION

Gastric cancer is the fifth most prevalent malignancy in the world and the fourth most lethal cancer type, with a 5-year survival rate less than 20.0% [1,2]. Nonmetastatic gastric and gastroesophageal adenocarcinomas in randomized clinical trials have shown a positive response to combinational treatments [3]. Advanced gastric malignancies can be treated with different cytotoxic substances, including platinum-based compounds, taxanes, fluoropyrimidines (FPs), and irinotecan [3]. The efficacy of chemotherapy, which plays a key role in treatment of both locally advanced and metastatic gastric cancers, is often hampered

by the development of chemoresistance. Complex mechanisms are involved in chemoresistance in gastric cancer [4].

5-Fluorouracil (5-FU) is a frequently used FP in various malignancies [5]. The principal target of FPs is the thymidylate synthase (TS) enzyme, which plays a vital role in DNA synthesis. There are opposing associations between TS expression level and tumor vulnerability to FPs [5-7]. Genetic variants in the thymidylate synthetase (*TYMS*) gene, encoding the TS protein, have been used to predict drug toxicity risk [8]. Variations in the 5' untranslated regions (5'-UTRs) of the *TYMS* gene have gained notable attention for their unique ability to affect the stability of *TYMS* mRNA and gene expression and TS levels

**Received:** July 23, 2024 **Revised:** October 29, 2024 **Accepted:** November 5, 2024

**Corresponding Author:** Iman Salahshourifar, PhD

Department of Biology, Science and Research Branch, Islamic Azad University, Tehran 1416753955, Iran

Tel: +98-9199300923, Fax: +98-21-66911705, E-mail: isalahshouri@gmail.com

This is an Open Access article distributed under the terms of the Creative Commons Attribution Non-Commercial License (<https://creativecommons.org/licenses/by-nc/4.0/>) which permits unrestricted non-commercial use, distribution, and reproduction in any medium, provided the original work is properly cited.

© 2025 The Korean Society of Pathologists/The Korean Society for Cytopathology

[9]. In particular, there are significant associations of change in gene expression, response to 5-FU treatment, and toxic effects with a 28-bp variable number tandem repeat (VNTR) in the *TYMS* 5'-UTR [6,10-12]. Studies have revealed distinct connections between the 2R and 3R alleles of this VNTR in *TYMS* expression, 5-FU reactivity, and toxicity [10,13]. The 3R allele is associated with a significant increase in *TYMS* expression, potentially necessitating higher doses of 5-FU for effective treatment, resulting in a less favorable prognosis and reduced drug efficacy [10,12]. Specifically, the 3R/3R genotype displays greater *TYMS* expression than the 2R/2R genotype [10,12,14]. In contrast, the 2R/2R genotype has been linked with increased toxicity in patients receiving FP-based chemotherapy, resulting in significant adverse reactions [8,11,15].

Adjacent to the *TYMS* gene, the enolase superfamily member 1 (*ENOSF1*) gene seems to have dual roles as a protein-coding gene and an antisense transcript that modulates *TYMS* mRNA expression and protein levels [10,16-19]. The rs2612091 variant influences the expression of *ENOSF1* mRNA and is associated with an increased risk of toxicity induced by capecitabine treatment [16,17].

The rs2741171 variant (located downstream of *TYMS* and in the intronic region of *ENOSF1*) has been implicated in the development of hand-foot syndrome (HFS) [13]. Hence, we designed the current study to investigate associations of the 28-bp VNTR in the *TYMS* gene and of the rs2612091 and rs2741171 variants in the *ENOSF1* gene and *TYMS* gene expression with 5-FU therapy in patients with gastric cancer.

## MATERIALS AND METHODS

### Participants

We recruited 100 matched tumor and normal formalin-fixed, paraffin-embedded (FFPE) samples from patients with gastric cancer who underwent gastrectomy at Imam Khomeini Hospital, Tehran, Iran, from 2012 to 2018. The cohort consisted of 70 male and 30 female participants, with an average age of  $58.10 \pm 11.43$  years. All patients were treated with 5-FU before surgery. The FFPE blocks of all patients were examined by a pathologist, and matched tumor and normal tissues were punched. The evaluation of chemotherapy effectiveness was categorized based on the standards established by the College of American Pathologists [20]. This guideline classifies the treatment responses into four groups: comprehensive response (with a score of 0), nearly comprehensive response (with a score of 1), partial

response (with a score of 2), and minimal or nonexistent response (with a score of 3). Patients were then classified into two groups of positive treatment response (with scores 0 to 2) and inadequate or absent response (with a score of 3).

### DNA extraction and genotyping revisions

DNA of matched normal and tumor tissues were extracted using QIAamp DNA FFPE Tissue kit (Qiagen, Hilden, Germany). Genotyping of the 5'-UTR-*TYMS* VNTR variant was performed using previously reported primers [6,21]. Polymerase chain reaction (PCR) was conducted with a total volume of 22  $\mu$ L as follows: 50 ng of genomic DNA, 5.0% dimethyl sulfoxide, 10 picomoles of each primer, and the 12  $\mu$ L of 2 $\times$  Hot Start PCR mix (Amplicon Co., Copenhagen, Denmark).

The PCR program was carried out with an initial denaturation at 95°C for 15 minutes, followed by 37 cycles of denaturation at 95°C for 1 minute, annealing at 64°C for 45 seconds, and extension at 72°C for 45 seconds and then a final extension step at 72°C for 10 minutes.

### Genotyping

Specific primers were designed for genotyping of the VNTR at the 5'-UTR of the *TYMS* gene (Table 1). The 2R allele with a size of 210 bp and 3R allele with a size of 238 bp were identified using agarose gel electrophoresis. Tetra-ARMS PCR was used for genotyping of rs2612091 and rs2741171 variants in the *ENOSF1* gene (Table 1). Tetra-ARMS PCR primers were designed using the Primer 1 online program (primer1.soton.ac.uk/primer1.html).

The PCR mixture reaction for tetra-ARMS PCR comprised between 50 and 100 ng of genomic DNA, 2 $\times$  Hot start PCR Master Mix Blue (Amplicon Co.), and 5 pmol of each primer. The PCR conditions were 95°C for 10 minutes; 40 cycles of 95°C for 1 minute, 62°C for 1 minute, and 72°C for 1 minute; and a final extension for 10 minutes at 72°C. Amplification products were examined, and genotypes were identified on a 3.0% agarose gel.

### RNA extraction and gene expression analysis

The total RNA from FFPE matched tumor and normal tissues of 100 patients was extracted using the Hybrid-R GeneAll Kit (GeneAll Co., Seoul, Korea). cDNA was synthesized using a commercial kit (Yekta Tajhiz Azma, Tehran, Iran). Then, quantitative real-time PCR (qPCR) analysis was performed using the Cyber Green method with previously published primers for

**Table 1.** Primer sequences for *ENOSF1* and *TYMS* variants

Gene	Variant	Primer	Product size (bp)	
<i>ENOSF1</i>	rs2612091	Forward inner primer (A allele)	CTGGACATCCAGTGGCTCCTCAATCA	247
		Reverse inner primer (G allele)	GGTACAGTCTTTAGGAGGAGCCGTGCAC	197
		Forward outer primer	TGTGCATGATTCAGAATGTGACAAAATGG	390
		Reverse outer primer	AAAAGAGACTCTTCACAGGGAGGTCAGCC	
	rs2741171	Forward inner primer (A allele)	GGGTTTCACCATGTTGATCAGGTGGA	222
		Reverse inner primer (G allele)	GCGGATCACCTGAGGTCAGGAGTATGATAC	288
		Forward outer primer	CAATTCCTGCCACAGCCAAAATTTCTC	454
		Reverse outer primer	TGACTCTCAGAGTGACAAGCAGCACTT	
<i>TYMS</i>	<i>TYMS</i> 28-bp VNTR	Forward primer	CGTGGCTCCTGCGTTTCC	210 (2R)
		Reverse primer	GAGCCGGCCACAGGCAT	238 (3R)

The tetra-ARMS polymerase chain reaction (PCR) method was used for *ENOSF1* and normal PCR was used for *TYMS* genotyping. *ENOSF1*, enolase superfamily member 1; *TYMS*, thymidylate synthetase; VNTR, variable number tandem repeat.

*TYMS* gene expression [22]. In addition, specific primers were designed for the *ENOSF1* gene expression analysis as follows: forward primer (5'-ACAGGCACTTCCAATTCCGA-3') and reverse primer (5'-AGAGCTGCTTCAACGTGTCA-3'). The *GAPDH* gene was used as the reference control with the following primer sequences: forward primer (5'-TCACCAGGGCT-GCTTTTAAC-3') and reverse primer (5'-GACAAGCTTC-CCGTTCTCAG-3').

For each assay, the total volume of the PCR reaction was 20 µL comprised of 2 µL of cDNA, 10 pmol of each primer, and 10 µL of Cyber Green 2× master mix (Amplicon Co.). The qPCR was performed using an initial denaturation step at 95°C for 15 minutes. This was followed by 40 cycles of denaturation at 95°C for 30 seconds, annealing at 60°C for 60 seconds, and extension at 72°C for 30 seconds. To ensure the robustness and reliability of the results, each sample underwent analysis in triplicate.

**Statistical analysis**

Data analysis was conducted using REST 2000 and SPSS ver. 26.0 software (IBM Corp., Armonk, NY, USA). The chi-square test, a two-sided independent t-test, and one-way ANOVA were applied to examine the relationships between variables. A significant difference was established at .05. Patient survival times were estimated using the log-rank test and Kaplan-Meier survival analysis. The Cox regression semi-parametric model assessed the mortality risk ratio across variant states. Changes in expression levels were measured using the 2<sup>-ΔΔCT</sup> method.

**RESULTS**

**Patient characteristics**

In this study of 100 patients with gastric cancer, 43 experienced resistance to chemotherapy. The average age of the patients was 58.10 ± 11.43 years 22 had grade 1 disease, 35 had grade 2, and 43 had grade 3. The stage of disease was 1 in 22 cases, 2 in 34, 3 in 39 cases, and 4 in five cases. Among the 57 patients who responded to treatment, 13 experienced complete remission (rated as score 0), 15 achieved near-complete remission (score 1), and 29 demonstrated a partial response (score 2). Over a maximum follow-up period of 5 years, 24 patients showed disease progression, 47 patients died, and 29 patients maintained a favorable condition.

**Genotypic variations and chemotherapeutic response**

A significant association was observed between VNTR genotype and the effectiveness of neoadjuvant chemotherapy (p = .032) (Tables 2, 3). The 2R3R genotype was found more frequently in patients with a positive response to the treatment (66.7%), followed by the 2R2R genotype. Conversely, the 3R3R genotype was more common in those who did not respond to the treatment.

Additionally, a significant association was found between the rs2612091 variant and the efficacy of treatment (p = .017), with the AG genotype more frequent in non-responders. However, no significant association was found between rs2741171 genotype and treatment outcome (p < .05).

**Variant impact on survival outcomes**

A significant association between overall survival and *TYMS* VNTR genotype was identified ( $p = .003$ ). Those with the 3R3R genotype had longer survival times in contrast to those with the 2R3R genotype, who had the shortest survival time (Table 4, Fig. 1A). Mortality risk analysis using the Cox model showed that patients with the 3R3R or 2R3R genotype had reduced hazard ratio (HR) of 0.24 and 0.47, respectively, compared to those with the 2R2R genotype. Despite the lack of significance ( $p = .170$ ), individuals carrying the GG or AA genotype of the

rs2612091 variant showed longer and shorter survival, respectively, after treatment with 5-FU (Table 4, Fig. 1B).

Similarly, the Cox model analysis showed no significant difference in HR for mortality among patients with GG or AG genotype compared to those with the AA genotype ( $p > .05$ ). For the rs2741171 variant, patients with AG genotype were associated with the longest survival after 5-FU treatment, whereas those with GG genotype had the shortest (Table 4, Fig. 1C). However, this observation was not statistically significant ( $p = .970$ ).

**Table 2.** Frequency distribution of genotypes in the studied variants

Gene	Variant	Genotype	Frequency, n (%)
<i>TYMS</i>	5'-UTR- <i>TYMS</i> VNTR	2R3R	54 (54.0)
		2R2R	25 (25.0)
		3R3R	21 (21.0)
<i>ENOSF1</i>	rs2612091	GG	23 (23.0)
		AG	48 (48.0)
		AA	29 (29.0)
	rs2741171	GG	48 (48.0)
		AA	16 (16.0)
		AG	36 (36.0)

The 2R3R genotype was the most frequent (54.0%) among all cases with 5'-UTR-*TYMS* VNTR, followed by the 2R2R (25.0%) and 3R3R (21.0%) genotypes. In rs2612091, the highest frequency was related to the AG genotype at 48.0%, and the frequencies of AA and GG genotypes were 29.0% and 23.0%, respectively. Genotypes with rs2741171 were 48.0% GG, 16.0% AA, and 36.0% AG.

*TYMS*, thymidylate synthetase; 5'-UTR, 5' untranslated region; VNTR, variable number tandem repeat; *ENOSF1*, enolase superfamily member 1.

**Gene expression analysis**

The *TYMS* gene was overexpressed in 61 tumor samples, while the remaining 39 did not reveal significant variations in gene expression. An association between *TYMS* gene expression and the 28-bp allele of the VNTR variant was found ( $p = .001$ ). The *TYMS* gene expression was downregulated among samples with the 2R2R genotype and overexpressed among samples with the 3R3R genotype (Table 5). No statistical significance was found between *TYMS* gene expression and treatment response ( $p = .206$ ).

Even though this result was not significant, the *ENOSF1* gene was downregulated in most tumor tissue samples (69%) compared to adjacent normal tissue samples that showed overexpression (31.0%) (Table 5).

***TYMS* and *ENOSF1* gene expression analysis**

No significant association was found between survival time and *TYMS* or *ENOSF1* gene expression (Table 6, Fig. 2). Further-

**Table 3.** Associations between genotypes and treatment response

Variant	Genotype	No. of patients (n = 100)	Treatment response		Chi-square test p-value
			Responder	Nonresponder	
5'-UTR- <i>TYMS</i> VNTR	2R2R	25 (25.0)	14 (56.0)	11 (44.0)	.032 <sup>a</sup>
	2R3R	54 (54.0)	36 (66.7)	18 (33.3)	
	3R3R	21 (21.0)	7 (33.3)	14 (66.7)	
rs2612091	AA	29 (29.0)	15 (51.7)	14 (48.3)	.017 <sup>b</sup>
	AG	48 (48.0)	23 (47.9)	25 (52.1)	
	GG	23 (23.0)	19 (82.6)	4 (17.4)	
rs2741171	AA	16 (16.0)	11 (68.8)	5 (31.3)	.065
	AG	36 (36.0)	15 (41.7)	21 (58.3)	
	GG	48 (48.0)	31 (64.6)	17 (35.4)	

Values are presented as number (%).

5'-UTR, 5' untranslated region; *TYMS*, thymidylate synthetase; VNTR, variable number tandem repeat.

<sup>a</sup>Among the studied genotypes, a significant correlation was found between VNTR genotype and treatment response ( $p = .032$ ). The 2R3R genotype was more common in responders, and the 3R3R genotype was more common among non-responders; <sup>b</sup>Genotypes of rs2612091 showed a significant association ( $p = .017$ ), patients who did not respond to treatment showed more frequent AG genotype.

**Table 4.** Survival time and HR among patients with different genotypes

Variant	Genotype	Survival time (mo)		HR (95% CI)	p-value
		Mean (95% CI)	p-value		
5'-UTR- <i>TYMS</i> VNTR	2R2R	23.44 (13.84–33.04)	.003 <sup>a</sup>	1 (reference group)	-
	2R3R	39.36 (32.62–46.1)		0.47 (0.25–0.87)	.020
	3R3R	47.17 (37.3–57.04)		0.24 (0.09–0.64)	.005
rs2612091	AA	30.71 (21.37–40.04)	.170	1 (reference group)	-
	AG	36.39 (28.97–43.8)		0.73 (0.39–1.37)	.320
	GG	45.80 (36.17–55.44)		0.47 (0.2–1.08)	.080
rs2741171	AA	36.84 (24.62–49.07)	.970	1 (reference group)	-
	AG	37.41 (28.93–45.88)		0.92 (0.39–2.16)	.850
	GG	36.79 (29.31–44.28)		1 (0.45–2.23)	.990

HR, hazard ratio; CI, confidence interval; 5'-UTR, 5' untranslated region; *TYMS*, thymidylate synthetase; VNTR, variable number tandem repeat; 5-FU, 5-fluorouracil.

<sup>a</sup>The highest and lowest average survival times of people after 5-FU treatment were in patients with 3R3R and 2R2R genotypes, respectively, and the observed difference was significant ( $p = .003$ ). Such a different also was observed in the Cox model, where the risk of death in those with 3R3R and 2R3R variants was lower than in those with 2R2R variants (reference group) at 0.24 and 0.47, respectively. The overall survival of patients with rs2612091 or rs2741171 after 5-FU treatment was not significant ( $p = .170$  and  $p = .970$ , respectively). In the Cox model, the risk ratio of death in patients with different genotypes of rs2612091 or rs2741171 variants compared to the reference group was not significant ( $p > .05$ ).

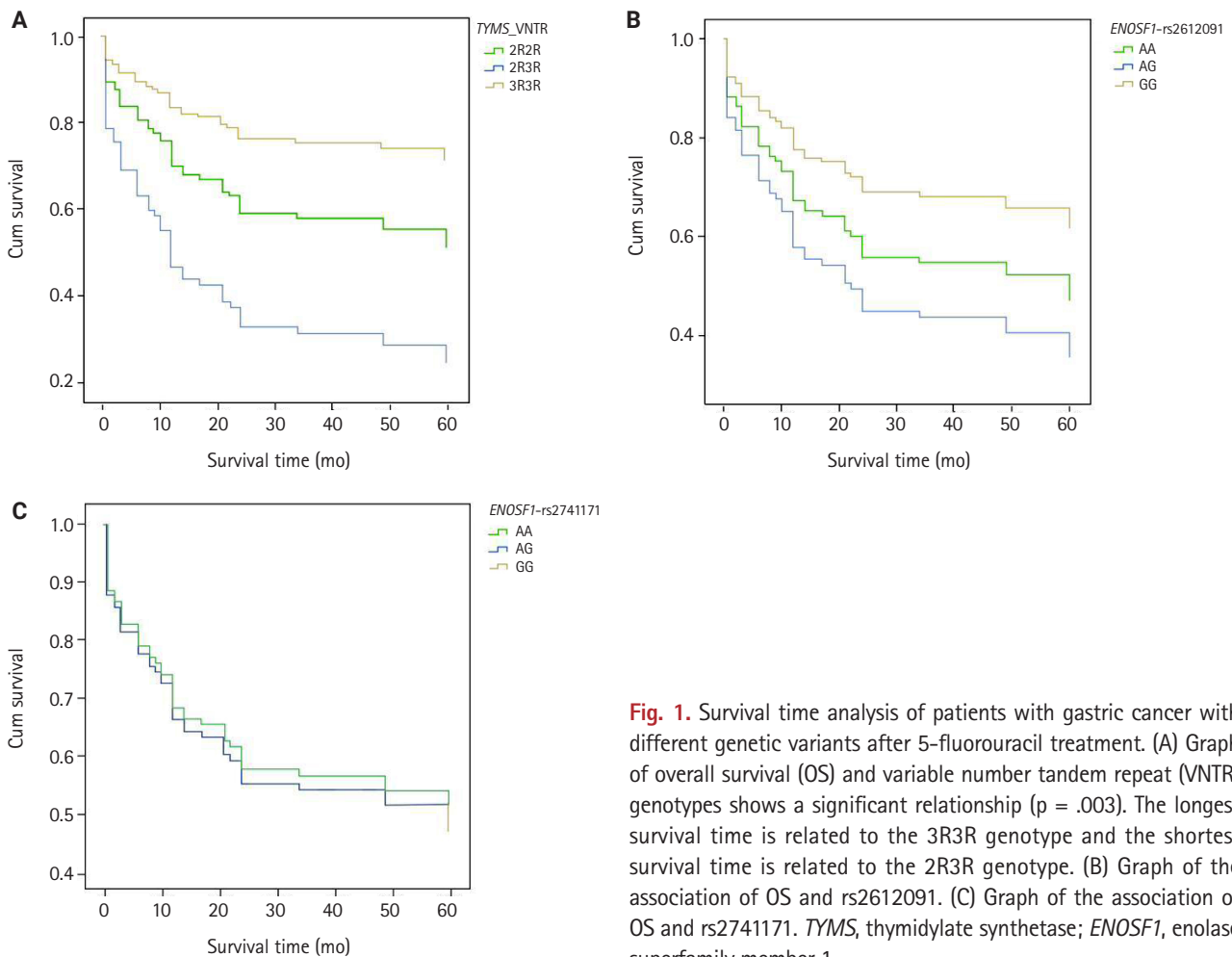


**Fig. 1.** Survival time analysis of patients with gastric cancer with different genetic variants after 5-fluorouracil treatment. (A) Graph of overall survival (OS) and variable number tandem repeat (VNTR) genotypes shows a significant relationship ( $p = .003$ ). The longest survival time is related to the 3R3R genotype and the shortest survival time is related to the 2R3R genotype. (B) Graph of the association of OS and rs2612091. (C) Graph of the association of OS and rs2741171. *TYMS*, thymidylate synthetase; *ENOSF1*, enolase superfamily member 1.

**Table 5.** Correlation between *TYMS* and *ENOSF1* expression and the examined genotypes

Variant	Genotype	<i>ENOSF1</i> expression, n (%)		p-value
		Low	High	
5'-UTR- <i>TYMS</i> VNTR	2R2R	25 (100)	0	<.001 <sup>a</sup>
	2R3R	36 (66.7)	18 (33.3)	
	3R3R	0	21 (21)	
<i>ENOSF1</i> rs2612091	GG	17 (73.9)	6 (26.1)	.160
	AG	36 (75.0)	12 (25.0)	
	AA	16 (25.2)	13 (44.8)	
<i>ENOSF1</i> rs2741171	GG	36 (75.0)	12 (25.0)	.310
	AG	21 (58.3)	15 (41.7)	
	AA	12 (75.0)	4 (25.0)	

*TYMS*, thymidylate synthetase; *ENOSF1*, enolase superfamily member 1; 5'-UTR, 5' untranslated region; VNTR, variable number tandem repeat.  
<sup>a</sup>There was a significant relationship between *TYMS* gene expression and the VNTR variant ( $p < .001$ ). The 2R2R genotype of the VNTR *TYMS* variant was associated with low *TYMS* expression, and the 3R3R genotype of the VNTR *TYMS* variant was associated with high *TYMS* expression. There was no significant association between *ENOSF1* expression and the investigated genotypes.

more, no significant association was detected between *TYMS* or *ENOSF1* gene expression and mortality risk (Table 6, Fig. 2).

As shown in Table 7, there was an adverse significant association between *TYMS* and *ENOSF1* gene expression ( $p = .001$ ; odds ratio, 5.95; 95% confidence interval, 2.36 to 15.01), as sample tissues with overexpression of the *TYMS* gene showed reduced expression of the *ENOSF1* gene in tumor tissues.

## DISCUSSION

Genetic variants have a critical impact on gene expression in anti-tumor drug reactions, with a particular emphasis on FPs and their impact on gastric cancer [10,13,23-25].

TS, a key target of FPs, plays a crucial role in DNA synthesis and repair. Variations in the *TYMS* gene encoding the TS protein are linked with survival rates and toxicity levels in patients treated with 5-FU chemotherapy [26,27]. The *ENOSF1* gene, closely related to and overlapping the *TYMS*, has also been

**Table 6.** Mean survival time and HR of patients according to *TYMS* and *ENOSF1* gene expression

Gene	Variant expression	Survival time (mo)		HR (95% CI)	p-value
		Mean (95% CI)	p-value		
<i>TYMS</i>	Low	1.553 (0.828–2.908)	.218	0.633 (0.344–1.167)	.165
	High	0.644 (0.343–1.207)			
<i>ENOSF1</i>	Low	1.063 (0.540–2.087)	.810	1.353 (0.601–3.042)	.464
	High	0.941 (0.479–1.849)			

No significant relationship was observed between expression of these genes and the survival time of patients ( $p = .218$  and  $p = .810$ , respectively). HR, hazard ratio; *TYMS*, thymidylate synthetase; *ENOSF1*, enolase superfamily member 1; CI, confidence interval.

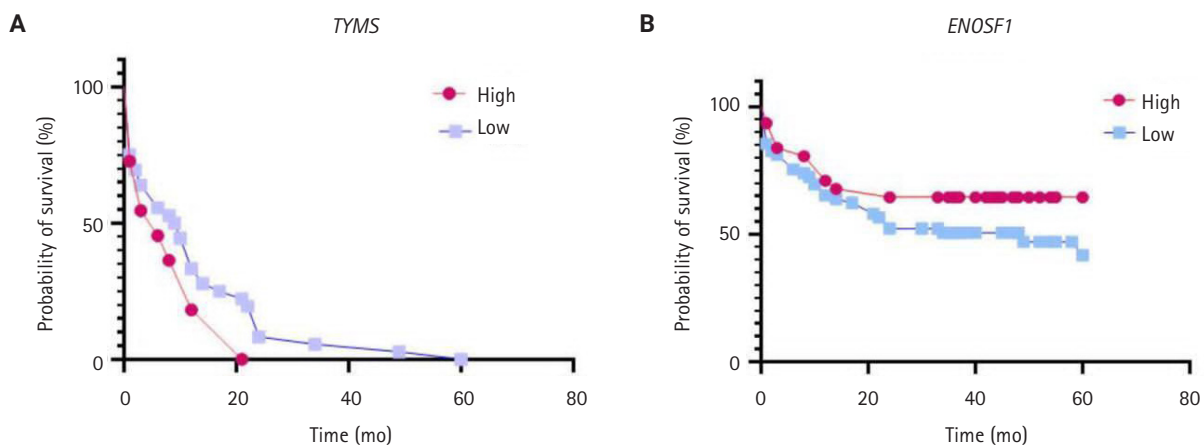


**Fig. 2.** Survival time analysis of gastric cancer patients after 5-fluorouracil treatment according to change in thymidylate synthetase (*TYMS*) gene expression. (A) Survival and gene expression graph of *TYMS*. (B) Survival and gene expression graph of enolase superfamily member 1 (*ENOSF1*). There was no correlation between expression changes of *TYMS* and *ENOSF1* genes and overall survival ( $p = .218$ ,  $p = .810$ ).

**Table 7.** Relationship between *TYMS* and *ENOSF1* expression

	OR	95% CI for OR		p-value
		Lower	Upper	
<i>ENOSF1</i>	5.95	2.36	15.01	<.001

Data analysis showed increased expression of *TYMS* with decreased expression of *ENOSF1* in tumor tissues.

*TYMS*, thymidylate synthetase; *ENOSF1*, enolase superfamily member 1; OR, odds ratio; CI, confidence interval.

identified as a potential factor in chemotherapy resistance, especially in 5-FU treatment [28,29]. This study meticulously investigated the 28-bp VNTR in the 5'-UTR of *TYMS*, along with the rs2612091 and rs2741171 variants in *ENOSF1*, in 100 gastric cancer patients undergoing 5-FU-based neoadjuvant chemotherapy. In addition, *TYMS* and *ENOSF1* gene expression was measured on matched tumor and normal tissue samples.

A significant association was found between the *TYMS* 28-bp VNTR variant and neoadjuvant chemotherapy response ( $p = .032$ ). The 2R3R genotype was more common in patients responding well to treatment than was the 3R3R genotype. In gastric cancer, *TYMS* overexpression has been detected in association with reduced 5-FU efficacy [11]. In addition, the 3R3R genotype is associated with *TYMS* overexpression and a poor response to 5-FU [11,30]. Similar patterns were observed in rectal cancer, where the 2R3R genotype is associated with better treatment outcomes [31]. In contrast, the 2R2R genotype may indicate a higher toxicity risk with FP treatment [8,11,15,26,32].

We also found a relationship between heightened toxicity and improved response to treatment in patients possessing the 2R2R genotype. Although the connection between the *TYMS* gene variant and treatment effectiveness is well-established, its association with survival time is uncertain. A previous study has reported significant disparity in survival time following 5-FU treatment between patients with the 3R3R and 2R2R genotypes ( $p = .003$ ). However, other studies have reported that patients with the 3R2R genotype have a longer survival time than those with the 3R3R and 2R2R genotypes [33], with similar findings observed in lung cancer [34]. Nevertheless, some research did not identify noteworthy variations in survival time linked to *TYMS* 5'-UTR variants [32,34-38]. A significant relationship has been established between *TYMS* gene expression and the 28-bp VNTR variant ( $p < .001$ ). The 2R2R genotype is associated with reduced *TYMS* expression, while the 3R3R genotype is linked to increased expression. This indicates the interaction between *TYMS* gene expression and VNTR alleles [11,32,39,40],

emphasizing the predictive role of the 3R allele in intratumoral *TYMS* expression and 5-FU response. Patients with the 2R2R genotype, exhibiting lower levels of *TYMS* mRNA, tend to demonstrate a more favorable response to 5-FU [39]. However, reduced *TYMS* expression in normal tissues, particularly in lung and gastrointestinal cancers, increases the risk of 5-FU toxicity [11,32,40]. Nonetheless, the correlation between the 28-bp VNTR and *TYMS* expression remained inconclusive in certain studies [11,23,41]. Rosmarin et al. [17] underscored the influence of *ENOSF1* on cell sensitivity to FPs, where the *ENOSF1* rs2612091 G/G genotype in colorectal cancer is linked to shorter survival. That investigation also assessed the impact of the *ENOSF1* rs2612091 variant on survival in advanced gastric cancer, indicating poorer outcomes with each additional G allele [42]. Furthermore, the G allele has been associated with increased capecitabine-related toxicity [17]. Different studies have explored adverse reactions to capecitabine, yielding mixed findings of the significance of these associations [9,28,43]. The involvement of the *ENOSF1* c.742-227G>A variant in the development of FP-dependent HFS has also been acknowledged [44]. Palles et al. [45] have suggested modifying HFS management based on rs2612091 testing. The research has revealed a notable correlation between rs2612091 genotypes and the efficacy of 5-FU-based therapies ( $p = .017$ ), with a greater frequency of non-responsiveness in individuals carrying the AG genotype. Nonetheless, the variance in survival duration following 5-FU treatment among genotypes was not significant ( $p = .170$ ).

The rs2741171 variant downstream of *TYMS* and within *ENOSF1* has shown no significant association with treatment response, patient survival, or *ENOSF1* expression. Yang et al. reported that gastric cancer tumors exhibited twice the *ENOSF1* expression levels of controls, identifying two peptide regions as potential diagnostic biomarkers [46,47]. In the present study, no substantial relationship was observed between the expression of *ENOSF1* and either the response to treatment or the mean survival duration ( $p = .810$ ).

Furthermore, the Cox model did not reveal a significant risk for mortality based on *ENOSF1* expression levels. Previous research has supported the notion that *ENOSF1* overexpression, functioning as a reverse *TYMS*, reduces *TYMS* expression through antisense RNA production and rTS- $\beta$  protein synthesis to influence *TYMS* activity at post-transcriptional and post-translational levels [48,49].

In summary, we revealed a substantial association between the 28-bp *TYMS* VNTR and *TYMS* gene expression in the effi-

cacy of neoadjuvant chemotherapy employing 5-FU in patients with gastric cancer. Those harboring the 2R3R genotype of *TYMS* showed superior treatment outcomes. Conversely, individuals bearing the 3R3R genotype showed elevated *TYMS* gene expression when juxtaposed with their counterparts possessing the 2R2R genotype. Nevertheless, an augmented response was discerned among subjects exhibiting a mixture of 3R and 2R alleles. This implies that the complex interaction between these two genetic repeats may be an unrecognized determinant influencing the response to 5-FU in the cohort under investigation. These findings suggest the need for analysis of interactions of other *TYMS* genetic variations with the 28-bp VNTR.

In addition, individuals with the AG genotype of the rs2612091 variant displayed a weaker response to neoadjuvant chemotherapy. However, this genetic variant did not demonstrate a significant correlation with overall survival rate or the expression level of the *ENOSF1* gene.

The rs2741171 variant showed no apparent correlation with survival rate, neoadjuvant chemotherapy efficacy, or gene expression pattern in patients with gastric cancer. However, several limitations in this study should be considered. One major limitation is that a multivariate analysis was not performed but is crucial to adjust for confounding variables, such as age, sex, and other clinical factors, which may independently influence the outcomes. Without this analysis, it is difficult to assess the true relationships between the genetic variants and neoadjuvant chemotherapy response.

Additionally, the sample size in our study was relatively small, which can limit the statistical power and increase the risk of type II errors, and real associations might not be detected. Another limitation is that the study focused on a specific patient population, which may limit the generalizability of the findings to broader or more diverse groups. Moreover, environmental and lifestyle factors that were not considered may have impacted the observed outcomes. Therefore, future studies should include larger and more diverse populations, perform multivariate analyses, and consider additional factors such as gene-environment interactions to provide a more comprehensive understanding of the role of *TYMS* and *ENOSF1* genetic variants in neoadjuvant chemotherapy response.

### Ethics Statement

This study was approved by the ethics committee (ID IR.IAU.SRB.REC.1397.110 on October 23, 2017). A consent form was obtained from patients before using their samples in this study.

### Availability of Data and Material

The datasets generated or analyzed during the study are available from the corresponding author on reasonable request.

### Code Availability

Not applicable.

### ORCID

Khadijeh Arjmandi <https://orcid.org/0009-0006-8003-9475>  
 Iman Salahshourifar <https://orcid.org/0000-0001-9987-1188>  
 Shiva Irani <https://orcid.org/0000-0002-4202-9931>  
 Fereshteh Ameli <https://orcid.org/0000-0003-1965-9035>  
 Mohsen Esfandbod <https://orcid.org/0000-0002-6497-2306>

### Author Contributions

Conceptualization: KA, IS, SI, FA, ME. Data curation: KA, IS, SI, FA, ME. Formal analysis: KA, IS, SI, FA, ME. Writing—original draft: KA. Writing—review & editing: KA, IS, SI, FA, ME. Approval of final manuscript: all authors.

### Conflicts of Interest

The authors declare that they have no potential conflicts of interest.

### Funding Statement

No funding to declare.

## REFERENCES

- Ilic M, Ilic I. Epidemiology of stomach cancer. *World J Gastroenterol* 2022; 28: 1187-203.
- Sung H, Ferlay J, Siegel RL, et al. Global cancer statistics 2020: GLOBOCAN estimates of incidence and mortality worldwide for 36 cancers in 185 countries. *CA Cancer J Clin* 2021; 71: 209-49.
- Joshi SS, Badgwell BD. Current treatment and recent progress in gastric cancer. *CA Cancer J Clin* 2021; 71: 264-79.
- Shi WJ, Gao JB. Molecular mechanisms of chemoresistance in gastric cancer. *World J Gastrointest Oncol* 2016; 8: 673-81.
- Biagioni A, Staderini F, Peri S, et al. 5-Fluorouracil conversion pathway mutations in gastric cancer. *Biology (Basel)* 2020; 9: 265.
- De Mattia E, Roncato R, Palazzari E, Toffoli G, Cecchin E. Germline and somatic pharmacogenomics to refine rectal cancer patients selection for neo-adjuvant chemoradiotherapy. *Front Pharmacol* 2020; 11: 897.
- Hernando-Cubero J, Matos-Garcia I, Alonso-Orduna V, Cap-

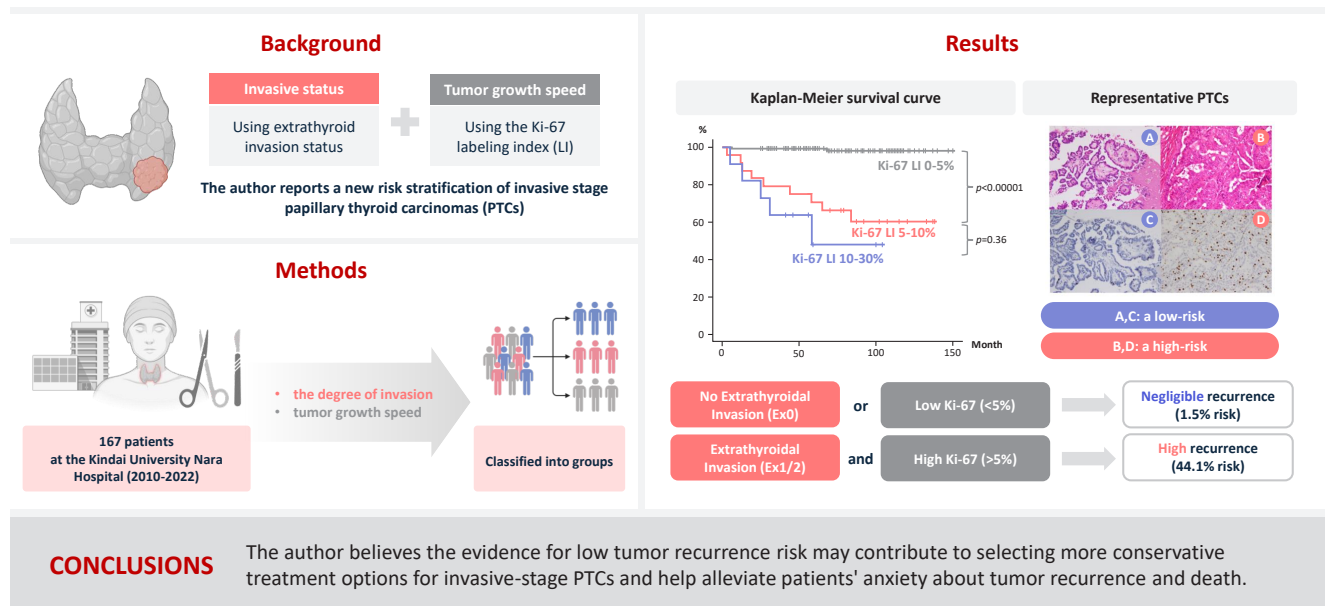
- devila J. The role of fluoropyrimidines in gastrointestinal tumours: from the bench to the bed. *J Gastrointest Cancer* 2017; 48: 135-47.
8. Castro-Rojas CA, Esparza-Mota AR, Hernandez-Cabrera F, et al. Thymidylate synthase gene variants as predictors of clinical response and toxicity to fluoropyrimidine-based chemotherapy for colorectal cancer. *Drug Metab Pers Ther* 2017; 32: 209-18.
  9. De Mattia E, Roncato R, Dalle Fratte C, Ecça F, Toffoli G, Cecchin E. The use of pharmacogenetics to increase the safety of colorectal cancer patients treated with fluoropyrimidines. *Cancer Drug Resist* 2019; 2: 116-30.
  10. Ab Mutalib NS, Md Yusof NF, Abdul SN, Jamal R. Pharmacogenomics DNA biomarkers in colorectal cancer: Current Update. *Front Pharmacol* 2017; 8: 736.
  11. Romiti A, Roberto M, D'Antonio C, et al. The TYMS-TSER polymorphism is associated with toxicity of low-dose capecitabine in patients with advanced gastrointestinal cancer. *Anticancer Drugs* 2016; 27: 1044-9.
  12. Vazquez C, Orlova M, Angriman F, et al. Prediction of severe toxicity in adult patients under treatment with 5-fluorouracil: a prospective cohort study. *Anticancer Drugs* 2017; 28: 1039-46.
  13. Matsusaka S, Lenz HJ. Pharmacogenomics of fluorouracil-based chemotherapy toxicity. *Expert Opin Drug Metab Toxicol* 2015; 11: 811-21.
  14. Lima A, Azevedo R, Sousa H, Seabra V, Medeiros R. Current approaches for TYMS polymorphisms and their importance in molecular epidemiology and pharmacogenetics. *Pharmacogenomics* 2013; 14: 1337-51.
  15. Gallegos-Arreola MP, Zuniga-Gonzalez GM, Sanchez-Lopez JY, et al. TYMS 2R3R polymorphism and DPYD [IVS]14+1G>A gene mutation in Mexican colorectal cancer patients. *Acta Biochim Pol* 2018; 65: 227-34.
  16. Meulendijks D, Rozeman EA, Cats A, et al. Pharmacogenetic variants associated with outcome in patients with advanced gastric cancer treated with fluoropyrimidine and platinum-based triplet combinations: a pooled analysis of three prospective studies. *Pharmacogenomics J* 2017; 17: 441-51.
  17. Rosmarin D, Palles C, Pagnamenta A, et al. A candidate gene study of capecitabine-related toxicity in colorectal cancer identifies new toxicity variants at DPYD and a putative role for ENOSF1 rather than TYMS. *Gut* 2015; 64: 111-20.
  18. Liang P, Nair JR, Song L, McGuire JJ, Dolnick BJ. Comparative genomic analysis reveals a novel mitochondrial isoform of human rTS protein and unusual phylogenetic distribution of the rTS gene. *BMC Genomics* 2005; 6: 125.
  19. Dolnick BJ, Angelino NJ, Dolnick R, Sufrin JR. A novel function for the rTS gene. *Cancer Biol Ther* 2003; 2: 364-9.
  20. Shi C, Berlin J, Branton P, et al. Protocol for the examination of specimens from patients with carcinoma of the stomach. Northfield: College of American Pathologists, 2020.
  21. Mandola MV, Stoehlmacher J, Muller-Weeks S, et al. A novel single nucleotide polymorphism within the 5' tandem repeat polymorphism of the thymidylate synthase gene abolishes USF-1 binding and alters transcriptional activity. *Cancer Res* 2003; 63: 2898-904.
  22. Jiang H, Li B, Wang F, Ma C, Hao T. Expression of ERCC1 and TYMS in colorectal cancer patients and the predictive value of chemotherapy efficacy. *Oncol Lett* 2019; 18: 1157-62.
  23. Shitara K, Muro K, Ito S, et al. Folate intake along with genetic polymorphisms in methylenetetrahydrofolate reductase and thymidylate synthase in patients with advanced gastric cancer. *Cancer Epidemiol Biomarkers Prev* 2010; 19: 1311-9.
  24. Li SC, Ma R, Wu JZ, et al. Delineation of gastric cancer subtypes by co-regulated expression of receptor tyrosine kinases and chemosensitivity genes. *Am J Transl Res* 2015; 7: 1429-39.
  25. Meulendijks D, Jacobs BA, Aliev A, et al. Increased risk of severe fluoropyrimidine-associated toxicity in patients carrying a G to C substitution in the first 28-bp tandem repeat of the thymidylate synthase 2R allele. *Int J Cancer* 2016; 138: 245-53.
  26. Smyth E, Zhang S, Cunningham D, et al. Pharmacogenetic analysis of the UK MRC (Medical Research Council) MAGIC Trial: association of polymorphisms with toxicity and survival in patients treated with perioperative epirubicin, cisplatin, and 5-fluorouracil (ECF) chemotherapy. *Clin Cancer Res* 2017; 23: 7543-9.
  27. Wu J, Li S, Ma R, et al. Tumor profiling of co-regulated receptor tyrosine kinase and chemoresistant genes reveal different targeting options for lung and gastroesophageal cancers. *Am J Transl Res* 2016; 8: 5729-40.
  28. Garcia-Gonzalez X, Cortejoso L, Garcia MI, et al. Variants in CDA and ABCB1 are predictors of capecitabine-related adverse reactions in colorectal cancer. *Oncotarget* 2015; 6: 6422-30.
  29. Garcia-Gonzalez X, Lopez-Fernandez LA. Using pharmacogenetics to prevent severe adverse reactions to capecitabine. *Pharmacogenomics* 2017; 18: 1199-213.
  30. Kawakami K, Graziano F, Watanabe G, et al. Prognostic role of thymidylate synthase polymorphisms in gastric cancer patients treated with surgery and adjuvant chemotherapy. *Clin Cancer Res* 2005; 11: 3778-83.
  31. Yang YC, Wu GC, Jin L, et al. Association of thymidylate synthase polymorphisms with the tumor response to preoperative chemo-

- radiotherapy in rectal cancer: a systematic review and meta-analysis. *Pharmacogenomics J* 2017; 17: 265-73.
32. Lecomte T, Ferraz JM, Zinzindohoue F, et al. Thymidylate synthase gene polymorphism predicts toxicity in colorectal cancer patients receiving 5-fluorouracil-based chemotherapy. *Clin Cancer Res* 2004; 10: 5880-8.
  33. Chen J, Ying X, Zhang L, Xiang X, Xiong J. Influence of TS and ABCB1 gene polymorphisms on survival outcomes of 5-FU-based chemotherapy in a Chinese population of advanced gastric cancer patients. *Wien Klin Wochenschr* 2017; 129: 420-6.
  34. Arevalo E, Castanon E, Lopez I, et al. Thymidylate synthase polymorphisms in genomic DNA as clinical outcome predictors in a European population of advanced non-small cell lung cancer patients receiving pemetrexed. *J Transl Med* 2014; 12: 98.
  35. Gao J, He Q, Hua D, Mao Y, Li Y, Shen L. Polymorphism of TS 3'-UTR predicts survival of Chinese advanced gastric cancer patients receiving first-line capecitabine plus paclitaxel. *Clin Transl Oncol* 2013; 15: 619-25.
  36. Gusella M, Frigo AC, Bolzonella C, et al. Predictors of survival and toxicity in patients on adjuvant therapy with 5-fluorouracil for colorectal cancer. *Br J Cancer* 2009; 100: 1549-57.
  37. Martinez-Balibrea E, Abad A, Martinez-Cardus A, et al. UGT1A and TYMS genetic variants predict toxicity and response of colorectal cancer patients treated with first-line irinotecan and fluorouracil combination therapy. *Br J Cancer* 2010; 103: 581-9.
  38. Seo BG, Kwon HC, Oh SY, et al. Comprehensive analysis of excision repair complementation group 1, glutathione S-transferase, thymidylate synthase and uridine diphosphate glucuronosyl transferase 1A1 polymorphisms predictive for treatment outcome in patients with advanced gastric cancer treated with FOLFOX or FOLFIRI. *Oncol Rep* 2009; 22: 127-36.
  39. Pullarkat ST, Stoehlmacher J, Ghaderi V, et al. Thymidylate synthase gene polymorphism determines response and toxicity of 5-FU chemotherapy. *Pharmacogenomics J* 2001; 1: 65-70.
  40. Shintani Y, Ohta M, Hirabayashi H, et al. New prognostic indicator for non-small-cell lung cancer; quantitation of thymidylate synthase by real-time reverse transcription polymerase chain reaction. *Int J Cancer* 2003; 104: 790-5.
  41. Lima A, Seabra V, Martins S, Coelho A, Araujo A, Medeiros R. Thymidylate synthase polymorphisms are associated to therapeutic outcome of advanced non-small cell lung cancer patients treated with platinum-based chemotherapy. *Mol Biol Rep* 2014; 41: 3349-57.
  42. Taddia L, D'Arca D, Ferrari S, et al. Inside the biochemical pathways of thymidylate synthase perturbed by anticancer drugs: novel strategies to overcome cancer chemoresistance. *Drug Resist Updat* 2015; 23: 20-54.
  43. Lam SW, Guchelaar HJ, Boven E. The role of pharmacogenetics in capecitabine efficacy and toxicity. *Cancer Treat Rev* 2016; 50: 9-22.
  44. Hamzic S, Kummer D, Froehlich TK, et al. Evaluating the role of ENOSF1 and TYMS variants as predictors in fluoropyrimidine-related toxicities: an IPD meta-analysis. *Pharmacol Res* 2020; 152: 104594.
  45. Palles C, Fotheringham S, Chegwidzen L, et al. An evaluation of the diagnostic accuracy of a panel of variants in DPYD and a single variant in ENOSF1 for predicting common capecitabine related toxicities. *Cancers (Basel)* 2021; 13: 1497.
  46. He QY, Cheung YH, Leung SY, Yuen ST, Chu KM, Chiu JF. Diverse proteomic alterations in gastric adenocarcinoma. *Proteomics* 2004; 4: 3276-87.
  47. Yang J, Xiong X, Wang X, Guo B, He K, Huang C. Identification of peptide regions of SERPINA1 and ENOSF1 and their protein expression as potential serum biomarkers for gastric cancer. *Tumour Biol* 2015; 36: 5109-18.
  48. Dolnick BJ. The rTS signaling pathway as a target for drug development. *Clin Colorectal Cancer* 2005; 5: 57-60.
  49. Chu E, Koeller DM, Casey JL, et al. Autoregulation of human thymidylate synthase messenger RNA translation by thymidylate synthase. *Proc Natl Acad Sci U S A* 1991; 88: 8977-81.

# Low Ki-67 labeling index is a clinically useful predictive factor for recurrence-free survival in patients with papillary thyroid carcinoma

Takashi Masui<sup>1</sup>, Katsunari Yane<sup>1</sup>, Ichiro Ota<sup>1</sup>, Kennichi Kakudo<sup>2,3</sup>, Tomoko Wakasa<sup>2</sup>, Satoru Koike<sup>1</sup>, Hirotaka Kinugawa<sup>1</sup>, Ryuji Yasumatsu<sup>4</sup>, Tadashi Kitahara<sup>5</sup>

## Graphical abstract



# Low Ki-67 labeling index is a clinically useful predictive factor for recurrence-free survival in patients with papillary thyroid carcinoma

Takashi Masui<sup>1</sup>, Katsunari Yane<sup>1</sup>, Ichiro Ota<sup>1</sup>, Kennichi Kakudo<sup>2,3</sup>, Tomoko Wakasa<sup>2</sup>, Satoru Koike<sup>1</sup>, Hiroataka Kinugawa<sup>1</sup>, Ryuji Yasumatsu<sup>4</sup>, Tadashi Kitahara<sup>5</sup>

<sup>1</sup>Department of Otolaryngology-Head and Neck Surgery, Kindai University Nara Hospital, Ikoma, Japan

<sup>2</sup>Department of Diagnostic Pathology, Kindai University Nara Hospital, Ikoma, Japan

<sup>3</sup>Department of Pathology and Thyroid Disease Center, Izumi City General Hospital, Izumi, Japan

<sup>4</sup>Department of Otolaryngology-Head and Neck Surgery, Kindai University, Osakasayama, Japan

<sup>5</sup>Department of Otolaryngology-Head and Neck Surgery, Nara Medical University, Kashihara, Japan

**Background:** We report a new risk stratification of invasive stage papillary thyroid carcinomas (PTCs) by combining invasive status, using extrathyroid invasion (Ex) status, and tumor growth speed using the Ki-67 labeling index (LI). **Methods:** We examined tumor recurrence in 167 patients with PTC who were surgically treated at the Kindai University Nara Hospital between 2010 and 2022. The patients were classified according to the degree of invasion [negative (Ex0) or positive (Ex1, Ex2, and Ex3)] and tumor growth speed expressed with Ki-67 LI, as low (<5%) or high (≥5%). This study confirmed previous findings that the disease-free survival (DFS) rate in PTCs significantly differed between patients with a high and low Ki-67 index. **Results:** When combining Ex status (negative or positive) and Ki-67 proliferation status (low or high), the DFS rate of invasion in the negative, low Ki-67 LI group was only 1.1%, while that of invasion in the positive, high Ki-67 LI was 44.1%. This study reports for the first time that recurrence risks can be stratified accurately when combining carcinoma's essential two features of extrathyroid invasion status and tumor growth speed. **Conclusions:** We believe the evidence for low tumor recurrence risk may contribute to use of more conservative treatment options for invasive-stage PTCs and help alleviate patient anxiety about tumor recurrence and death.

**Keywords:** Thyroid cancer, papillary; Recurrence-free survival; Ki-67 labeling index; Extracapsular invasion; Lymphatic metastasis

## INTRODUCTION

Papillary thyroid carcinoma (PTC) usually has an indolent nature with a very slow rate of tumor growth, even though it often (7%–23%) involves cervical lymph node metastases [1-4]. Due to this evidence, a choice of surgery or clinical follow-up of patients with early invasive PTC can be challenging for endocrinologists and endocrine surgeons. Clinical factors such as age, sex, and tumor size and histopathologic parameters such as extrathyroidal invasion, lympho-vascular invasion, and lateral cervical lymph node metastasis are predictive factors for PTC

recurrence [5-7]. However, those clinical parameters do not distinguish PTC, and a number of cases with these characteristics does not develop recurrence. Simultaneously, a number of patients without these characteristics can present with locoregional recurrence. Thus, more accurate risk stratification of PTC is needed for proper postoperative follow-up strategy to reduce unnecessary surgery. The 2015 American Thyroid Association (ATA) published management guidelines regarding estimated risk of structural disease recurrence in patients without structurally identifiable disease after initial therapy into low-risk, intermediate-risk, and high-risk [8]. However,

**Received:** September 28, 2024 **Revised:** November 7, 2024 **Accepted:** November 8, 2024

**Corresponding Author:** Takashi Masui, MD, PhD

Department of Otolaryngology-Head and Neck Surgery, Kindai University Nara Hospital, 1248-1 Otoda-cho, Ikoma, Nara 630-0293, Japan

Tel: +81-743-77-0880, FAX: +81-743-77-0902, E-mail: 1813a5@med.kindai.ac.jp

This is an Open Access article distributed under the terms of the Creative Commons Attribution Non-Commercial License (<https://creativecommons.org/licenses/by-nc/4.0/>) which permits unrestricted non-commercial use, distribution, and reproduction in any medium, provided the original work is properly cited.

© 2025 The Korean Society of Pathologists/The Korean Society for Cytopathology

more than 10 parameters were used in this risk stratification, included more than 10 independent features seen in PTCs, including (1) gross extrathyroidal extension (Ex2/3), (2) incomplete tumor resection, (3) distant metastasis or (4) lymph node metastasis more than 3 cm in size for ATA high-risk for disease recurrence, (5) aggressive histological subtypes of PTC, (6) minor extrathyroidal extension (Ex1), (7) vascular invasion, or (8) more than five involved lymph nodes (2–30 mm in size) for ATA intermediate-risk for recurrence, and (9) intrathyroidal differentiated thyroid carcinomas (Ex0) or (10) less than five involved lymph node micrometastasis (<2 mm) for ATA low-risk for recurrence, in addition to encapsulation, multifocality, *TERT* promoter mutation, and *BRAFV600E* mutation. Thus, we believe that outcome prediction of well-differentiated thyroid carcinomas (PTC, follicular subtype PTC, oncocytic thyroid carcinoma and follicular thyroid carcinoma) using only one of these clinicopathological parameters is not reliable. Although all 14 variables are useful prognostic and predictive factors, this ATA risk stratification for structural disease recurrence is complicated and not perfect in real-world practice. Although a small fraction of ATA low-risk and intermediate-risk patients develop tumor recurrence, most patients and clinicians choose treatment with total thyroidectomy (TTX) just in case. This results in significant overtreatment of low-risk small PTCs. More than 80% of small (less than 20 mm) PTCs in the United States in 2014 were treated with TTX [9], and more than 40% of PTCs eligible for lobectomy in two North American institutes in 2019 were treated with TTX [10]. These findings underscore the need for carefully consideration in medical treatment policies for this subgroup.

The Ki-67 labeling index (LI) is a well-established method in pathology practice in a variety of malignancies including medullary thyroid carcinoma [11–13] but rarely is used for clinical prognostic risk stratification of PTC. We report a new method to predict risk of tumor recurrence in invasive PTC by combining invasion status, positive or negative extrathyroid extension, and tumor growth rate (high or low using the Ki-67 LI).

Staining for Ki-67 is routinely conducted for neuroendocrine tumors, breast carcinomas, malignant lymphomas, brain tumors, and sarcoma [14–16]. However, the Ki-67 LI does not play a diagnostic role in other organs, and its prognostic value remains a controversial issue [17].

The grade of extrathyroid invasion (Ex0, Ex1, Ex2, and Ex3) is a well-known prognostic and predictive factor in PTCs and constitutes a significant component in TNM stage category [18]

and other prognostic categories [19] such as AGES [20] and MACIS [21]. As some studies demonstrated that the Ki-67 LI alone has promising results in predicting recurrence-free survival rates [6,22,23] and cause-specific survival rates of PTCs regardless of TNM stage, the present study examined Ki-67 LI combined with invasion capacity (extrathyroid extension as Ex0, Ex1, Ex2, or Ex3) in 167 cases of curatively treated PTCs in a single tertiary hospital in Japan. This is the first study to successfully demonstrate prognostic and predictive values of Ki-67 LI after risk stratification based on a combination of invasive capacity and Ex category.

## MATERIALS AND METHODS

### Patients and our protocol

The demographic characteristics, TN category, and stage of the 167 patients are detailed in Tables 1 and 2 [18]. Between 2010 and 2022, 167 patients with PTC underwent either lobectomy (113 cases, 67.7%) or TTX (54 cases, 32.3%) (Table 2), with or without paratracheal and lateral cervical lymph node dissection, at Kindai University Nara Hospital. Patients that were excluded included those with distant metastasis diagnosed by computed tomography (CT) at initial presentation, severe calcification or bone formation unsuitable for sensitive Ki-67 immunohistochemistry, benign lesions, malignant lymphoma, follicular variant papillary carcinoma, oncocytic carcinoma, follicular carcinoma, medullary carcinoma, poorly differentiated carcinoma, high-grade differentiated carcinoma, anaplastic carcinoma including anaplastic transformation, and incidental

**Table 1.** T and N categories and stages of 167 patients with papillary thyroid carcinoma according to the American Joint Committee on Cancer (8th edition)

	< 55 years old		≥ 55 years old	
	N category 0	N category 1	N category 0	N category 1
T category				
1a	10	6	23	4
1b	3	8	10	6
2	4	10	3	1
3	7	20	8	26
4	1	4	0	13
Stage				
I	73		36	
II	0		45	
III	-		13	

**Table 2.** Comparison of patient characteristics using univariate analysis by log-rank test for disease-free survival

Characteristic	Total patients	Patients with recurrence (n = 19)	Patients without recurrence (n = 154)	Univariate analysis by log-rank test, p-value
Age (yr)				.254
≤55	78	6	72	
>55	89	11	78	
Sex				.023
Male	31	6	25	
Female	136	11	125	
Tumor diameter (mm)				<.001
>20	57	14	43	
≤20	110	3	107	
Lympho-vascular invasion				.059
Yes	17	4	13	
No	150	13	137	
Extrathyroidal invasion				<.001
Yes	78	16	62	
No	89	1	88	
Lateral cervical lymph node metastasis				.233
Yes	39	6	33	
No	128	11	117	
Ki-67 LI				<.001
>5%	35	15	20	
≤5%	132	2	130	
Surgical methods <sup>a</sup>				
Lobectomy	113			
Total thyroidectomy	54			
Recurrence case	17			
Local	3			
Cervical lymph node	11			
Lung	9			
Liver	1			
Skin	1			
Outcome				
Alive and well	160			
Cancer-bearing survival	5			
Cause-specific death	2			
Observation period (mo)	13–144 (median, 77)			

LI, labeling index.

<sup>a</sup>Duplicate counted if there are more than 2.

carcinoma. Additionally, cases in which patient consent was not obtained for publication were excluded.

### Surgical treatment strategies for patients with PTC at the Kindai University Nara Hospital

We recommend TTX for patients younger than 70 years with high-risk clinical features (tumors > 40 mm, metastatic lymph

nodes > 30 mm, gross Ex2 and 3, or metastatic lymph nodes in the lateral cervical region). In contrast, lobectomy is generally recommended in patients younger than 70 years without high-risk clinical features and in patients older than 70 years of age. Lymph node dissection in the central (paratracheal) compartment is usually performed including the lateral compartment if nodal metastatic disease is clinically suspected. Radioisotope

therapy (30 mCi) is mainly administered to high-risk patients < 70 years of age who have undergone TTX and to patients > 70 years of age with  $^{131}\text{I}$  uptake in distant metastases.

### Thyroid nodule practice at the Kindai University Nara Hospital

Fine-needle aspiration cytology was used to diagnose PTC and facilitate the preoperative evaluation. We conducted thyroid function tests, including thyroglobulin (TG), and performed neck ultrasonography to detect and localize tumor recurrence during the postoperative follow-up. CT was performed annually. Recurrence was defined as the appearance of a new postoperative lesion that was not present prior to the initial radical surgery. After histological confirmation of lymph node metastasis at the second surgery, we usually conducted an image review to identify suspicious nodal lesions before the initial surgery. Recurrence was noted after confirmation of no suspicious nodal disease before the initial surgery. When suspicious

nodal enlargements were present, we excluded those cases from recurrence and classified them as residual diseases curatively treated with a second surgery. Immunohistochemistry was performed using a Histostainer 36 A (Nichirei Biosciences, Tokyo, Japan) according to the manufacturers' instructions (SP6 Anti Ki67 rabbit monoclonal antibody). The Ki-67 LI was calculated by two pathologists (K.K. and T.W.) by manually counting the Ki-67-positive tumor cell nuclei and dividing by the total tumor cell nuclei in the hotspot regions, counting at least 1,000 cells twice each. Ki-67 LI was expressed as the range between the lower and higher values in the percentile. Representative PTCs, low-risk (Fig. 1A, C) and high-risk (Fig. 1B, D) cases are shown (Fig. 1).

First, the 167 patients were divided into Ki-67 LI low-risk (<5%) and moderate (5%–10%)-to-high-proliferation index (10%–30%) groups to examine the differences in recurrence rates. Next, to identify independent prognostic factors for disease-free survival (DFS), univariate analyses were performed

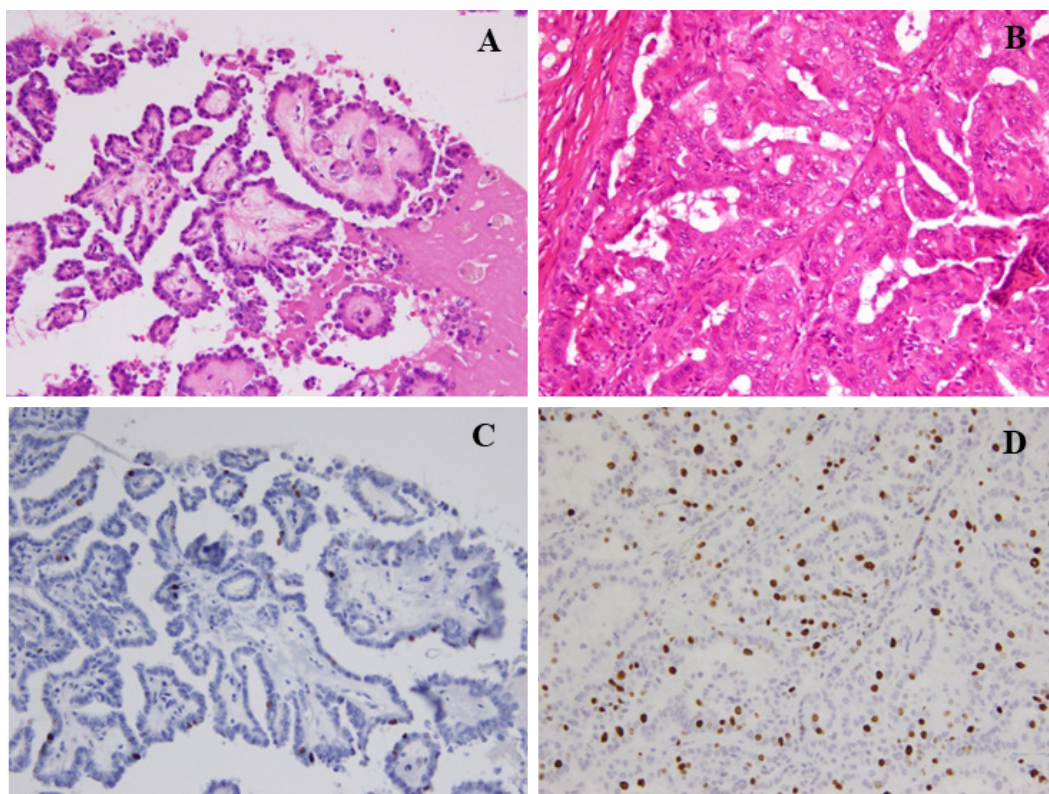


**Fig. 1.** Representative papillary thyroid carcinomas (PTCs) of low-risk (A, C) and high-risk (B, D). (A) A low-risk PTC. Case 01 was disease-free for 80 months after lobectomy. Conventional PTC showing focal micro-papillary and hobnail features. (B) A high-risk PTC with oncocytic features and conventional papillary growth. Case 160 was disease-free for 59 months after total thyroidectomy plus lateral cervical lymph node dissection. (C) The Ki-67 labeling index (LI) of Fig. 1A was 1%. Ki-67 immunohistochemistry with hematoxylin nuclear counter stain. (D) The Ki-67 LI of Fig. 1B was 20%. Ki-67 immunohistochemistry with hematoxylin nuclear counter stain.

for each patient characteristic, and multivariate analyses were performed for factors that differed significantly (Tables 2, 3). The patients were stratified into the following three groups according to the degree of extrathyroid invasiveness (there were no Ex3 cases in this patient series): Ex-group 1, early non-invasive stage (Ex0, anyN, and M0); Ex-group 2, early invasive stage (Ex1, any N, and M0); and Ex-group 3, advanced invasive stage (Ex2 and 3, anyN, and M0). Tested combinations of these two features were examined for tumor recurrence: (1) tumor growth rate as the Ki-67 LI and (2) invasive capacity (Ex-group 1, Ex-group 2, and Ex-group 3) (Table 4).

**Statistical analysis**

All statistical analyses were performed using EZR (Saitama Medical Center, Jichi Medical University, Saitama, Japan), which is a graphical user interface for R (R Foundation for Statistical Computing, Vienna, Austria). The chi-square test and the log-rank test were used for univariate analysis, and the Cox proportional hazards model was used for multivariate analysis. p-values < .05 were considered statistically significant.

**RESULTS**

**Multivariate analysis for DFS**

To identify independent prognostic factors for disease-free survival, univariate analyses were performed for each patient characteristic, and multivariate analyses were performed for factors that differed significantly (Tables 2, 3). Univariate anal-

ysis showed that male, tumor diameter >20 mm, Ex1/2, and Ki-67 LI >5% were the four possible prognostic factors. Therefore, multivariate analysis of these four factors showed that Ki-67 LI >5% was an independent prognostic factor (Tables 2, 3).

**Ki-67 LI and other clinicopathologic factors of recurrence-free survival rate**

In this study, we classified the cases into three groups based on Ex status (Ex-group 1 for Ex0, any N, and M0; Ex-group 2 for Ex1, any N, and M0; and Ex-group 3 for Ex2 and 3, any N and M0) and into three groups based on Ki-67 LI (Ki-67-group 1 for Ki-LI of 0%–5%, Ki-67-group 2 of 5%–10%, and Ki-67-group 3 of 10%–30%) (Table 4). The recurrence rate in Ex-group 1 was 1/89 (1.1%), and the recurrent patients exhibited a Ki-67 <5%; however, only one patient with Ex-group 1 PTC exhibited Ki-67 ≥5%. In contrast, recurrence occurred in 11 of 62 patients (17.7%) in Ex-group 2 and in five of 16 patients (31.3%) in Ex-group 3 PTCs. A statistically significant difference between Ex-

**Table 3.** Multivariate analysis of the risk factors of recurrence of papillary thyroid carcinoma

Variable	Odds ratio	95% CI	p-value
Male sex	2.74	0.94–7.99	.065
Tumor diameter >20 mm	3.15	0.86–11.45	.081
Ex1/2	2.88	0.33–25.24	.339
Ki-67 LI >5%	13.26	2.66–66.12	.002

Ki-67 LI >5% was an independent prognostic factor. CI, confidence interval; Ex, extrathyroid invasion; LI, labeling index.

**Table 4.** Recurrence rates in Ex-group 1, 2, and 3 regardless of Ki-67 LI and recurrence rates in Ki-67-groups 1, 2, and 3 regardless of Ex status

	Total cases	rec+	rec-	p-value
Ex-group 1 (Ex0, any N and M0)	89	1	88	<.001
Ex-group 2 (Ex1, any N and M0)	62	11	51	
Ex-group 1 (Ex0, any N and M0)	89	1	88	<.001
Ex-group 3 (Ex2/3, any N and M0)	16	5	11	
Ex-group 2 (Ex1, any N and M0)	62	11	51	.298
Ex-group 3 (Ex2/3, any N and M0)	16	5	11	
Group 1 (Ki-67 LI >5% and Ex0)	1	0	1	.425
Group 2 (Ki-67 LI >5% and Ex1)	23	10	13	
Group 3 (Ki-67 LI >5% and Ex2/3)	11	5	6	
Ki-67-group 1 (Ki-67 LI <5%)	132	2	130	<.001
Ki-67-group 2 (Ki-67 LI 5%–10%)	24	9	15	
Ki-67-group 3 (Ki-67 LI 10%–30%)	11	6	5	

After combining these two (Ex status and Ki-67 LI of ≥5%) parameters, recurrence (rec) rates were compared. Ex, extrathyroid invasion; LI, labeling index.

group 1 and the other two groups ( $p < .001$ ) (Table 4) was observed. When recurrence was examined only in cases with high ( $\geq 5\%$ ) Ki-67 LI, it was found in zero of 1 (0%) in group 1 (Ki-67 LI  $\geq 5\%$  and Ex0), 10 of 23 (43.5%) in group 2 (Ki-67 LI  $\geq 5\%$  and Ex1), and five of 11 (45.5%) in Group 3 (Ki-67 LI  $\geq 5\%$  and Ex2) (Table 4). As the disease progressed, both the number of cases with Ki-67 LI  $\geq 5\%$  and the recurrence rate increased. However, there were no significant differences ( $p = .425$ ).

As illustrated in the Kaplan-Meier method of Fig. 2, patients were classified based on Ki-67 LI status, Ki-67-group 1 (Ki-LI of 0%–5%), Ki-67-group 2 (Ki-67 LI of 5%–10%), and Ki-67-group 3 (Ki-67 LI of 10%–30%), and their relationship with tumor recurrence was investigated. A higher recurrence rate in the Ki-67-group 2 (37.5%, 9/24 cases,  $p < .001$ ) and Ki-67-group 3 (54.5%, 6/11 cases,  $p < .001$ ) than that of the Ki-67-group 1 (1.5%, 2/132 cases) is shown in the Fig. 2. A statistically significant difference was observed between the Ki-67-group 1 and group 2, and between Ki-67-group 1 and group 3 ( $p < .001$ ), but not between Ki-67-group 2 and group 3 ( $p = .360$ ) (Fig. 2). As there were a small number of cases in this study, we combined Ki-67 LI 5%–10% and 10%–30% groups in one group (Ki-67 LI of  $\geq 5\%$ ) and Ex1 and Ex2 groups in a second group (Ex1 and 2) (Table 5), and the recurrence rates were analyzed. We confirmed the recurrence is rare (1.5%) in cases with  $< 5\%$  Ki-67 LI regardless of Ex status. There was only one case with Ex0 and Ki-67 LI of 10%–30%, and that case did not recur.

There were two cases of tumor death. They were a case of Ex1 and Ki-67 LI 5%–10% and a case of Ex2 and Ki-67 LI 20%–30%. Because of the small number of carcinoma deaths, analysis for cause-specific death was not carried out.

Further studies in larger patient cohorts are necessary to confirm our observation (negligible risk of recurrence in Ki-67

LI of  $< 5\%$  patients regardless of Ex status and in Ex0 patients regardless of Ki-67 LI).

## DISCUSSION

Overdiagnosis and overtreatment of carcinomas, including thyroid carcinoma, are significant issues in healthcare communities worldwide [9,22]. Identifying potential lethal malignancies for radical surgical intervention (TTX) and indolent thyroid carcinomas for more conservative surgery (lobectomy) or non-surgical observation is essential to reducing overdiagnosis and overtreatment of thyroid carcinomas. Several strategies have been proposed for thyroid carcinoma treatment to resolve

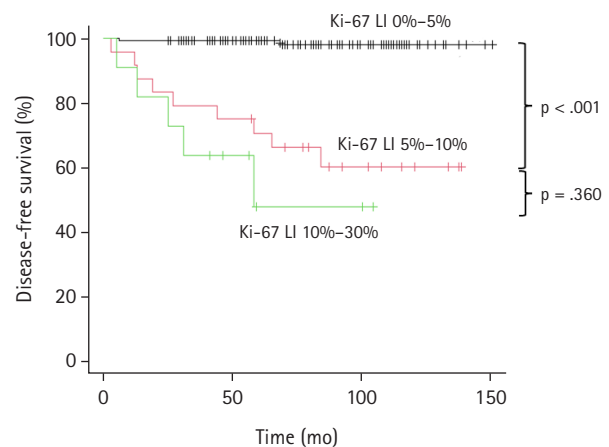


**Fig. 2.** Disease-free survival curves of three groups of 167 total papillary thyroid carcinoma patients classified by Ki-67 labeling index [LI]  $< 5\%$ , 5%–10%, and 10%–30%. The disease-free survival rate of Ki-67 LI  $< 5\%$  is 98.0% at 10 years, that of Ki-67 LI of 5%–10% is 60.2% at 10 years, and that of Ki-67 LI of 10%–30% is 47.7% at 5 years (Kaplan-Meier method).

**Table 5.** Recurrence rates of 167 PTC patients classified by Ex status (Ex0 vs. Ex1 and 2/3) and Ki-67 LI ( $< 5\%$  vs. 5%–30%)

	Ki-67 labeling index		Subtotal
	$< 5\%$	5%–30%	
Ex0	1/88 (1.1)	0/1 (0)	1/89 (1.1)
Ex1 and 2	1/44 (2.3)	15/34 (44.1)	16/78 (20.5)
Subtotal	2/132 (1.5)	15/35 (42.9)	

Values are presented as number (%).

Low-risk: Risk of recurrence is 1.5% (0%–2.3%) 2/132.

High-risk: Risk of recurrence is 44.1% (15/34).

Ex0: no Ex, Ex1: microscopic Ex; Ex2: gross and clinical Ex.

The recurrence rate of 34 patients with both Ki-67 LI 5%–30% and Ex1/2/3 is significantly higher (44.1%) than the other groups (either Ki-67 LI  $< 5\%$  or Ex0) (1.1%) with a median follow-up period of 64 months. Statistically significant differences were observed ( $p < .001$ ).

PTC, papillary thyroid carcinoma; Ex, extrathyroid invasion; LI, labeling index.

these uncertainties: (1) do not include asymptomatic adults in thyroid carcinoma screening [23], (2) do not apply fine-needle aspiration cytology to low-risk small thyroid nodules [24], (3) downgrade low-risk neoplasms from carcinoma category to non-malignant (borderline) tumor category [25], (4) active surveillance (non-surgical option) to low-risk small PTCs [8,26,27], and (5) do not apply TTX and radioactive iodine to low-risk thyroid carcinomas [24]. However, these five strategies did not improve the overtreatment of thyroid carcinomas sufficiently, and a paradoxical phenomenon that early-stage thyroid carcinoma patients can live longer than the general population has been reported [28]. We speculated that there are a significant number of invasive thyroid carcinomas (Ex1 or Ex2) that do not cause disease-specific death as they are not targets of the above five strategies and are still treated with unnecessary aggressive carcinoma surgery (TTX). This study was conducted to identify low-risk carcinomas for recurrence in invasive PTCs, which are almost synonymous with the so-called “very-slow growing carcinoma” defined by Welch and Black [9] to never progress to clinically significant carcinoma. Among 167 surgically treated PTCs in a single institute under a conservative treatment strategy in Japan were few studies focusing on recurrence, comprising 17 (10.2%) cases who developed tumor recurrence with a median of 64 months of follow-up and two cases of cause-specific death (1.2%).

Recurrence rates between Ex-group 1 (Ex0, any N and M0) and 2 (Ex1, any N and M0) were statistically different ( $p < .001$ ), as were those between Ex-group 1 and 3 (Ex2, any N and M0) ( $p < .001$ ). Recurrence rates in Ki-67-groups 1 (<5%), 2 (5%–10%), and 3 (10%–30%) were 1.5% (2/132), 37.5% (9/24), and 54.5% (6/11), respectively (Table 3). When recurrence rates based on Ex status (Ex-groups 1, 2, and 3) were examined in only cases with Ki-67 LI  $\geq 5\%$  (combined Ki-67 LI  $\geq 5\%$  and Ex status), recurrence rates of group 1 (Ex0 and Ki-67 LI  $\geq 5\%$ ), group 2 (Ex1 and Ki-67 LI  $\geq 5\%$ ), and group 3 (Ex2/3 and Ki-67 LI  $\geq 5\%$ ) were 0% (0/1), 43.5% (10/23), and 45.5% (5/11), respectively (Tables 3, 4). There were no significant differences. When combining Ex status into two groups (Ex0 and Ex1/2/3) and Ki-67 proliferation status into two groups (<5% and  $\geq 5\%$ ), the DFS rate of the Ex0 and Ki-67 LI <5% group was only 1.1%, while that of Ex1/2/3 and Ki-67 LI 5%–30% was 44.1% (Table 4). No recurrence was found among patients with Ex0, N0, and Ki-67 LI <5% (data not shown).

Dwivedi et al. [29] analyzed the expression of Ki-67 and observed a greater expression of this marker in PTCs than in

non-neoplastic lesions. Miyauchi et al. [23] found that Ki-67 in PTCs was an independent prognostic factor for disease-free survival. However, most previous studies neglected tumor stage and invasion status (T, N, M, and Ex status). We further incorporated invasive status (Ex0, Ex1, and Ex2/3) into analysis of the Ki-67 proliferation index for tumor recurrence for the first time because both are essential criteria of carcinoma (uncontrolled proliferation and invasion into nearby tissue). This means that a tumor cannot be a biologically malignant progressive lethal carcinoma when either one of the two essential carcinoma criteria is missing or insufficient. This study is the first to successfully show a higher recurrence rate in cases with both high ( $\geq 5\%$ ) Ki-67 LI and Ex 1 or Ex 2/3 invasive status, while there is a negligible risk of recurrence in cases with either one or without these two features (Ex0 [no invasion into nearby tissue] and Ki-67 LI <5% [low tumor growth rate]).

Matsuse et al. [30] reported that Ki67 LI and *BRAF/TERT* gene mutations are risk factors for the recurrence of PTCs. Although *BRAF* and *TERT* mutations are prognostically important oncogene mutations in patients with PTC, *TERT* mutations are rarely present in patients younger than 45 years. Therefore, this method cannot be applied to many young patients with PTC. Our method, using invasive status and Ki-67 LI, can be applied in more patients and does not involve the cost burden related to genetic testing. However, *TERT*, *BRAF*, and Ki-67 LI may be used to extract and confirm high-grade PTCs in older patients with advanced-stage tumors.

A cutoff of 5% for Ki-67 LI was introduced in the 3rd edition World Health Organization (WHO) classification [31] and by several authors, including Kakudo et al. in 2015 [30,32]. Ki-67 LI is a continuous variable that should not be divided into two groups, <5% and  $\geq 5\%$ . Even in cases higher than 5%, a difference between 5%–10% and 10%–30% is expected, as confirmed in this study (Table 4). These PTCs with a high Ki-67 LI of 10%–30% might have covered lesions equivalent to poorly differentiated carcinoma introduced in the 3rd edition WHO classification [31] and high-grade differentiated thyroid carcinoma introduced in the 5th edition WHO classification [33]. In their diagnostic criteria, increased mitoses and/or tumor necrosis have very similar implications to Ki-67 LI greater than 10%. Therefore, we recommend pathologists include the absolute value of Ki-67 LI in their pathology reports so that clinical doctors can understand risk of recurrence and carcinoma death more precisely. This can inform clinicians about the risk of recurrence and grading of tumor death risk, as Ki-67 LI is a

continuous variable with a higher value associated with worse prognosis.

Using a larger number of cases than ours (312 cases with 5% or less), Miyauchi et al. [23] reported a recurrence prognosis of 86.4% at 10 years for PTC with a Ki-67 LI <5%, a lower figure (higher recurrence rate) than our 98.5%. Possible explanations for this include the following. (1) There are differences in the methods of measuring Ki-67 LI. Standardization of measurement methods is desired as a solution. (2) Tumor specimens in advanced stages of disease may show diversity in proliferative potential within the specimen. In such cases, the value of the examined site with the highest proliferative potential (hot spot) was used in this study, although it is possible that the hot spot did not have the maximum potential in the specimen. In addition, (3) if the values used for comparison are not hot spots but average values, differences in the conclusions are expected. However, the studies agree about the importance of a higher Ki-67 LI and a higher recurrence rate. (4) Two different cutoff values, 3% and 5%, have been proposed to identify high-grade MTCs by two independent groups [10,34]. While the international consensus has adopted the cutoff of 5% [12], Australia (Sydney Group) is still using 3% [8]. Thus, the value of the cutoff for the Ki-67 labeling rate needs to be determined by the pathology laboratory.

We also considered a situation with a Ki-67 labeling rate cutoff of 4%, but this resulted in a recurrence rate of 1.6% for the 0%–4% Ki-67 labeling group ( $n = 123$ ) and 20.7% for the 4%–10% Ki-67 labeling group ( $n = 29$ ). Due to this large difference, we ultimately adopted the cutoff value of 5% as in the study by Kakudo et al. [32].

In the present study, we stratified 167 PTCs according to invasive status combined with tumor growth rate using Ki-67 LI for recurrence. At the same time, we excluded exceptional PTCs that were likely to show anaplastic transformation (high-grade PTCs with a high Ki-67 labeling rate >30% and with an anaplastic carcinoma component). We believe that this strategy allowed us to elucidate a clear difference between cases with Ki-67 LI  $\geq 5\%$  and <5% in PTCs, and recurrence was seen in PTCs with Ki-67 LI <5% was only 2/132 patients (1.5%). Therefore, this prognostic characteristic (a negligible risk of recurrence at 1.5% for a median 64-month follow-up in PTCs with Ki-67 LI <5%) is essential information for a patient immediately after surgery, when the typical patient most frequently experiences carcinoma anxiety. As there are rare exceptional occurrences in low Ki-67 LI cases, we cannot guarantee absence of recurrence.

However, a 1.5% risk is negligible in invasive PTCs, and no recurrence was found among patients with Ex0, N0, and Ki-67 LI <5%. Doctors could comfort patients with Ki-67 LI <5%, N0, and Ex0 suffering from severe carcinoma anxiety immediately after surgery when planning postoperative follow-up strategies. Even in patients with Ex0-3 and/or N1/2 PTCs, curative surgery was possible in 98.5% if the Ki-67 LI was <5%. This is important data for alleviating the fear of carcinoma recurrence, metastasis, and tumor mortality. However, for advanced-stage PTCs in which curative resection is not possible and the disease is persistent, an alternative strategy is required to predict patient outcomes, and the serum TG doubling time and doubling rate, proposed by Miyauchi et al. [23], play a significant role in predicting patient outcomes in such cases. Based on the results obtained in this study, we believe that patients with a Ki-67 LI <5% should be followed up as usual. Conversely, patients with a Ki-67 LI  $\geq 5\%$  are at high risk of recurrence and should be followed with imaging studies at relatively short intervals.

Ki-67 LI is a clinically useful predictive factor for recurrence-free survival in patients with papillary thyroid carcinoma. We believe the evidence for low tumor recurrence risk may contribute to use of more conservative treatment options for invasive-stage PTCs and help alleviate patient anxiety about tumor recurrence and death.

A limitation of this study was the small number of patients analyzed. However, the results showed significant differences even in this small patient cohort, which indicates that the difference between high ( $\geq 5\%$ ) Ki-67 LI PTCs and low (<5%) Ki-67 LI PTCs is clear and biologically meaningful. However, further confirmatory studies in a large patient series and different ethnic populations are required before our proposal is widely accepted worldwide. A second limitation is our indication for thyroid surgery. The choice of lobectomy or TTX deviated slightly from Western thyroid nodule practice, and most patients were treated with lobectomy even in a significant number of patients with lateral nodal metastasis (N1b). However, all surgeries were performed by a single surgeon (K.Y.) and his team, and we believe that the indications for surgery and choice of surgery type were constant during this rather extended (2010–2022) study period. A third limitation of this study is the lack of a genetic profile of the PTCs studied, as the health insurance system in Japan does not cover genetic tests for diagnosis of PTCs. Last, another key limitation is the lack of interlaboratory reproducibility of Ki-67 LI measurements due to multiple sources of variation, including antibody clones,

antibody formats, staining methods, testing personnel, and staining platforms. Technical standardization of the Ki-67 immunohistochemical assay among laboratories is essential for establishing a reliable risk classification for thyroid carcinomas. As expected, our determination of the Ki-67 LI threshold varies from those reported in other publications by Miyauchi et al. [22,23] due to inherent challenges in the Ki-67 immunostaining and LI measurement methods, particularly antigen preservation, antibody clones, antibody incubation time, DAB reaction time, reaction temperature, and immuno-staining method used. Consequently, a cutoff value established for one assay system might not universally apply to others. In clinical practice, it is imperative to account for the specific measurement system employed and its validated cutoff values rather than relying exclusively on generalized thresholds.

### Ethics Statement

This study was performed was approved by the Kindai University, Nara Hospital (protocol no. 23-54). Informed consent was obtained from the participant included in the study.

### Availability of Data and Material

The datasets generated or analyzed during the study are available from the corresponding author on reasonable request.

### Code Availability

Not applicable.

### ORCID

Takashi Masui	<a href="https://orcid.org/0000-0002-9567-2947">https://orcid.org/0000-0002-9567-2947</a>
Katsunari Yane	<a href="https://orcid.org/0009-0003-7990-4386">https://orcid.org/0009-0003-7990-4386</a>
Ichiro Ota	<a href="https://orcid.org/0000-0003-3815-8877">https://orcid.org/0000-0003-3815-8877</a>
Kennichi Kakudo	<a href="https://orcid.org/0000-0002-0347-7264">https://orcid.org/0000-0002-0347-7264</a>
Tomoko Wakasa	<a href="https://orcid.org/0000-0002-3328-5677">https://orcid.org/0000-0002-3328-5677</a>
Satoru Koike	<a href="https://orcid.org/0009-0006-5710-6414">https://orcid.org/0009-0006-5710-6414</a>
Hirota Kinugawa	<a href="https://orcid.org/0009-0007-0248-7157">https://orcid.org/0009-0007-0248-7157</a>
Ryuji Yasumatsu	<a href="https://orcid.org/0000-0001-6199-0341">https://orcid.org/0000-0001-6199-0341</a>
Tadashi Kitahara	<a href="https://orcid.org/0000-0002-5260-6202">https://orcid.org/0000-0002-5260-6202</a>

### Author Contributions

Conceptualization: TM, KY, IO, KK, TW, SK, HK, RY, TK. Data curation: TM, KK, SK, HK. Formal analysis: TM, KK, KY, IO. Funding acquisition: TM. Methodology: TM, KK, TW, RY, TK. Resources: TM, KK. Writing—original draft: TM, KK. Writing—review & editing: TM, KY, IO, KK, TW, SK, HK, RY, TK.

Approval of final manuscript: all authors.

### Conflicts of Interest

K.K., a contributing editor of the *Journal of Pathology and Translational Medicine*, was not involved in the editorial evaluation or decision to publish this article. All remaining authors have declared no conflicts of interest.

### Funding Statement

No funding was received for this study.

## REFERENCES

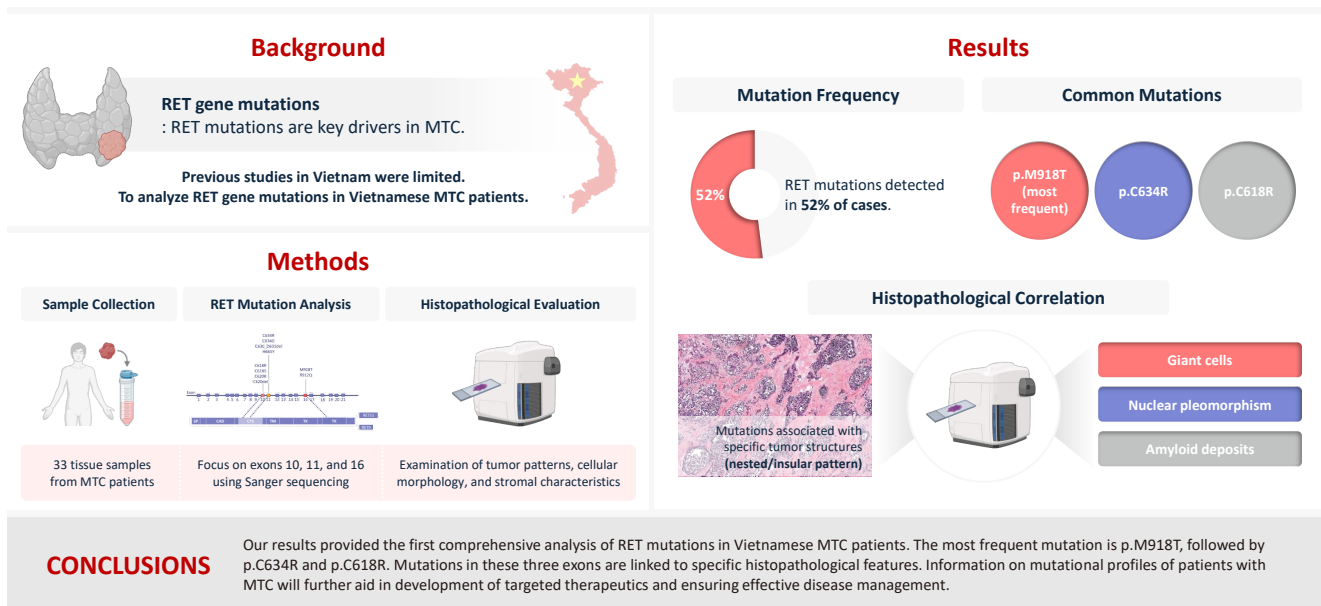
1. Popadich A, Levin O, Lee JC, et al. A multicenter cohort study of total thyroidectomy and routine central lymph node dissection for cN0 papillary thyroid cancer. *Surgery* 2011; 150: 1048-57.
2. Hartl DM, Mamelle E, Borget I, Leboulleux S, Mirghani H, Schlumberger M. Influence of prophylactic neck dissection on rate of retreatment for papillary thyroid carcinoma. *World J Surg* 2013; 37: 1951-8.
3. Liu J, Zhang Z, Huang H, et al. Total thyroidectomy versus lobectomy for intermediate-risk papillary thyroid carcinoma: a single-institution matched-pair analysis. *Oral Oncol* 2019; 90: 17-22.
4. Song E, Han M, Oh HS, et al. Lobectomy is feasible for 1-4 cm papillary thyroid carcinomas: a 10-year propensity score matched-pair analysis on recurrence. *Thyroid* 2019; 29: 64-70.
5. Guo K, Wang Z. Risk factors influencing the recurrence of papillary thyroid carcinoma: a systematic review and meta-analysis. *Int J Clin Exp Pathol* 2014; 7: 5393-403.
6. Ito Y, Higashiyama T, Takamura Y, et al. Risk factors for recurrence to the lymph node in papillary thyroid carcinoma patients without preoperatively detectable lateral node metastasis: validity of prophylactic modified radical neck dissection. *World J Surg* 2007; 31: 2085-91.
7. Baek SK, Jung KY, Kang SM, et al. Clinical risk factors associated with cervical lymph node recurrence in papillary thyroid carcinoma. *Thyroid* 2010; 20: 147-52.
8. Haugen BR, Alexander EK, Bible KC, et al. 2015 American Thyroid Association management guidelines for adult patients with thyroid nodules and differentiated thyroid cancer: the American Thyroid Association Guidelines Task Force on Thyroid Nodules and Differentiated Thyroid Cancer. *Thyroid* 2016; 26: 1-133.
9. Welch HG, Black WC. Overdiagnosis in cancer. *J Natl Cancer Inst* 2010; 102: 605-13.

10. Caulley L, Eskander A, Yang W, et al. Trends in diagnosis of non-invasive follicular thyroid neoplasm with papillarylike nuclear features and total thyroidectomies for patients with papillary thyroid neoplasms. *JAMA Otolaryngol Head Neck Surg* 2022; 148: 99-106.
11. Fuchs TL, Nassour AJ, Glover A, et al. A proposed grading scheme for medullary thyroid carcinoma based on proliferative activity (Ki-67 and mitotic count) and coagulative necrosis. *Am J Surg Pathol* 2020; 44: 1419-28.
12. Xu B, Fuchs TL, Ahmadi S, et al. International medullary thyroid carcinoma grading system: a validated grading system for medullary thyroid carcinoma. *J Clin Oncol* 2022; 40: 96-104.
13. Bai Y, Guo T, Niu D, et al. Clinical significance and interrelations of PD-L1 expression, Ki-67 index, and molecular alterations in sporadic medullary thyroid carcinoma from a Chinese population. *Virchows Arch* 2022; 481: 903-11.
14. Weigel MT, Dowsett M. Current and emerging biomarkers in breast cancer: prognosis and prediction. *Endocr Relat Cancer* 2010; 17: R245-62.
15. Berney DM, Gopalan A, Kudahetti S, et al. Ki-67 and outcome in clinically localised prostate cancer: analysis of conservatively treated prostate cancer patients from the Trans-Atlantic Prostate Group study. *Br J Cancer* 2009; 100: 888-93.
16. Kloppel G. Classification and pathology of gastroenteropancreatic neuroendocrine neoplasms. *Endocr Relat Cancer* 2011; 18 Suppl 1: S1-16.
17. La Rosa S. Diagnostic, prognostic, and predictive role of Ki67 proliferative index in neuroendocrine and endocrine neoplasms: past, present, and future. *Endocr Pathol* 2023; 34: 79-97.
18. Amin MB, Edge SB, Greene FL, et al. *AJCC cancer staging manual*. 8th ed. Cham: Springer International Publishing, 2016.
19. D'Avanzo A, Ituarte P, Treseler P, et al. Prognostic scoring systems in patients with follicular thyroid cancer: a comparison of different staging systems in predicting the patient outcome. *Thyroid* 2004; 14: 453-8.
20. Hay ID, Grant CS, Taylor WF, McConahey WM. Ipsilateral lobectomy versus bilateral lobar resection in papillary thyroid carcinoma: a retrospective analysis of surgical outcome using a novel prognostic scoring system. *Surgery* 1987; 102: 1088-95.
21. Voutilainen PE, Siironen P, Franssila KO, Sivula A, Haapiainen RK, Haglund CH. AMES, MACIS and TNM prognostic classifications in papillary thyroid carcinoma. *Anticancer Res* 2003; 23: 4283-8.
22. Miyauchi A. Clinical trials of active surveillance of papillary microcarcinoma of the thyroid. *World J Surg* 2016; 40: 516-22.
23. Miyauchi A, Kudo T, Hirokawa M, et al. Ki-67 labeling index is a predictor of postoperative persistent disease and cancer growth and a prognostic indicator in papillary thyroid carcinoma. *Eur Thyroid J* 2013; 2: 57-64.
24. Ahn HS, Kim HJ, Welch HG. Korea's thyroid-cancer "epidemic": screening and overdiagnosis. *N Engl J Med* 2014; 371: 1765-7.
25. U. S. Preventive Services Task Force, Bibbins-Domingo K, Grossman DC, et al. Screening for thyroid cancer: US Preventive Services Task Force Recommendation Statement. *JAMA* 2017; 317: 1882-7.
26. Lloyd RV, Osamura RY, Kloppel G, Rosai J. *WHO classification of tumours of endocrine organs*. 4th ed. Lyon: International Agency for Research on Cancer, 2017.
27. Sugitani I, Ito Y, Takeuchi D, et al. Indications and strategy for active surveillance of adult low-risk papillary thyroid microcarcinoma: consensus statements from the Japan Association of Endocrine Surgery Task Force on Management for Papillary Thyroid Microcarcinoma. *Thyroid* 2021; 31: 183-92.
28. Sugitani I, Ito Y, Miyauchi A, Imai T, Suzuki S. Active surveillance versus immediate surgery: questionnaire survey on the current treatment strategy for adult patients with low-risk papillary thyroid microcarcinoma in Japan. *Thyroid* 2019; 29: 1563-71.
29. Dwivedi SS, Khandeparkar SG, Joshi AR, et al. Study of immunohistochemical markers (CK-19, CD-56, Ki-67, p53) in differentiating benign and malignant solitary thyroid nodules with special reference to papillary thyroid carcinomas. *J Clin Diagn Res* 2016; 10: EC14-9.
30. Matsuse M, Yabuta T, Saenko V, et al. TERT promoter mutations and Ki-67 labeling index as a prognostic marker of papillary thyroid carcinomas: combination of two independent factors. *Sci Rep* 2017; 7: 41752.
31. DeLellis RA, Lloyd RV, Heitz PU, Eng C. *World Health Organization classification of tumours: pathology and genetics of tumours of endocrine organs*. Lyon: IARC Press, 2004.
32. Kakudo K, Wakasa T, Ohta Y, Yane K, Ito Y, Yamashita H. Prognostic classification of thyroid follicular cell tumors using Ki-67 labeling index: risk stratification of thyroid follicular cell carcinomas. *Endocr J* 2015; 62: 1-12.
33. Baloch ZW, Asa SL, Barletta JA, et al. Overview of the 2022 WHO classification of thyroid neoplasms. *Endocr Pathol* 2022; 33: 27-63.
34. Alzumaili B, Xu B, Spanheimer PM, et al. Grading of medullary thyroid carcinoma on the basis of tumor necrosis and high mitotic rate is an independent predictor of poor outcome. *Mod Pathol* 2020; 33: 1690-701.

# Characteristics of *RET* gene mutations in Vietnamese medullary thyroid carcinoma patients: a single-center analysis

Van Hung Pham<sup>1,2</sup>, Quoc Thang Pham<sup>3</sup>, Minh Nguyen<sup>1</sup>, Hoa Nhat Ngo<sup>3</sup>, Thao Thi Thu Luu<sup>3</sup>, Nha Dao Thi Minh<sup>1</sup>, Trâm Đặng<sup>1</sup>, Anh Tu Thai<sup>4</sup>, Hoang Anh Vu<sup>3</sup>, Dat Quoc Ngo<sup>3</sup>

## Graphical abstract



# Characteristics of *RET* gene mutations in Vietnamese medullary thyroid carcinoma patients: a single-center analysis

Van Hung Pham<sup>1,2</sup>, Quoc Thang Pham<sup>3</sup>, Minh Nguyen<sup>1</sup>, Hoa Nhat Ngo<sup>3</sup>, Thao Thi Thu Luu<sup>3</sup>, Nha Dao Thi Minh<sup>1</sup>, Trâm Đặng<sup>1</sup>, Anh Tu Thai<sup>4</sup>, Hoang Anh Vu<sup>3</sup>, Dat Quoc Ngo<sup>3</sup>

<sup>1</sup>Faculty of Nursing and Medical Technology, University of Medicine and Pharmacy at Ho Chi Minh City, Ho Chi Minh City, Vietnam

<sup>2</sup>University Medical Center Ho Chi Minh City, Ho Chi Minh City, Vietnam

<sup>3</sup>Pathology Department, University of Medicine and Pharmacy at Ho Chi Minh City, Ho Chi Minh City, Vietnam

<sup>4</sup>Faculty of Pathology, Ho Chi Minh City Oncology Hospital, Ho Chi Minh City, Vietnam

**Background:** The *RET* gene point mutation is the main molecular alteration involved in medullary thyroid carcinoma (MTC) tumorigenesis. Previous studies in Vietnam mainly consisted of case reports, with limited data on larger sample sizes. In this study, we investigated *RET* gene mutations in exons 10, 11, and 16 and analyzed clinicopathological features of a series of Vietnamese MTC patients. **Methods:** We collected 33 tissue samples from patients with MTC and analyzed *RET* mutations using the Sanger sequencing method. The relationship between hotspot *RET* mutations (exons 10, 11, 16) and clinicopathological features were investigated. **Results:** Among the 33 analyzed cases, 17 tumors (52%) harbored *RET* mutations in exon 10, 11, or 16. A total of 10 distinct genetic alterations were identified, including eight missense mutations and two short indels. Of these, seven were classified as pathogenic mutations based on previous publications, with p.M918T being the most frequent (4 cases), followed by p.C634R (3 cases) and p.C618R (3 cases). Mutations were significantly associated with specific histological patterns, such as the nested/insular pattern ( $p=.026$ ), giant cells ( $p=.007$ ), nuclear pleomorphism ( $p=.018$ ), stippled chromatin ( $p=.044$ ), and amyloid deposits ( $p=.024$ ). No mutations were found in germline analyses, suggesting these were somatic alterations. **Conclusions:** Our results provided the first comprehensive analysis of *RET* mutations in Vietnamese MTC patients. The most frequent mutation was p.M918T, followed by p.C634R and p.C618R. Mutations in these three exons were linked to specific histopathological features. Information on mutational profiles of patients with MTC will further aid in the development of targeted therapeutics to ensure effective disease management.

**Keywords:** Thyroid neoplasms; Carcinoma, medullary; Proto-oncogene protein c-ret; Mutation

## INTRODUCTION

According to the data from GLOBOCAN 2022, the global incidence of new thyroid cancer cases is 821,214, ranking seventh among all cancer types and claiming the lives of 47,507 individuals annually [1]. In Vietnam, the age-standardized incidence rate of thyroid cancer increased from 2.4 per 100,000 during 1996–2000 to 7.5 per 100,000 during 2011–2015; furthermore, the age of patients at diagnosis decreased gradually [2]. Most

thyroid cancer subtypes are derived from follicular cells, except medullary thyroid carcinoma (MTC), which originates from parafollicular C cells. MTC is a well-differentiated thyroid tumor that accounts for about 5% to 10% of all thyroid carcinomas, and shows an intermediate prognostic outcome between papillary and anaplastic thyroid cancer [3,4].

The primary genetic change implicated in the development of MTC is point mutation in the *RET* gene [5]. *RET*-mutant MTC exhibits more aggressive clinical behavior, including a

**Received:** October 22, 2024 **Revised:** December 23, 2024 **Accepted:** December 27, 2024

**Corresponding Author:** Quoc Thang Pham, MD, PhD

Pathology department, University of Medicine and Pharmacy at Ho Chi Minh City, Ho Chi Minh City 748010, Vietnam

Tel: +84-783-332-527, Fax: +84-28-3855-2304, E-mail: phamquocthang@ump.edu.vn

This is an Open Access article distributed under the terms of the Creative Commons Attribution Non-Commercial License (<https://creativecommons.org/licenses/by-nc/4.0/>) which permits unrestricted non-commercial use, distribution, and reproduction in any medium, provided the original work is properly cited.

© 2025 The Korean Society of Pathologists/The Korean Society for Cytopathology

higher incidence of lymph node metastasis and distant metastasis, as well as worse survival [6-8]. Notably, patients have most benefited from the genetic screening for germline mutations of the *RET* proto-oncogene in the diagnosis, prevention, and treatment of MTC [9]. The allelic frequencies of *RET* mutations vary in different populations, and thus it is critical to ascertain population-specific mutation frequencies [10].

Takahashi et al. first described the *RET* oncogene in 1985 [11]. Situated on chromosome 10q11.2, the *RET* proto-oncogene encodes a cellular tyrosine kinase transmembrane receptor. Structurally, *RET* comprises three distinct domains: an extracellular segment at the N-terminus housing four cadherin-like regions, a cysteine-rich region housing a transmembrane domain, and a cytoplasmic domain with tyrosine kinase activity [12]. Upon binding with the ligand-co-receptor complex, *RET* undergoes dimerization and autophosphorylation on intracellular tyrosine residues, which then recruit adaptor and signaling proteins to activate multiple downstream pathways [13]. The activation of *RET* stimulates various downstream pathways involved in cell growth, proliferation, survival, and differentiation [14]. Consequently, alterations leading to the dysregulation of *RET* activity contribute to several human cancers [13].

For patients with thyroid carcinoma undergoing *RET* testing, the method typically begins by sequencing the commonly mutated *RET* cysteine codons within exons 10 and 11, along with hot spots found in exons 13 to 16. Alternatively, all *RET* exons may be sequenced from the outset [9,15]. Frequently observed somatic mutation M918T occurs in up to 40% of individuals with sporadic MTC and is linked to the aggressive nature of the disease [8,16]. In this study, none of the patients had a family history, thus we selected exons 10, 11, and 16 for analysis. MTC commonly exhibits single amino acid substitutions as well as minor insertions or deletions [15]. Since the Sanger sequencing method is the most suitable technique for analyzing single nucleotide variants and short indels, we employed the Sanger method to achieve the objectives of this study.

Research examining *RET* gene mutations in patients with MTC has been conducted in many countries worldwide. However, research in Vietnam remains limited. Therefore, this investigation aims to provide additional data on *RET* gene mutations in Vietnamese individuals, potentially contributing to diagnostic and molecular-targeted treatment applications.

## MATERIALS AND METHODS

### Tissue samples

We retrospectively collected primary tumors of 33 thyroid cancer patients with diagnosed MTC who had undergone thyroid resection at the Oncology Hospital (Ho Chi Minh City, Vietnam) between 2020 and 2022.

Sections were cut at 3- $\mu$ m thickness and stained with hematoxylin-eosin. Experienced pathologists Q.T.P. and H.N.N. evaluated indicative regions from both cancerous and non-cancerous tissues on histopathological slides. Pathological features were classified according to the updated World Health Organization (WHO) 2022 criteria [17]. For each sample, 10 slices, each 10  $\mu$ m thick, were obtained from corresponding paraffin-embedded tissue blocks for subsequent DNA extraction. Normal thyroid tissue was selected from these blocks for germline analysis.

### DNA isolation

DNA extraction from formalin-fixed paraffin-embedded (FFPE) tissue blocks was carried out using the ReliaPrep FFPE gDNA Miniprep System kit (Promega, Madison, WI, USA) following the instructions of the manufacturer. The purity of the DNA samples was assessed using Nanodrop technology before polymerase chain reaction (PCR) and sequencing. Samples with insufficient DNA yield were excluded from further analysis.

### PCR and Sanger sequencing

The primers of *RET* exons 10, 11, and 16 that target hot spot regions are shown in the [Supplementary Table S1](#). All primers used in this study were newly designed. PCR was performed in 15  $\mu$ L mixtures of 0.1  $\mu$ M of each forward and reverse primer, 1 $\times$  PCR Buffer, 1.5 mM MgCl<sub>2</sub>, 200  $\mu$ M each dNTP, 0.5 U Taq Hot Start Polymerase (Takara Bio, Shiga, Japan) and 25–50 ng of genomic DNA.

PCR was denatured at 98°C for 3 minutes followed by 45 cycles of 98°C for 10 seconds, 58°C for 30 seconds and 72°C for 40 seconds, and a final elongation at 72°C for 2 minutes. PCR products were checked for size and purity using 2% agarose gel electrophoresis.

PCR products were purified enzymatically using the ExoSAP IT PCR Product Cleanup Reagent (Thermo Scientific, Waltham, MA, USA) for removal of excess primers and dNTPs before Sanger sequencing using the BigDye Terminator v3.1 Kit

and the ABI 3500 Genetic Analyzer (Applied Biosystems, Foster City, CA, USA). Sequences were compared to the reference sequence of the *RET* gene (GenBank accession number: NG 07489.1). CLC Main Workbench Software version 5.5 (Qiagen, Frederick, MD, USA) was utilized to analyze mutations. All detected alterations were functionally classified using the available databases (such as NCBI, COSMIC, etc.) and previous reports. Pathogenicity of variants was estimated by Polymorphism Phenotyping-2 (PolyPhen-2; Havard, Boston, MA, USA) or MutationTaster (Neurocure Cluster of Excellence/Berlin Institute of Health, Berlin, Germany).

**Statistical methods**

Statistical analysis was performed using STATA ver. 14.2 (Stata Corp., College Station, TX, USA). Comparisons between the two groups were conducted using the chi-square or Fisher exact test. Differences between the two groups with a significance level of  $p < .05$  were considered statistically significant.

**RESULTS**

**Characteristics of MTC patients and their clinicopathological features**

Our research investigated 33 MTC patients. There were more females than males, with a female-to-male ratio of 1.4:1. The average age at diagnosis of MTC was 46.67 years. Of the cases studied, 85% exhibited a solitary tumor, and 88% had the tumor confined to a single lobe of the thyroid gland. The smallest tumor observed grossly measured 6 mm, whereas the largest measured 80 mm (Table 1). Among the morphological features, solid and nest/insular patterns were the most commonly observed in MTC cases (Supplementary Fig. S1). Typical cells were identified in 91% of the cases, exhibiting a round or polyhedral shape with coarsely granular chromatin (Supplementary Fig. S2). Four cases exhibited clearly defined nuclei, while only three cases displayed tumor cells with nuclear inclusions (Supplementary Fig. S3). In the stroma, 52% showed amyloid deposits; in addition, fibrosis was noted in 64% of cases and hemorrhage in 61%, with calcifications occurring in approximately 30% of the cases (Supplementary Fig. S4).

In total, 45% of MTC patients were diagnosed with lymph node metastasis. High-grade histological features included a high mitotic count ( $\geq 5$  per  $2 \text{ mm}^2$ ) in six cases, necrosis in three cases, and lymphovascular invasion in four cases.

**Table 1.** Relationship between molecular alterations and clinicopathological features

Variable	Wild-type tumors (n=16)	Tumor with <i>RET</i> mutations (n=17)	p-value
Sex (male/female)	10/6	4/13	.024
Age (yr), median (range)	45 (30–65)	50 (35–70)	.112
Tumor size (mm)	25 (6–80)	30 (10–75)	.145
<b>Morphological features</b>			
Solid pattern	13	17	.103
Nested/insular pattern	8	15	.026
Trabecular pattern	2	4	.656
Papillary pattern	4	2	.398
Follicular pattern	4	3	.688
Others	4	4	>.99
<b>Tumor cell characteristics</b>			
Admixtures	9	14	.141
Round or polyhedral cells	14	16	.601
Spindle cells	4	6	.708
Plasmacytoid cells	4	5	>.99
Giant cells	0	7	.007
Oncocytic cells	2	3	>.99
Small cells	1	0	.485
Nuclear pleomorphism	0	6	.018
Nuclear inclusions	2	1	.601
Stippled chromatin	12	17	.044
Nucleoli	2	2	>.99
<b>Stromal tissue characteristics</b>			
Necrosis	3	0	.103
Sclerosis	11	10	.554
Amyloid deposits	5	12	.024
Hemorrhage	9	11	.619
Calcification	3	7	.259
<b>Prognostic features</b>			
Vascular invasion	3	1	.335
Nodal metastases	9	6	.227
High mitotic count ( $\geq 5$ per $2 \text{ mm}^2$ )	4	2	.398
<b>TNM staging</b>			
pT1	7	5	.412
pT2	8	9	.209
pT3	1	3	.112
pN0	10	7	.354
pN1	6	10	.227
pM0	16	17	N/A
<b>AJCC stage</b>			
Stage I	9	5	.121
Stage II	7	10	.278
Stage III	0	2	.189

AJCC, American Joint Committee on Cancer.

**Table 2.** RET gene alterations of samples

Location	Variants	Protein changes	No. of cases	Type of variants	Classification
Exon 10	c.1852T>C	p.C618R (p.Cys618Arg)	3	Missense	Pathogenic
	c.1853G>C	p.C618S (p.Cys618Ser)	1	Missense	Pathogenic
	c.1858T>C	p.C620R (p.Cys620Arg)	1	Missense	Pathogenic
	c.1858_1860del	p.C620del (p.Cys620del)	1	Deletion	Disease causing (predicted score by MutationTaster: 0.99)
Exon 11	c.1900T>C	p.C634R (p.Cys634Arg)	3	Missense	Pathogenic
	c.1900T>G	p.C634G (p.Cys634Gly)	1	Missense	Pathogenic
	c.1887_1893delinsA	p.C630_D631del (p.Cys630_Asp631del)	1	Deletion	Polymorphism (predicted score by MutationTaster: 0.58)
	c.1993C>T	p.H665Y (p.His665Tyr)	1	Missense	Possibly Damaging (predicted score by PolyPhen-2: 0.89)
Exon 16	c.2753T>C	p.M918T (p.Met918Thr)	4	Missense	Pathogenic
	c.2735G>A	p.R912Q (p.Arg912Gln)	1	Missense	Pathogenic

**The landscape of RET gene mutations**

The prevalence of RET gene alterations in the hot spot region was approximately 52% in our population. As shown in Table 2 and Fig. 1, among the 33 analyzed samples, 10 alterations were identified across exons 10, 11, and 16, with frequencies of six (18%), six (18%), and five (15%), respectively. All alterations indicate heterozygous status, and no germline mutations were detected in normal tissue among these cases, suggesting that these variants were somatic mutations. The p.M918T mutation had the highest frequency with four identified cases, followed by p.C634R and p.C618R mutations with three cases each. There were two mutations at the hot spot codon p.C618 (TGC>CGC, TGC>TCC) in exon 10 and two mutations at the hot spot codon p.C634 (TGC>CGC, TGC>GGC) in exon 11.

Alongside the eight single nucleotide variants (p.C618R, p.C618S, p.C620R, p.C634R, p.C634G, p.H665Y, p.M918T and p.R912Q), two short in-frame insertions/deletions were observed: a 2-amino acid deletion in exon 11 (p.C630\_D631del) and a 1-amino acid deletion in exon 16 (p.C620del). Out of the detected alterations, seven were pathogenic mutations according to prior publications. Two alterations were categorized as either ‘disease-causing’ or ‘possibly damaging,’ with PolyPhen-2 and MutationTaster assigning scores of 0.89 and 0.99, respectively. Additionally, one alteration was classified as a polymorphic variant, with a score of 0.58 on MutationTaster (Table 2).

Our data showed that there are relationships between the detected mutations and histopathological features, including nested or insular pattern, giant cells, nuclear pleomorphism, stippled chromatin, and amyloid deposit (Table 1). The number

of cases with detected mutations was also higher in females (p=.024). Other clinicopathological characteristics did not show any statistically significant associations with the presence or absence of mutations.

**DISCUSSION**

In this study, the absence of a family history along with classification of the identified variants as somatic indicated that these MTC cases harbored somatic gene alterations. With an average age of 46.67±13.93 years, this population is consistent with the age range reported by the American Thyroid Association, which notes that sporadic MTC typically presents later, often between the fourth and sixth decades of life, in contrast to hereditary MTC, which tends to manifest at an earlier age [9]. The study results also indicate that most MTC cases presented as a single tumor, with the predominant histological pattern being solid. The typical cells were round or polygonal, exhibiting coarsely granular chromatin, with a low incidence of clear nuclei and nuclear inclusions, consistent with WHO classification [17]. In addition to amyloid deposition in the stroma, our study population was characterized by a high prevalence of fibrosis and hemorrhage, both exceeding 60%.

Our research described RET gene mutations in a series of cases of Vietnamese patients with MTC. To the best of our knowledge, only one previous study investigated RET gene mutations in Vietnamese patients with MTC; however, that analysis was limited to a single case. Ha et al. [18] reported that a c.2753C>T transition resulted in a missense mutation of methi-

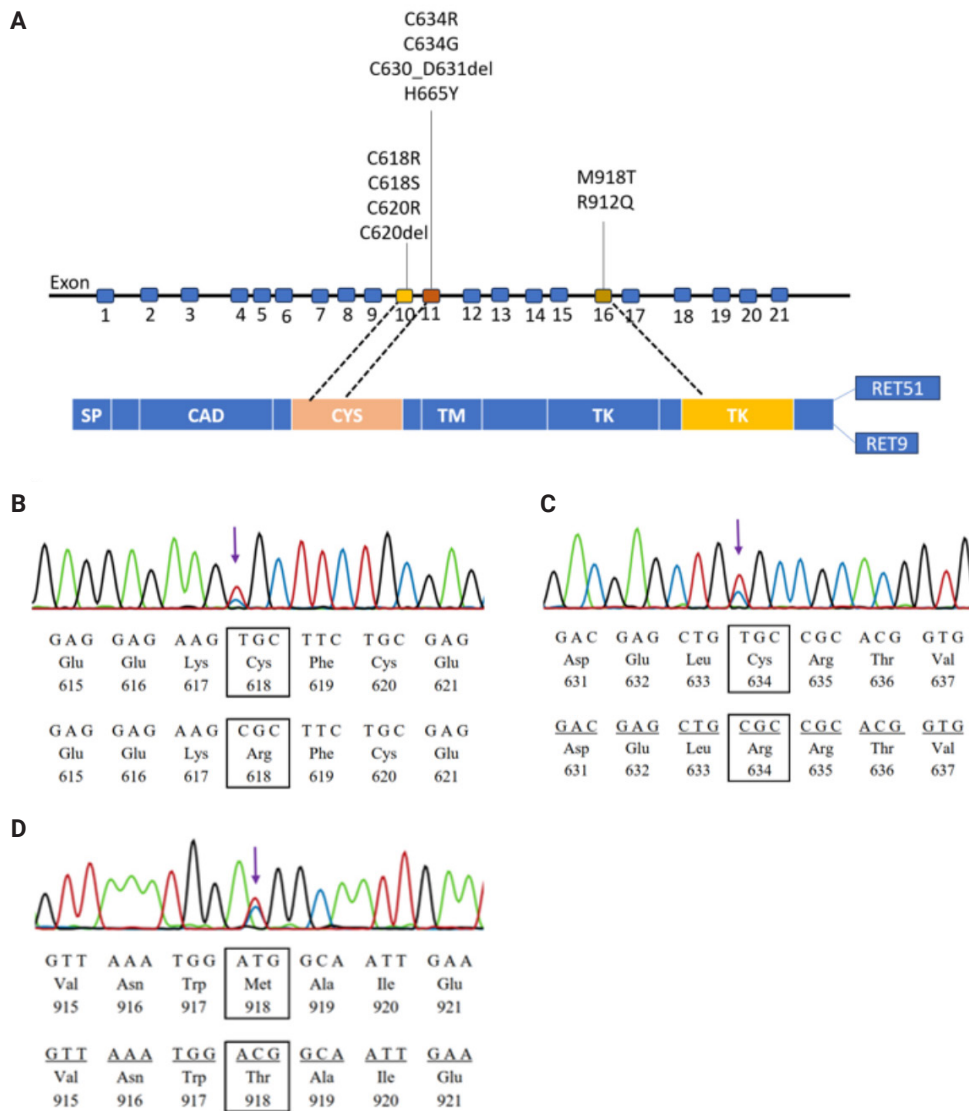


**Fig. 1.** The spectrum of mutations in the *RET* gene. (A) The distribution of mutations in the *RET* gene identified in this study. (B–D) The most frequently detected mutations include p.C618R in exon 10 (B), p.C634R in exon 11 (C), and p.M918T in exon 16 (D).

onine to threonine (p.M918T) in the RET protein. According to the American Thyroid Association, around half of sporadic MTC patients exhibit somatic *RET* mutations [9]. Additionally, Ciampi et al. [8] reported that somatic *RET* mutations are detected in as many as 55% of sporadic MTC patients. Our data showed mutations in exons 10, 11, and 16 in 17 cases out of a total of 33 cases of MTC with no family history, accounting for 52%.

In our study, a total of 10 different alterations in the *RET* gene were identified, including point mutations and short indels. All the point mutations were missense mutations and all the short

indels were in-frame changes. In general, missense mutations with a single amino acid change were the most common ones causing loss of function of the *RET* protein in cases of MTC. Similar results have been reported in other studies [8,16].

This study detected the p.M918T mutation in exon 16 in four cases, and the p.C634R mutation in exon 11 and the p.C618R mutation in exon 10 in three cases each, suggesting that they are common in Vietnamese patients with MTC. Several publications reported that p.M918T has the highest frequency in similar studies [8,19], and cysteine mutations have been noted in sporadic MTC cases [12]. Moreover, the *RET* gene p.C634

codon was mutated in four cases with different amino acid alterations, similar to previous report [8]. The p.C634R mutation was observed in three cases. However, the p.C634 codon was mutated in four cases, including three cases of p.C634R and one additional case of p.C634G. Our data differs from a Slovakian study involving patients with MTC, where the p.C618R mutation in exon 10 was more common than p.C634R and p.M918T mutations in patients with a negative family history [20]. In this study, mutations at codon C618 were detected in four cases, more than at codon C620, which were found in two cases. These results differ from those reported by Yeganeh et al. [21], where p.C611Y and p.C620R were the most prevalent mutations in exon 10.

Asai et al. [22] and Santoro et al. [23] previously elucidated the molecular mechanisms of *RET* activation by cysteine mutations. When a non-cysteine residue replaces a cysteine residue, it releases a neighboring cysteine normally engaged in forming an intramolecular disulfide bond. This freed cysteine then creates an abnormal intermolecular covalent disulfide bond between two mutant *RET* molecules, triggering their dimerization and subsequent activation [22,23]. p.M918T mutations enhance kinase activity both as monomers and by presenting substrates for trans-autophosphorylation [23]. This effect arises from structural alterations in the activation loop of the kinase domain [24]. *RET* mutations of extracellular cysteines, which include mutations in exon 10 and exon 11, facilitate dimerization and kinase activation, whereas mutations in the *RET* kinase coding domain, including those in exon 16, drive dimerization-independent kinase activation. Thus, *RET* kinase inhibition is an attractive therapeutic target in patients with *RET* alterations. Initially, this method was accomplished through multikinase inhibitors, impacting various dysregulated pathways involving *RET* kinase. In clinical settings, employing multikinase inhibitors for advanced thyroid cancer patients yielded therapeutic benefits, although often accompanied by notable and occasionally severe side effects [15]. Nevertheless, significant advancements have emerged with the discovery of potent and specific *RET* kinase inhibitors for treating advanced thyroid cancer. While further clinical confirmation through future trials is necessary, the consistent antitumoral effectiveness and enhanced safety profile of these new compounds herald a promising era in precision oncology for *RET*-driven cancers [15]. In 2020, the U.S. Food and Drug Administration (FDA) sanctioned selpercatinib and pralsetinib for *RET*-mutated MTC necessitating systemic treatment. Drawing from these data

and FDA endorsements, the National Comprehensive Cancer Network Panel advocated for both of these *RET* inhibitors as primary choices for patients with *RET*-mutant conditions [25]. Somatic genotyping for *RET* should be conducted in patients who exhibit germline wild-type status or whose germline status remains undetermined [25].

Kaserer et al. [26] highlighted that, in comparison to sporadic tumors, hereditary tumors were significantly more likely to exhibit multifocality, bilaterality, association with desmoplastic stroma, and the presence of C cell hyperplasia. Our study identified a significant association between sporadic *RET* mutations and distinct histological patterns, including a nested/insular pattern and the presence of giant cells, nuclear pleomorphisms, and amyloid deposits. To the best of our knowledge, no previous studies have reported a correlation between *RET* sporadic mutations and specific histopathological patterns. Interestingly, Verga et al. [27] reported that cutaneous lichen amyloidosis was exclusively identified in MEN2A/FMTC families carrying a *RET* pathogenic variant at codon 634. Since the number of MTC patients included in our research was relatively small, additional studies are required to better investigate the association between sporadic *RET* mutations and histological characteristics.

Our study revealed a landscape of *RET* gene mutations in exons 10, 11 and 16 in cases of MTC in Vietnamese patients. The most common mutation was p.M918T, followed by p.C634R and p.C618R. Mutations detected in these three exons are associated with histopathological features including histological patterns (nested/insular pattern), cellular features (giant cells, nuclear pleomorphism, and stippled chromatin), and stromal features (amyloid deposition). Moreover, clinical characteristics including patient sex also have a relationship with the detected mutations. The results of this study indicate that when considering *RET* gene mutations in a Vietnamese population with sporadic MTC, attention should be paid to exons 10, 11, and 16 first.

### Supplementary Information

The Data Supplement is available with this article at <https://doi.org/10.4132/jptm.2025.01.18>.

### Ethics Statement

This study received approval from the Board of Ethics in Biomedical Research of the University of Medicine and Pharmacy in Ho Chi Minh City, Vietnam, under approval number 916/

HDDD-DHYD. The consent forms for the patients were obtained.

### Availability of Data and Material

The datasets generated or analyzed during the study are available from the corresponding author on reasonable request.

### Code Availability

Not applicable.

### ORCID

Van Hung Pham <https://orcid.org/0009-0007-0289-9952>  
 Quoc Thang Pham <https://orcid.org/0000-0001-8787-367X>  
 Minh Nguyen <https://orcid.org/0000-0002-9159-147X>  
 Hoa Nhat Ngo <https://orcid.org/0009-0008-7981-896X>  
 Thao Thi Thu Luu <https://orcid.org/0009-0006-8369-7676>  
 Nha Dao Thi Minh <https://orcid.org/0009-0005-5353-9311>  
 Trâm Đặng <https://orcid.org/0009-0007-9455-9065>  
 Anh Tu Thai <https://orcid.org/0009-0002-0668-8339>  
 Hoang Anh Vu <https://orcid.org/0000-0003-4232-6001>  
 Dat Quoc Ngo <https://orcid.org/0000-0003-1461-0216>

### Author Contributions

Conceptualization: VHP, QTP, DQN. Data curation: VHP, HNN, TD, TTTL, NDTM. Formal analysis: VHP, HAV, MN. Funding acquisition: DQN. Investigation: VHP. Methodology: QTP, ATT, HAV, DQN. Project administration: QTP. Resources: ATT, HAV. Software: HAV, VHP. Supervision: QTP, DQN, MN. Validation: ATT, QTP, DQN. Visualization: NDTM. Writing—original draft: VHP, QTP. Writing—review & editing: VHP, QTP, HNN, MN, HAV. Approval of final manuscript: all authors.

### Conflicts of Interest

The authors declare that they have no potential conflicts of interest.

### Funding Statement

This study was funded by a grant from the University of Medicine and Pharmacy at Ho Chi Minh City (grant number 114/2023/HĐ-ĐHYD).

### Acknowledgments

The authors express their gratitude to the Center for Molecular Biomedicine at the University of Medicine and Pharmacy in Ho

Chi Minh City, as well as the Department of Pathology at the Ho Chi Minh City Oncology Hospital, for their support and facilitation in completing this study.

## REFERENCES

1. Ferlay J, Ervik M, Lam F, et al. Global cancer observatory: cancer today [Internet]. Lyon: International Agency for Research on Cancer, 2024 [cited 2024 Dec 10]. Available from: <https://gco.iarc.who.int/today>.
2. Pham DX, Nguyen HD, Phung AH, et al. Trends in incidence and histological pattern of thyroid cancer in Ho Chi Minh City, Vietnam (1996-2015): a population-based study. *BMC Cancer* 2021; 21: 296.
3. DeLellis RA, Lloyd RV, Heitz PU, Eng C. World Health Organization classification of tumours: pathology and genetics of tumours of endocrine organs. Lyon: IARC Press, 2004.
4. Pusztaszeri MP, Bongiovanni M, Faquin WC. Update on the cytologic and molecular features of medullary thyroid carcinoma. *Adv Anat Pathol* 2014; 21: 26-35.
5. Matrone A, Gambale C, Prete A, Elisei R. Sporadic medullary thyroid carcinoma: towards a precision medicine. *Front Endocrinol (Lausanne)* 2022; 13: 864253.
6. Romei C, Casella F, Tacito A, et al. New insights in the molecular signature of advanced medullary thyroid cancer: evidence of a bad outcome of cases with double *RET* mutations. *J Med Genet* 2016; 53: 729-34.
7. Moura MM, Cavaco BM, Pinto AE, et al. Correlation of *RET* somatic mutations with clinicopathological features in sporadic medullary thyroid carcinomas. *Br J Cancer* 2009; 100: 1777-83.
8. Ciampi R, Romei C, Ramone T, et al. Genetic landscape of somatic mutations in a large cohort of sporadic medullary thyroid carcinomas studied by next-generation targeted sequencing. *iScience* 2019; 20: 324-36.
9. Wells SA Jr, Asa SL, Dralle H, et al. Revised American Thyroid Association guidelines for the management of medullary thyroid carcinoma. *Thyroid* 2015; 25: 567-610.
10. Rovcanin B, Damjanovic S, Zivaljevic V, Diklic A, Jovanovic M, Paunovic I. The results of molecular genetic testing for *RET* proto-oncogene mutations in patients with medullary thyroid carcinoma in a referral center after the two decade period. *Hipokratia* 2016; 20: 187-91.
11. Takahashi M, Ritz J, Cooper GM. Activation of a novel human transforming gene, *ret*, by DNA rearrangement. *Cell* 1985; 42: 581-8.

12. Romei C, Ciampi R, Elisei R. A comprehensive overview of the role of the *RET* proto-oncogene in thyroid carcinoma. *Nat Rev Endocrinol* 2016; 12: 192-202.
13. Mulligan LM. *RET* revisited: expanding the oncogenic portfolio. *Nat Rev Cancer* 2014; 14: 173-86.
14. Arighi E, Borrello MG, Sariola H. RET tyrosine kinase signaling in development and cancer. *Cytokine Growth Factor Rev* 2005; 16: 441-67.
15. Salvatore D, Santoro M, Schlumberger M. The importance of the *RET* gene in thyroid cancer and therapeutic implications. *Nat Rev Endocrinol* 2021; 17: 296-306.
16. Elisei R, Cosci B, Romei C, et al. Prognostic significance of somatic *RET* oncogene mutations in sporadic medullary thyroid cancer: a 10-year follow-up study. *J Clin Endocrinol Metab* 2008; 93: 682-7.
17. Ghossein RA, Mete O, Osamura AJ, et al. WHO classification of tumours of endocrine and neuroendocrine tumours. 5th ed. Vol. 8. WHO Classification of Tumours online. Lyon: International Agency for Research on Cancer, 2022.
18. Ha NH, Yen TT, Nhung VP, Thuong MT, Ton ND, Hai NV. Identification of mutation in the *RET* gene in a patient with medullary thyroid cancer. *Viet J Biotechnol* 2016; 14: 405-10.
19. Marsh DJ, Learoyd DL, Andrew SD, et al. Somatic mutations in the *RET* proto-oncogene in sporadic medullary thyroid carcinoma. *Clin Endocrinol (Oxf)* 1996; 44: 249-57.
20. Milicevic S, Bergant D, Zagar T, Peric B. Crude annual incidence rate of medullary thyroid cancer and *RET* mutation frequency. *Croat Med J* 2021; 62: 110-9.
21. Yeganeh MZ, Sheikholeslami S, Dehbashi Behbahani G, Farashi S, Hedayati M. Skewed mutational spectrum of *RET* proto-oncogene Exon10 in Iranian patients with medullary thyroid carcinoma. *Tumour Biol* 2015; 36: 5225-31.
22. Asai N, Iwashita T, Matsuyama M, Takahashi M. Mechanism of activation of the *ret* proto-oncogene by multiple endocrine neoplasia 2A mutations. *Mol Cell Biol* 1995; 15: 1613-9.
23. Santoro M, Carlomagno F, Romano A, et al. Activation of *RET* as a dominant transforming gene by germline mutations of *MEN2A* and *MEN2B*. *Science* 1995; 267: 381-3.
24. Takahashi M, Kawai K, Asai N. Roles of the *RET* proto-oncogene in cancer and development. *JMA J* 2020; 3: 175-81.
25. Haddad RI, Bischoff L, Ball D, et al. Thyroid carcinoma, version 2.2022, NCCN clinical practice guidelines in oncology. *J Natl Compr Canc Netw* 2022; 20: 925-51.
26. Kaserer K, Scheuba C, Neuhold N, et al. Sporadic versus familial medullary thyroid microcarcinoma: a histopathologic study of 50 consecutive patients. *Am J Surg Pathol* 2001; 25: 1245-51.
27. Verga U, Fugazzola L, Cambiaghi S, et al. Frequent association between MEN 2A and cutaneous lichen amyloidosis. *Clin Endocrinol (Oxf)* 2003; 59: 156-61.

# Uncommon granulomatous manifestation in Epstein-Barr virus–positive follicular dendritic cell sarcoma: a case report

Henry Goh Di Shen<sup>1\*</sup>, Yue Zhang<sup>1\*</sup>, Wei Qiang Leow<sup>1,2,3</sup>

<sup>1</sup>Duke-NUS Medical School, Singapore

<sup>2</sup>Department of Anatomical Pathology, Singapore General Hospital, Singapore

<sup>3</sup>School of Biological Sciences, Nanyang Technological University, Singapore

Hepatic Epstein-Barr virus–positive inflammatory follicular dendritic cell sarcoma (EBV+ IFDCS) represents a rare form of liver malignancy. The absence of distinct clinical and radiological characteristics, compounded by its rare occurrence, contributes to a challenging diagnosis. Here, we report a case of a 54-year-old Chinese female with a background of chronic hepatitis B virus treated with entecavir and complicated by advanced fibrosis presenting with a liver mass found on her annual surveillance ultrasound. Hepatectomy was performed under clinical suspicion of hepatocellular carcinoma. Immunomorphologic characteristics of the tumor were consistent with EBV+ IFDCS with distinct non-caseating granulomatous inflammation. Our case illustrates the importance of considering EBV+ IFDCS in the differential diagnosis of hepatic inflammatory lesions. Awareness of this entity and its characteristic features is essential for accurately diagnosing and managing this rare neoplasm.

**Keywords:** Dendritic cell sarcoma, follicular; Epstein-Barr virus infections; Hepatitis B, chronic; Granuloma; Case report

## INTRODUCTION

Epstein-Barr virus–positive inflammatory follicular dendritic cell sarcoma (EBV+ IFDCS), previously known as inflammatory pseudotumor-like follicular/fibroblastic dendritic cell sarcoma, is a rare, indolent malignancy arising from follicular dendritic cells (FDCs). The condition is characterized by spindle-shaped neoplastic cells dispersed in a dense lymphoplasmacytic infiltrate, primarily affects the liver and spleen of middle-aged adults, and shows a significant female predominance [1,2]. The pathological diagnosis of this neoplasm presents challenges due to its wide range of histological features and close resemblance to inflammatory lesions [3]. The complexity of diagnosis is further highlighted by recent reports of gran-

uloma or eosinophilia-rich variants [4] and a lymphoma-like subtype [5]. Here, we present a rare case of EBV+ IFDCS with prominent epithelioid granulomas in a chronic hepatitis B virus (HBV) carrier with METAVIR F2 fibrosis. The presence of granulomas in this context adds to the evidence for emerging histopathological variants of EBV+ IFDCS. Through detailed clinical, histological, and immunohistochemical analysis, this report aims to underscore the challenges of diagnosis amid the complex interplay of chronic liver disease, viral infections, and rare hepatic neoplasms.

## CASE REPORT

A 54-year-old female patient has a history of hyperlipidemia,

**Received:** 1 July 2024 **Revised:** 10 September 2024 **Accepted:** 26 September 2024

**Corresponding Author:** Henry Goh Di Shen

Duke-NUS Medical School, 8 College Rd, 169857 Singapore

Tel: +65-88772440, E-mail: henry.g@u.duke.nus.edu

\*Henry Goh Di Shen and Yue Zhang contributed equally to this work.

This is an Open Access article distributed under the terms of the Creative Commons Attribution Non-Commercial License (<https://creativecommons.org/licenses/by-nc/4.0/>) which permits unrestricted non-commercial use, distribution, and reproduction in any medium, provided the original work is properly cited.

© 2025 The Korean Society of Pathologists/The Korean Society for Cytopathology

mitral valve prolapse, obsessive-compulsive behavior, epilepsy, and chronic hepatitis B treated with entecavir, complicated by advanced fibrosis with a liver stiffness of 11.4 kPa. She presented with an asymptomatic liver lesion, a cyst with septation and vascularity on annual surveillance ultrasound, suspicious for hepatocellular carcinoma (HCC). Baseline alanine transaminase, aspartate transaminase, and  $\alpha$ -fetoprotein levels remained within normal limits at 15 U/L (reference range, 6 to 66 U/L), 15 U/L (reference range, 12 to 42 U/L), and  $<2.7 \mu\text{g/L}$  (reference range,  $<7.1 \mu\text{g/L}$ ), respectively. The patient then underwent a computed tomography scan of the liver, which revealed a 1.3-cm arterial enhancing lesion in hepatic segment IVb with associated washout and capsule appearance, suspicious for HCC (Fig. 1A). No other suspicious hepatic lesions were identified, and the portal and hepatic veins were patent. The patient underwent elective laparoscopic cholecystectomy and segment IVb wedge resection for suspected HCC and gallstones. The patient tolerated the procedure well, and the surgical specimen was submitted for histopathological analysis.

The patient at 1 year of follow-up showed no palpable lymph nodes or abdominal masses. A positron emission tomography-computed tomography scan performed 2 weeks prior showed no evidence of hypermetabolic local recurrence at the surgical bed. Scattered nonspecific pulmonary nodules and clusters of centrilobular/tree-in-bud nodularities were noted, which may represent small airway infection or inflammation. No fluorodeoxyglucose-avid nodal metastases were detected. Liver function tests showed a slightly elevated alkaline phosphatase of 120 U/L (reference range, 39 to 99 U/L). HBV DNA load was detected at 11 IU/mL (1.06 log), for which she received tenofovir. The results of quantitative EBV polymerase chain reaction were undetectable, and alpha-fetoprotein level was within normal limits. The patient was planned for continued surveillance with a follow-up visit.

### Pathological examination

Gross examination of the resected specimen revealed a firm, white, multi-nodular mass within the subcapsular region of the liver, measuring 1.8×1.8×1.1 cm. Low-magnification microscopic examination identified a distinct, expansile nodule characterized by sharply demarcated borders (Fig. 1B). At higher magnifications, neoplastic cells, ranging from oval to spindle-shaped, were dispersed within the inflammatory infiltrate, accompanied by reactive lymphoid follicles. These tumor cells displayed varying cytoplasmic volumes, ill-defined cell

borders, irregular nuclear contours, and vesicular nuclei with distinct nucleoli, including some with binucleated and rare multinucleated forms (Fig. 1C). This background infiltration exhibited a pronounced lymphoplasmacytic inflammation interspersed with epithelioid histiocytes and micro-granulomas, along with the occasional presence of multinucleated giant cells (Fig. 1D, E). Notably, there was an absence of central caseation within the granulomas, and no foreign bodies were identified. In addition, fungal organisms were not detected with Grocott's methenamine silver and periodic acid-Schiff special stains (Fig. 1F), and no acid-fast bacilli were noted with Ziehl-Neelsen and Fite-Faraco special stains (Fig. 1G). Victoria blue staining identified hepatitis B surface antigens and occasional fibrous expansions of portal tracts with fibrous septa, consistent with METAVIR F2 fibrosis.

The granulomatous features observed in this case, characterized by epithelioid histiocytes, micro-granulomas, and multinucleated giant cells without central caseation, align with the rare granuloma-rich variant of EBV+ IFDCS. This variant remains underreported in the literature, particularly in the liver, where the differential diagnosis includes a wide range of infectious and inflammatory conditions [6]. Notably, the granulomas observed here lack central necrosis, distinguishing them from granulomas associated with infections such as tuberculosis or fungal diseases.

Immunohistochemical analysis showed that a subset of neoplastic cells variably expressed FDC markers CD21 and CD35 (Fig. 2A, B). Disrupted follicular dendritic networks, within which neoplastic cells emerged, were also highlighted. In situ hybridization for EBV-encoded small RNA (EBER) was positive, marking both large pleomorphic nuclei and slender, occasionally tadpole-shaped nuclei of tumor cells (Fig. 2C). A mixed population of CD20-positive B-cells, CD3-positive T cells, and CD68-positive histiocytes was observed in the background, alongside interspersed plasma cells. The cell proliferation marker MIB1 indicated a low proliferative index of approximately 10%.

## DISCUSSION

EBV+ IFDCS is closely associated with EBV infection, often showing positivity for EBV via EBER in situ hybridization, suggesting that EBV is contributory to the development of this tumor. While the precise pathogenetic mechanism by which EBV drives the tumorigenesis of EBV+ IFDCS is not fully un-

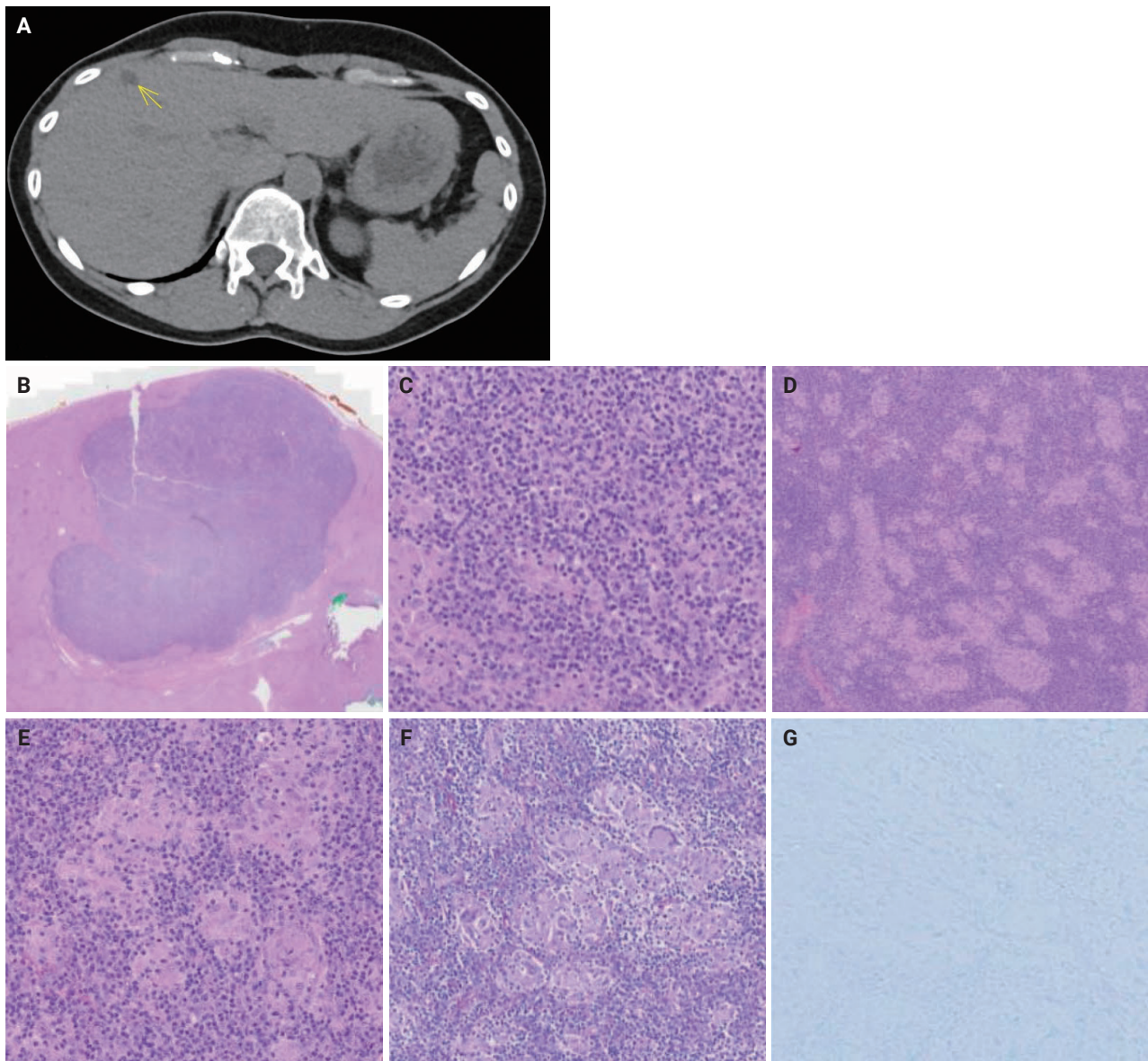


**Fig. 1.** Radiological and histological findings of hepatic tumor. (A) Computed tomography scan revealing a 1.3 cm lesion (arrow) in hepatic segment IVb. (B) Hematoxylin and eosin–stained image showing a well-demarcated tumor from the surrounding hepatic tissue. (C) The tumor contains a mixture of atypical spindle cells within a background of small lymphocytes and plasma cells. (D) Abundant prominent noncaseating epithelioid granulomas within the tumor. (E) Multinucleated histiocytes are more readily observable at higher magnification. (F) Periodic acid–Schiff staining did not detect fungal organisms. (G) Ziehl–Neelsen staining was also negative for acid-fast bacilli, such as *Mycobacterium tuberculosis*.

derstood, it is theorized that latent Type 1 EBV infection of B lymphocytes leads to opportunistic infection of follicular dendritic cells due to their close functional associations in the context of immune function. EBER and latent membrane protein-1 from EBV then lead to cellular proliferation and inhibition of apoptosis through amplification of CD40 signaling [7]. Other contributory mechanisms include immune dysregulation due

to latent EBV infection, supported by an observation of heavy IgG4+ plasma cell infiltration and activation in six cases of splenic EBV+ IFDCS [8].

The diagnosis of EBV+ IFDCS relies on the combination of histopathological key features of spindle cells within a prominent lymphoplasmacytic infiltrate and a high index of suspicion. Immunohistochemistry includes variable positivity for

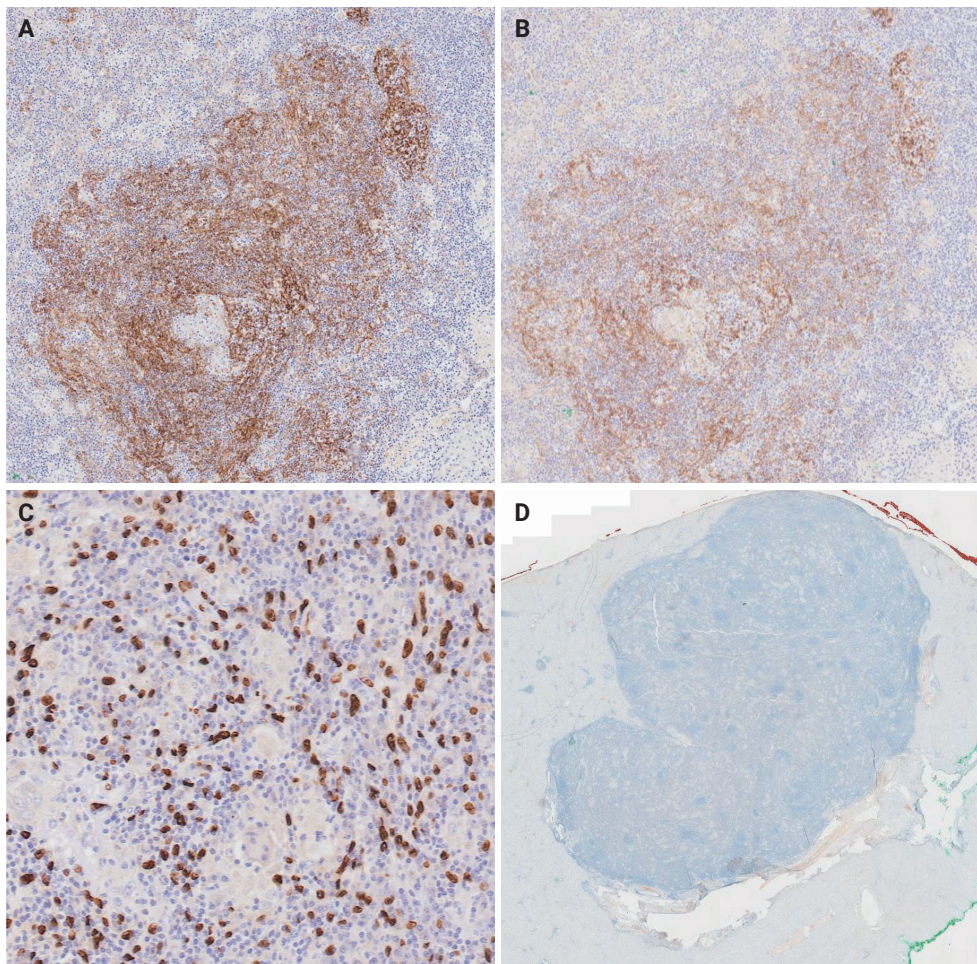


**Fig. 2.** Immunohistochemical profile of hepatic tumor. Immunohistochemistry shows that the neoplastic cells were strongly positive for CD23 (A) and CD35 (B) markers, consistent with a follicular dendritic cell phenotype. (C) In situ hybridization for Epstein-Barr virus–encoded RNA highlights the neoplastic cell nuclei. (D) Anaplastic lymphoma kinase immunostaining is negative.

FDC markers (CD21, CD23, CD35, CNA.42; with CD21 and CD35 having the highest specificity), and positive EBER in situ hybridization can help confirm the diagnosis. The diagnosis is further complicated by two identified morphological variants of the disease, which include the presence of epithelioid granulomas or pronounced tissue eosinophilia [4]. In addition, the lymphoma-like subtype and hemangioma-like subtype are also described in a recent publication [5]. These nuances highlight the intricate nature of this disease and the challenges in its diagnosis.

The differentials for EBV+ IFDCS include inflammatory myofibroblastic tumor (IMT), which is histologically similar, containing loose spindle cells and mixed inflammatory infiltrates, but is associated with gene fusions such as anaplastic lymphoma kinase (ALK) and ROS1, with more than 50% of IMTs contain-

ing ALK fusions, of which the ALK immunostain was negative in this case (Fig. 2D) [9]. It is also important to rule out mimics of hepatic inflammatory pseudotumor, including a benign inflammatory response to an adjacent abscess, IgG4-related sclerosing disease, and inflammatory variants of angiomyolipoma or hepatocellular adenomas. Granulomatous inflammation is an uncommon finding in EBV+ IFDCS and is particularly rare in hepatic presentations of this disease. The presence of granulomas in this case underscores the diagnostic challenge, as granulomas are often associated with a broad range of differential diagnoses, including infections (e.g., tuberculosis, fungal infections), autoimmune conditions (e.g., sarcoidosis), and other granulomatous diseases (e.g. Langerhans cell histiocytosis).

Recent reports have begun to describe granuloma-rich variants of EBV+ IFDCS [4,6], yet the pathophysiological significance of

granuloma formation in these cases remains unclear. The formation of granulomas in EBV+ IFDCS may be influenced by a combination of factors, including chronic viral infections such as EBV and HBV and the resultant immune dysregulation. It has been suggested that granulomas may represent a localized immune response to EBV-infected neoplastic cells or a secondary reaction to tumor necrosis or adjacent liver fibrosis [10]. EBV's role in chronic inflammation and immune activation could promote the recruitment and activation of macrophages and T cells, contributing to granuloma formation [6]. Furthermore, chronic liver disease with fibrosis may alter the local immune microenvironment, potentially enhancing granulomatous inflammation. This case adds valuable insight into this rare histopathological variant, particularly in the setting of chronic liver disease and hepatitis B infection, where immune modulation may play a critical role in granuloma formation.

The prognosis of EBV+ IFDCS is generally more favorable compared to classical follicular dendritic cell sarcoma (FDCS). While classical FDCS demonstrates a significant risk of local recurrence and distant metastasis, leading to a notable mortality rate, EBV+ IFDCS tends to exhibit less aggressive behavior, following an indolent course. A meta-analysis performed by Wu et al. [11] reported 1-year and 5-year progression-free survival of 91.5% and 56.1%, respectively, with a local and/or distant recurrence rate of 15.8% [11]. This calls into question whether the label of sarcoma in EBV+ IFDCS is better served than a label of tumor, considering that on the spectrum of EBV+ IFDCS, its behavior is more akin to an inflammatory pseudotumor rather than FDCS. Several factors, such as the size and location of the tumor, presence of atypia, necrosis, and metastasis, are known to influence the prognosis of FDCS. Of note, factors such as age, sex, tumor size, and specific pathological characteristics have not been significantly identified as predictors of disease progression in EBV+ IFDCS.

Surgical resection remains the standard of care for EBV+ IFDCS. The role of chemotherapy or radiotherapy, whether primary, adjuvant or neoadjuvant, is not well described and remains dependent on the combination of patient factors, tumor characteristics and clinical discretion [12]. Immunotherapy targeting programmed death-1/programmed death-ligand 1 presents a theoretical alternative, particularly for unresectable, recurrent, or metastatic EBV+ IFDCS.

In conclusion, this case highlights the importance of considering granuloma-rich variants of EBV+ IFDCS in the differential diagnosis of hepatic lesions with granulomatous inflam-

mation, particularly in patients with chronic liver disease and concurrent viral infections. The recognition of this rare variant is crucial for accurate diagnosis and appropriate management.

### Ethics Statement

Formal written informed consent was not required with a waiver by the SingHealth Centralised Institutional Review Board (CIRB).

### Availability of Data and Material

Data sharing not applicable to this article as no datasets were generated or analyzed during the study.

### Code Availability

Not applicable.

### ORCID

Henry Goh Di Shen <https://orcid.org/0009-0007-0145-3625>

Yue Zhang <https://orcid.org/0009-0006-8113-1185>

Wei Qiang Leow <https://orcid.org/0000-0001-6003-9837>

### Author Contributions

Conceptualization: WQL. Data curation: HGDS, YZ. Writing—original draft: HGDS, YZ. Writing—review & editing: all authors. Approval of final manuscript: all authors.

### Conflicts of Interest

The authors declare that they have no potential conflicts of interest.

### Funding Statement

No funding to declare.

## REFERENCES

1. Ge R, Liu C, Yin X, et al. Clinicopathologic characteristics of inflammatory pseudotumor-like follicular dendritic cell sarcoma. *Int J Clin Exp Pathol* 2014; 7: 2421-9.
2. Yan S, Yue Z, Zhang P, et al. Case report: Hepatic inflammatory pseudotumor-like follicular dendritic cell sarcoma: a rare case and review of the literature. *Front Med (Lausanne)* 2023; 10: 1192998.
3. Cheuk W, Chan JK, Shek TW, et al. Inflammatory pseudotumor-like follicular dendritic cell tumor: a distinctive low-grade malignant intra-abdominal neoplasm with consistent Epstein-Barr

- virus association. *Am J Surg Pathol* 2001; 25: 721-31.
4. Li XQ, Cheuk W, Lam PW, et al. Inflammatory pseudotumor-like follicular dendritic cell tumor of liver and spleen: granulomatous and eosinophil-rich variants mimicking inflammatory or infective lesions. *Am J Surg Pathol* 2014; 38: 646-53.
  5. Li Y, Yang X, Tao L, et al. Challenges in the diagnosis of Epstein-Barr virus-positive inflammatory follicular dendritic cell sarcoma: extremely wide morphologic spectrum and immunophenotype. *Am J Surg Pathol* 2023; 47: 476-89.
  6. Nie C, Xie X, Li H, et al. Epstein-Barr virus-positive inflammatory follicular dendritic cell sarcoma with significant granuloma: case report and literature review. *Diagn Pathol* 2024; 19: 34.
  7. Abe K, Kitago M, Matsuda S, et al. Epstein-Barr virus-associated inflammatory pseudotumor variant of follicular dendritic cell sarcoma of the liver: a case report and review of the literature. *Surg Case Rep* 2022; 8: 220.
  8. Choe JY, Go H, Jeon YK, et al. Inflammatory pseudotumor-like follicular dendritic cell sarcoma of the spleen: a report of six cases with increased IgG4-positive plasma cells. *Pathol Int* 2013; 63: 245-51.
  9. Coffin CM, Hornick JL, Fletcher CD. Inflammatory myofibroblastic tumor: comparison of clinicopathologic, histologic, and immunohistochemical features including ALK expression in atypical and aggressive cases. *Am J Surg Pathol* 2007; 31: 509-20.
  10. Dunleavy K, Roschewski M, Wilson WH. Lymphomatoid granulomatosis and other Epstein-Barr virus associated lymphoproliferative processes. *Curr Hematol Malig Rep* 2012; 7: 208-15.
  11. Wu H, Liu P, Xie XR, Chi JS, Li H, Xu CX. Inflammatory pseudotumor-like follicular dendritic cell sarcoma: literature review of 67 cases. *World J Meta-Anal* 2021; 9: 1-11.
  12. Pascariu AD, Neagu AI, Neagu AV, Bajenaru A, Betianu CI. Hepatic inflammatory pseudotumor-like follicular dendritic cell tumor: a case report. *J Med Case Rep* 2021; 15: 410.

# Mucocele of the rectal stump: mucinous cystic neoplasm with low-grade dysplasia simulating low-grade appendiceal mucinous neoplasm

Hasan Basri Aydin<sup>1</sup>, Maria Faraz<sup>1</sup>, A. David Chismark<sup>2</sup>, Haiyan Qiu<sup>1</sup>, Hwajeong Lee<sup>1</sup>

<sup>1</sup>Department of Pathology and Laboratory Medicine, Albany Medical Center, Albany, NY, USA

<sup>2</sup>Department of Surgery, Albany Medical Center, Albany, NY, USA

Mucoceles, commonly observed in the appendix, are mucin-filled, dilated structures arising from a range of etiologies. Cases associated with dysplastic or neoplastic epithelium can rupture and disseminate within the abdominopelvic cavity. Similar lesions in other parts of the colon are exceedingly rare, with only 16 colonic mucoceles having been reported. The first case of a colonic mucinous neoplasm with dysplasia resembling a low-grade appendiceal mucinous neoplasm involving rectal stump was described in 2016. Here, we present the second such case arising in the rectal stump, identified in a 44-year-old male with extensive surgical history. Microscopic examination revealed low-grade dysplastic epithelium lining the cyst and mucin dissecting into the stroma, without evidence of rupture or extramural mucin. The patient was followed for 16 months without recurrence or peritoneal disease. The exact etiology and outcome of these rare lesions remain unknown, requiring close follow-up.

**Keywords:** Cystic; Mucinous; Mucocele; Neoplasms; Rectum

## INTRODUCTION

Despite the relative prevalence of appendiceal mucocele, colonic mucoceles are extremely rare, with only sixteen cases reported in the literature [1-14]. The term 'mucocele' in pathology literature is traditionally a clinical or gross descriptive term used to describe a dilated, mucin-filled bowel segment or tissue cavity, most commonly the appendix [15]. It does not correspond to any specific diagnosis but rather denotes the macroscopic appearance and presentation of a lesion. Pathologically, mucoceles can result from various underlying processes, and the type of epithelial lining or lack thereof plays a critical role in determining their nature. The term 'mucinous neoplasm' however, refers to a pathologic entity characterized by the presence of dysplastic or neoplastic mucin-producing epithelium [16]. For clarity, in this study, 'mucocele' is not used as a synonym for

low-grade appendiceal mucinous neoplasm (LAMN) but rather in its general descriptive sense, consistent with its gross presentation.

LAMN is a distinct diagnostic entity with well-defined histopathologic criteria and significant clinical implications. The presence of low-grade dysplastic mucinous epithelium in the appendix in an appropriate clinical and histological context supports the diagnosis of LAMN [17]. Even in cases where acellular mucin pools are present in the appendiceal stroma without identifiable residual epithelial lining, the lesion may be classified as LAMN, as dysplastic epithelium may no longer be visible in sampled sections following mucin extravasation and rupture [16,18].

To date, only one case, reported by Tanaka et al. in 2016 [10], described a distal rectal stump mucocele with low-grade epithelial dysplasia resembling LAMN. More recently, in 2024, Chen

**Received:** October 18, 2024 **Revised:** December 23, 2024 **Accepted:** December 27, 2024

**Corresponding Author:** Hwajeong Lee, MD

Department of Pathology and Laboratory Medicine, Albany Medical Center, 47 New Scotland Ave., MC81, Albany, NY 12208, USA

Tel: +1-518-262-6254, Fax: +1-518-262-3663, E-mail: LeeH5@amc.edu

This is an Open Access article distributed under the terms of the Creative Commons Attribution Non-Commercial License (<https://creativecommons.org/licenses/by-nc/4.0/>) which permits unrestricted non-commercial use, distribution, and reproduction in any medium, provided the original work is properly cited.

© 2025 The Korean Society of Pathologists/The Korean Society for Cytopathology

et al. [14] reported five cases of mucinous neoplasms originating in extra-appendiceal segments of the colon, reminiscent of appendiceal mucinous neoplasms. In their discussion, they proposed the term “extra-appendiceal mucinous neoplasm” for such lesions. Three of the five cases grossly presented as mucoceles, similar in clinical context and pathologic findings to previously reported colorectal mucoceles, and are therefore included in our analysis. To the best of our knowledge, our case of a mucocele with dysplasia arising in a rectal stump represents the second reported instance. These cases collectively suggest a potential link between longstanding mucin stasis, mucocele formation, and neoplastic progression.

## CASE REPORT

A 44-year-old male who was born with imperforate anus with subsequent pull-through procedure underwent proctectomy with end-colostomy at age 12 due to poor anorectal function. Throughout his childhood, he suffered from draining sinuses from the perineum, which were ablated each time. His symptoms eventually dissipated in his 20s and he remained asymptomatic for the next 20 years. Recently he presented with a complaint of intractable lower back pain radiating down to his left leg. On initial presentation, he also had acute kidney injury

(AKI) with a creatinine level of 13.0 g/dL (reference, <1.0 g/dL). An abdominal computed tomography scan revealed a large cystic mass in the pelvis causing obstructive uropathy with bilateral hydronephrosis as well as compressive neuropathy, leading to lower back pain (Fig. 1). Bilateral percutaneous nephrostomy tubes were placed to address obstructive uropathy. This led to improvement of AKI and creatinine level trended down to 4.78 g/dL. Eventually, the pelvic mass was resected and sent to pathology. Other than severe intraabdominal adhesions, no implants, nodules, mucin, or other lesion were noted in the abdominopelvic cavity by the surgery team. The operative note did not specify the exact origin of the mass or any direct anatomical connection to a bowel segment. The resected mass appeared intact without any surface disruptions, excrescences or mucin, and measured 17.5 × 10.7 × 4.5 cm. Sectioning of the mass revealed a multiloculated cyst containing amorphous, tan and gelatinous material.

Sections revealed a cystic structure that was largely denuded but partially lined by attenuated anorectal-type mucosa, consisting of both colorectal glandular and anorectal transitional-type epithelium (Fig. 2). Notably, focal areas of low-grade dysplasia were identified. Pools of acellular mucin were observed dissecting into the stromal tissues, accompanied by degenerative changes such as calcifications and fibrosis (Fig.

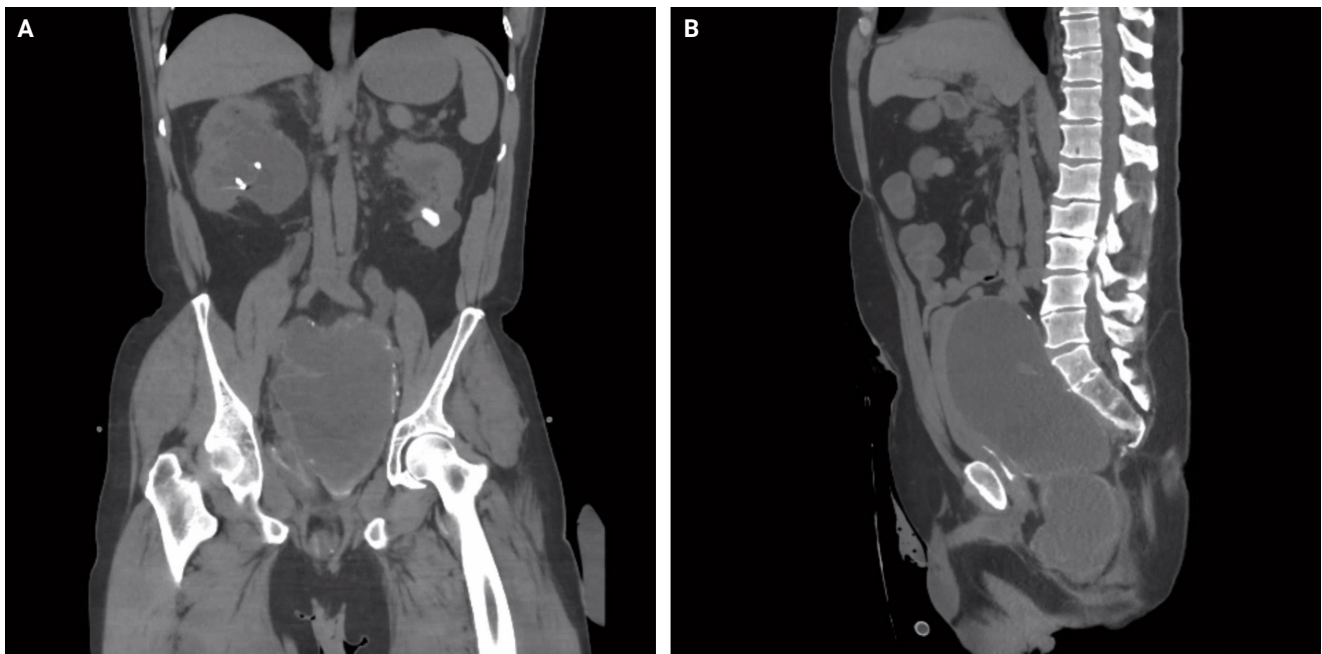


**Fig. 1.** Abdominal computed tomography scan demonstrating a large, multiloculated cystic mass within the pelvis (coronal [A] and sagittal [B] planes respectively).

3). Importantly, there was no evidence of high-grade dysplasia, invasive carcinoma, or metastasis.

The findings were reminiscent of a LAMN as defined by the Peritoneal Surface Oncology Group International (PSOGI), by fulfilling five of the six criteria, namely low-grade cytologic atypia (dysplastic mucin-producing epithelium), loss of the lamina propria and muscularis mucosae consistent with pressure-related atrophy and fibrosis, fibrosis of the submucosa, non-infiltrative pushing growth pattern without destructive stromal invasion and mucin dissection into the wall without evidence of extra-cystic mucin or peritoneal spread [17].

Given the absence of high-grade features, invasive carcinoma, or extra-cystic mucin/neoplastic cells, a descriptive diagnosis, mucinous cystic neoplasm of uncertain malignant potential, was rendered. The patient has been followed for 16 months without evidence of recurrence or peritoneal disease.

## DISCUSSION

Mucoceleles are most commonly encountered in the appendix within the luminal gastrointestinal tract. They are rarely symptomatic and rather incidentally found during clinical care for

other conditions. They constitute less than 1% of appendectomies [19]. However, their malignant potential is well recognized. Therefore, incidental identification of any dysplastic epithelium in an appendectomy usually prompts additional examination of the specimen. Cases of LAMN typically lack infiltrative growth pattern, destructive invasion, stromal desmoplastic reaction, or distant metastasis [20]. Nevertheless, if left untreated or incompletely excised, they can grow further and eventually rupture at weaker points of the appendiceal wall and result in mucin and dysplastic epithelium spreading within the abdominopelvic cavity, termed pseudomyxoma peritonei [21]. Despite the relative prevalence of appendiceal mucocele, colonic mucocele including colonic mucinous neoplasm similar to LAMN is exceedingly rare, with only seventeen cases including the present case [1-14] summarized in Table 1.

In brief, the mean age of the patients was 58 (range 12 to 92) years with female predominance (12 out of 17). Most patients had a complex surgical history including colostomy, endorectal pull-through, Hartmann's procedure, total colectomy, total hysterectomy, and hemorrhoidectomy. A number of patients had colonic diverticulosis and ended up developing mucoceles in a diverticulum [9,14]. The presentation commonly involved large

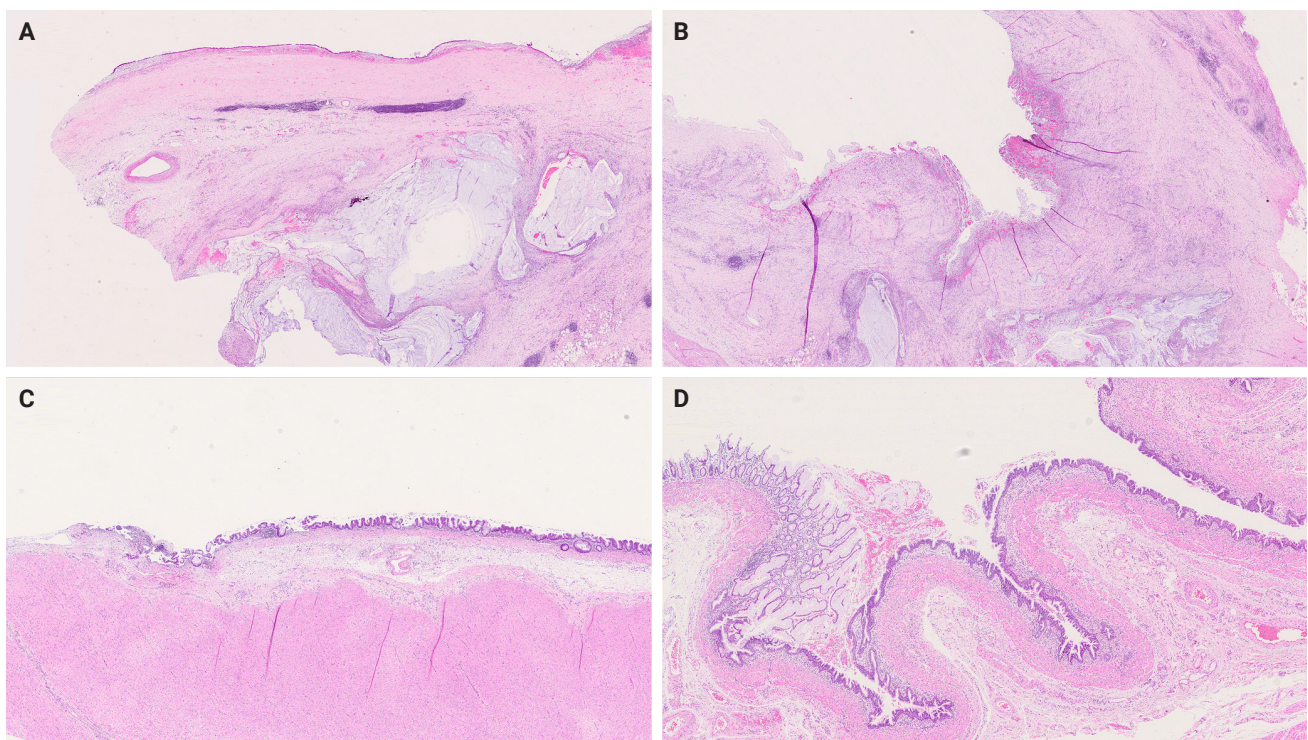


**Fig. 2.** Scanning view of the lumen lined by attenuated colorectal type mucosa (A), denuded area (B), colorectal mucosa (C), and anorectal transitional type mucosa (D).

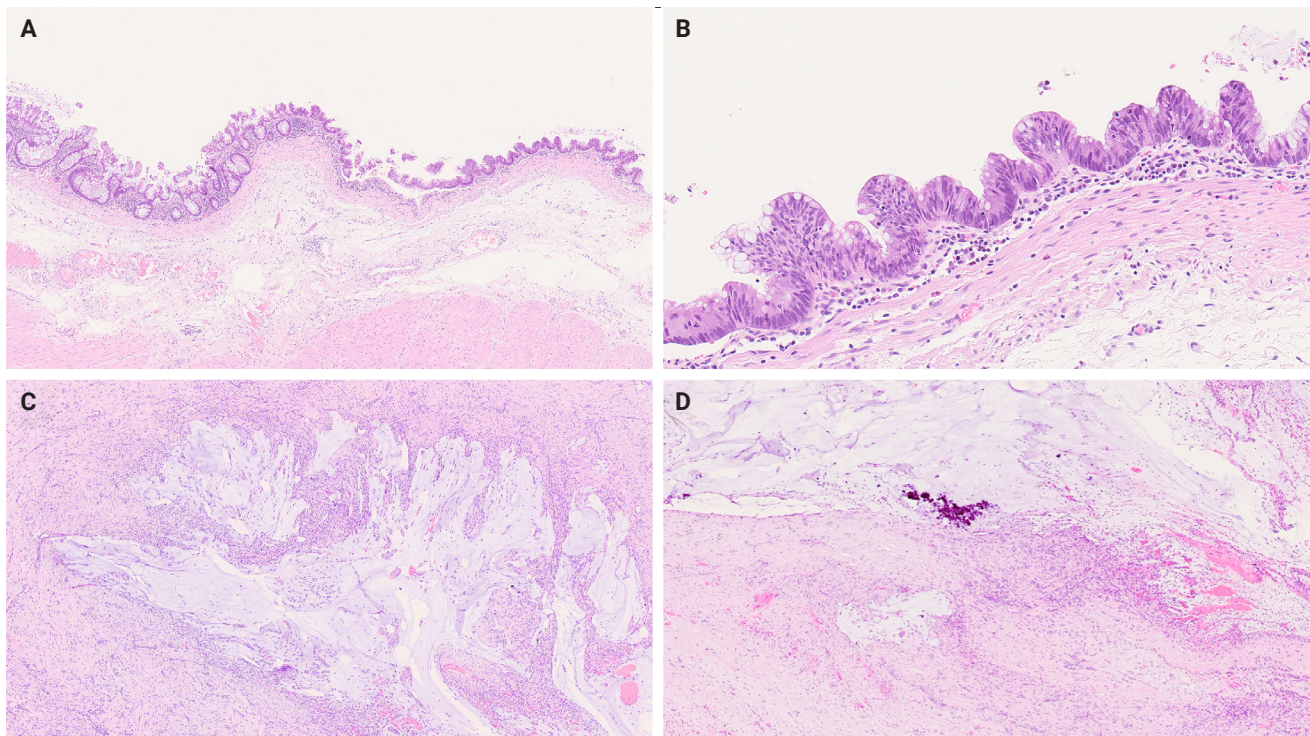


**Fig. 3.** (A) Scanning view of the lumen lined by attenuated colorectal type mucosa. (B) High-power view showing low-grade dysplasia. (C) Acellular mucin pools dissecting stroma. (D) Mucin pools with degenerative calcifications.

mucoceles, often distending the rectum or pelvic area, some causing compressive symptoms similar to our case. Typically, the unused bowel segment such as the pouch or diverticulum where the fecal stream is not present was the predilection site for mucin accumulation, similar to the present case. Histologic findings varied, with most cases showing nondysplastic benign epithelium, while five cases exhibited dysplastic changes similar to LAMN [9,10,14]. Another case (2014) displayed conventional colonic villous adenoma within the mucocele [8]. None of the cases showed invasive malignancy. Follow-up durations ranged from 13 days to 3 years, and no recurrence or malignant transformation were reported.

Taken together, chronic luminal stasis and resultant increased intraluminal pressure and impaired anal drainage associated with complex surgical history appear to contribute to mucocele development in the unused segment of colon [8]. The prolonged stasis within the surgically altered bowel segment creates an environment conducive to mucin accumulation. This mechanism is analogous to that observed in appendiceal mucoceles, where luminal obstruction and stasis are key factors [22]. Appendix is more prone to luminal obstruction, due to blind-ended anatomy and narrower lumen, explaining the rela-

tively high incidence of appendiceal mucinous neoplasms [22]. Likewise, postoperative intraabdominal adhesions can be another contributing factor as they can restrict luminal diameter, potentiate intraluminal pressure buildup, and impair drainage [13]. Extensive intraabdominal adhesions were noted in our case as well.

Histopathologically, our case exhibited features akin to LAMN, including epithelium with low-grade dysplasia and acellular mucin pools dissecting stromal tissues with degenerative features. Our and previous observations underscore the potential for neoplastic transformation in colonic mucoceles. However, dysplastic epithelium was observed in seven out of 17 (to include our current case) cases. Therefore, it is likely that mucoceles arise as passive processes in patients with complex surgical history, with neoplasia developing as a secondary event in a subset, possibly in those with genetic predisposition.

Given its rarity, there is currently no consensus or published guidelines on the management of colonic mucocele. Since the malignant potential of the appendiceal counterpart is well-documented, complete surgical resection might be appropriate. However, as the malignant potential of colonic mucoceles in general and those with dysplasia in particular, is unknown,

**Table 1.** Summary of seventeen cases of colonic mucoceles in the literature including the present case (1974–2024)

Case No.	Report year	Age (yr)/Sex	Presentation	Surgical history	Gross findings	Histologic findings	Follow-up duration	Outcome
1	1974 [1]	38/F	Pelvic mucocele	Colostomy and mucous fistula for traumatic colonic injury, stenosis of mucus fistula and anal canal	Mucocele of the distal colonic segment, 21 cm in size. The bowel was chronically inflamed, thickened (1 cm), and distended with mucus.	Marked mucosal atrophy with fibrosis of the muscularis mucosae and submucosa. Multiple histiocytes containing brown pigment and chronic inflammatory cells present in the terminal rectum	N/A	No known recurrence or malignant transformation
2	1987 [2]	12/M	Perirectal mucocele	Endorectal pull-through for imperforate anus	1,500 mL mucosal lined pelvic mucocele, obstructing the rectum and ureter	N/A	1 year	No known recurrence or malignant transformation
3	1991 [3]	59/F	Rectal mucocele	Hartmann's procedure for perforated diverticulitis	Retrouterine fluid collection (pelvic abscess) within the pelvis, 9 cm in diameter.	N/A	N/A	No known recurrence or malignant transformation
4	2011 [4]	39/F	Rectal mucocele	Hemorrhoidectomy	Two small lesions located in 6 and 10 o'clock direction and anal canal scarring	Mucocele with benign colorectal glands floating in mucin pool	9 mo	No known recurrence or malignant transformation
5	2011 [5]	73/F	Colonic mucocele	Ileo-sigmoid bypass surgery for adenocarcinoma of splenic flexure	Dilated ascending and transverse colon with features of mucocele (12 cm)	Closed loop obstruction of a colonic segment with subsequent mucin accumulation, no cystic lesion is present	6 wk	No known recurrence or malignant transformation
6	2011 [6]	36/M	Colonic mucocele	N/A	1.0 x 0.9 cm polyp at hepatic flexure, which was removed with hot snare	Mucocele without dysplasia, hyperplasia of the crypt epithelium, mucinous cystadenoma or mucinous cystadenocarcinoma	12 mo	No known recurrence or malignant transformation
7	2013 [7]	40/F	Rectal mucocele	Total colectomy and end ileostomy for Crohn's disease	Grossly distended rectal stump, 15 x 9 cm in size	Mucin was transectally drained, no sections are submitted for histologic examination.	1 mo	No known recurrence or malignant transformation
8	2014 [8]	92/M	Rectal mucocele	Subtotal colectomy and end ileostomy for ulcerative colitis	Grossly distended rectal stump filled with three liters of mucin	Benign, mucus secreting, rectal villous adenoma within the rectal stump, size unspecified	N/A	No known recurrence or malignant transformation
9	2015 [9]	66/F	Colonic mucocele in a cecal diverticulum	Total hysterectomy	3.5 x 3.0 cm cystic mass with mucin collection found within a cecal diverticulum	Mucin collection with dysplastic epithelial lining in muscularis propria with colonic lamina propria curving into muscularis propria, thus forming a diverticulum	12 mo	No known recurrence or malignant transformation
10	2016 [10]	37/F	Distal colonic stump mucocele	Transverse loop colostomy for colonic obstruction due to a yolk sac tumor, anterior of the sacrum	Yellowish mucin-filled cyst; no lesions suggestive of malignant change was found at the mucosal surface of the cyst and stricture segment	Dysplastic changes similar to that of low-grade appendiceal mucinous neoplasms, including pseudo-stratified nuclei, papillary-proliferating cells with mucin content, and loss of the lamina muscularis mucosae and the stroma in the lamina propria, mucosae replaced with fibrous tissue; no invasive carcinoma or severe atypia	1 mo	No known recurrence or malignant transformation

(Continued to the next page)

Table 1. Continued

Case No.	Report year	Age (yr)/ Sex	Presentation	Surgical history	Gross findings	Histologic findings	Follow-up duration	Outcome
11	2018 [11]	84/M	Rectal mucocele	Hemorrhoidectomy	5 x 7 cm in size, mucin-filled unilocular cyst, with a relatively strong firm and a mucosal interior	Unilocular cystic lesion with the majority of the wall formed of mucous columnar epithelium, with a component of laminated stratified squamous epithelium.	3 yr	No known recurrence or malignant transformation
12	2018 [12]	74/F	Rectal mucocele	Subtotal colectomy with end ileostomy and a mucous fistula at the descending colon due to Crohn's disease	Dilated rectum and sigmoid with large amounts of partly calcified mucus	No evidence of dysplasia, malignancy, or Crohn's manifestation in the completely obliterated proximal colon and the anus	13 days	No known recurrence or malignant transformation
13	2021 [13]	85/F	Rectal stump mucocele causing mechanical ileus	Hartmann's procedure	Digital rectal examination led to immediate drainage of a citrine viscous fluid, consistent with mucus. Consequently, a rectal catheter was placed in the stump, which drained approximately 2 L of fluid.	Cyst not excised surgically due to age and comorbidities of the patient, instead drained via catheter	6 mo	No known recurrence or malignant transformation
14	2024 [14]	77/F	Colonic mucocele in a diverticulum	Diverticulosis	1.7 cm cyst in sigmoid colon, arising in a diverticulum	Focal high-grade mucinous neoplasm of the colon arising in association with SSL extending into subserosal fat	N/A	No known recurrence or malignant transformation
15	2024 [14]	58/F	Rectosigmoid mucocele	Diverticulosis, possible duplication cyst	6.1 cm cyst in rectosigmoid colon without connection to the lumen	Focal high-grade mucinous neoplasm of the colon arising in a duplication cyst or obstructed diverticulum, extending into muscularis propria	N/A	No known recurrence or malignant transformation
16	2024 [14]	67/F	Colonic mucocele	Appendix with fibrous obliteration	4.6 cm submucosal mucin-filled cystic mass in cecum	Low-grade mucinous neoplasm, limited to submucosa	N/A	No known recurrence or malignant transformation
17	2024 (current study)	44/M	Distal colonic stump mucocele	Congenital imperforate anus with subsequent pull-through procedure, proctectomy with end-colostomy	17.5 x 10.7 x 4.5 cm cystic mass in distal rectal stump	Cyst partially lined by low-grade dysplastic epithelium with pools of acellular mucin dissecting stroma, associated calcifications and fibrosis	16 mo	No known recurrence or malignant transformation

F, female; M, male; N/A, not applicable; SSL, sessile serrated lesion.

vigilant long-term follow-up and monitoring for recurrence or progression to malignancy may be also justified. Further case documentation is needed to better understand the behavior and long-term outcomes of colonic mucocoeles, particularly those with dysplastic changes.

Our study has several limitations that warrant acknowledgment. First, a gross photograph of the cystic mass from our case is unavailable. Second, in our effort to curate and summarize previously reported cases of colonic mucocoeles, we encountered incomplete reporting in some of the cases, limiting our ability to perform a uniform comparison. This also highlights the need for more standardized reporting of such rare cases in the literature. Thirdly, we acknowledge that certain reported cases reflect dilated, mucin-filled segments of bowel secondary to outlet obstruction rather than true neoplastic or cystic lesions. These cases would appropriately fall under the category of “retention cysts” in a broader sense.

### Ethics Statement

Institutional Review Board approval was waived due to the use of retrospective, de-identified data.

### Availability of Data and Material

All data generated or analyzed during the study are included in this published article (and its supplementary information files).

### Code Availability

Not applicable.

### ORCID

Hasan Basri Aydin <https://orcid.org/0009-0000-4737-5107>  
 Maria Faraz <https://orcid.org/0009-0003-7303-2484>  
 A. David Chismark <https://orcid.org/0009-0008-1033-6444>  
 Haiyan Qiu <https://orcid.org/0009-0004-1439-1046>  
 Hwajeong Lee <https://orcid.org/0000-0001-7005-6278>

### Author Contributions

Conceptualization: HL. Investigation: HBA, MF, ADC, HQ. Supervision: HL. Writing—original draft: HBA. Writing—review & editing: MF, ADC, HQ. Approval of final manuscript: all authors.

### Conflicts of Interest

The authors declare that they have no potential conflicts of interest.

### Funding Statement

No funding to declare.

### Acknowledgments

The authors thank Dale Veasey for his contribution in grossing.

## REFERENCES

1. Nicosia JF, Abcarian H. Mucocele of the distal colonic segment, a late sequela of trauma to the perineum: report of a case. *Dis Colon Rectum* 1974; 17: 536-9.
2. Hitch DC, Patil UB, Panicek DM. Mucocele after endorectal pull-through for imperforate anus. *J Pediatr Surg* 1987; 22: 1023-4.
3. Creagh MF, Chan TY. Case report: rectal mucocele following Hartmann's procedure. *Clin Radiol* 1991; 43: 358-9.
4. Hsu KE, Hsieh CB, Yu JC, Chan DC, Wu CC, Jin JS, et al. Rare rectal mucocele mimic tumor following hemorrhoidectomy in an adult patient. *Rev Esp Enferm Dig* 2011; 103: 276-7.
5. Ali A, Krishnan A, Rehman S, Rao V, Pearson HJ. Giant colonic mucocele following palliative surgery for metastatic adenocarcinoma. *J Surg Case Rep* 2011; 2011: 1-4.
6. Ai XB, Feng JC, Gong FY, Wang A, Ren DH, Sui K. Endoscopic therapy of colonic liver flexure mucocele. *Case Rep Gastroenterol* 2011; 5: 433-7.
7. Teoh AY, Lee JF, Chong CC, Tang RS. Endoscopic ultrasonography-guided drainage of a rectal mucocele after total colectomy for Crohn's disease. *Endoscopy* 2013; 45 Suppl 2 UCTN: E252-3.
8. Appleton N, Day N, Walsh C. Rectal mucocele following subtotal colectomy for colitis. *Ann R Coll Surg Engl* 2014; 96: e13-4.
9. Nakatani K, Tokuhara K, Sakaguchi T, Ryota H, Yoshioka K, Kon M. Low-grade mucinous neoplasia in a cecal diverticulum: A case report. *Int J Surg Case Rep* 2015; 15: 66-9.
10. Tanaka T, Kawai K, Abe H, Muroto K, Otani K, Nishikawa T, et al. Giant mucocele of the colon at the distal stump due to low-grade mucinous neoplasia. *Surg Case Rep* 2016; 2: 117.
11. Ishii D, Aoki T, Inaba S, Yabuki H. Rectal mucocele in the anterior wall of the rectum. *BMJ Case Rep* 2018; 2018: bcr2018225097.
12. Schneider R, Kraljevic M, von Flue M, Fuglistaler I. Giant symptomatic rectal mucocele following subtotal colectomy. *Case Rep Gastroenterol* 2018; 12: 143-6.
13. Longchamp G, Colucci N, Ris F, Buchs NC. Rectal stump mucocele after a Hartmann's procedure causing mechanical ileus. *BMJ Case Rep* 2021; 14: e237543.
14. Chen F, Harvey SE, Young ED, Liang TZ, Larman T, Voltaggio L. Extra-appendiceal mucinous neoplasms: a tumour with clinico-

- pathologic similarities to low- and high-grade appendiceal counterpart. *Hum Pathol* 2024; 148: 23-31.
15. Faure M, Salgado R, Op de Beeck B, Bellinck P, Termote JL, Parizel PM. Mucocele of the appendix: case report and review of literature. *JBR-BTR* 2014; 97: 217-21.
  16. Carr NJ, Cecil TD, Mohamed F, Sobin LH, Sugarbaker PH, Gonzalez-Moreno S, et al. A consensus for classification and pathologic reporting of pseudomyxoma peritonei and associated appendiceal neoplasia: the results of the Peritoneal Surface Oncology Group International (PSOGI) modified Delphi process. *Am J Surg Pathol* 2016; 40: 14-26.
  17. Govaerts K, Lurvink RJ, De Hingh I, Van der Speeten K, Ville-neuve L, Kusamura S, et al. Appendiceal tumours and pseudomyxoma peritonei: literature review with PSOGI/EURACAN clinical practice guidelines for diagnosis and treatment. *Eur J Surg Oncol* 2021; 47: 11-35.
  18. Guner M, Aydin C. Low-grade appendiceal mucinous neoplasm: what is the best treatment? *Cureus* 2023; 15: e46591.
  19. Cristian DA, Grama FA, Becheanu G, Pop A, Popa I, Surlin V, et al. Low-grade appendiceal mucinous neoplasm mimicking an adnexal mass. *Rom J Morphol Embryol* 2015; 56: 837-42.
  20. Pai RK, Longacre TA. Appendiceal mucinous tumors and pseudomyxoma peritonei: histologic features, diagnostic problems, and proposed classification. *Adv Anat Pathol* 2005; 12: 291-311.
  21. Misdraji J. Mucinous epithelial neoplasms of the appendix and pseudomyxoma peritonei. *Mod Pathol* 2015; 28 Suppl 1: S67-79.
  22. Gupta P, Mishra AK, Deo A, Yadav R, K CM, Bhattarai A. Complete small intestinal obstruction due to band formation in low-grade appendiceal mucinous neoplasm: a rare case report and literature review. *Int J Surg Case Rep* 2023; 108: 108422.

# Erratum: Breast fine-needle aspiration cytology in the era of core-needle biopsy: what is its role?

Ahrong Kim<sup>1,2\*</sup>, Hyun Jung Lee<sup>1,3\*</sup>, Jee Yeon Kim<sup>1,3</sup>

<sup>1</sup>Department of Pathology, Pusan National University School of Medicine, Yangsan, Korea

<sup>2</sup>Department of Pathology, Biomedical Research Institute, Pusan National University Hospital, Busan, Korea

<sup>3</sup>Department of Pathology, Research Institute for Convergence of Biomedical Science and Technology, Pusan National University Yangsan Hospital, Yangsan, Korea

To the Editor:

We found an error in our published article.

Kim A, Lee HJ, Kim JY. Breast fine-needle aspiration cytology in the era of core-needle biopsy: what is its role? *J Pathol Transl Med.* 2025; 59(1): 26-38. <https://doi.org/10.4132/jptm.2024.11.01>.

The Funding Statement is marked incorrectly. The correct Funding Statement is as follows.

## Funding Statement

This work was supported by a 2-Year Research Grant of Pusan National University.

We apologize for the inconvenience caused by this error.

---

**Corresponding Author:** Jee Yeon Kim, MD, PhD

Department of Pathology, Pusan National University School of Medicine, 49 Busandaehak-ro, Mulgeum-eup, Yangsan 50612, Korea  
Tel: +82-55-360-1861, Fax: +82-55-360-1865, E-mail: [jeekim@pusan.ac.kr](mailto:jeekim@pusan.ac.kr)

\*Ahrong Kim and Hyun Jung Lee contributed equally to this work.

This is an Open Access article distributed under the terms of the Creative Commons Attribution Non-Commercial License (<https://creativecommons.org/licenses/by-nc/4.0/>) which permits unrestricted non-commercial use, distribution, and reproduction in any medium, provided the original work is properly cited.

© 2025 The Korean Society of Pathologists/The Korean Society for Cytopathology

**TABLES OF CONTENTS**

- INSTRUCTION
- ETHICS
- REVIEW PROCESS
- COVER LETTER
- MANUSCRIPT PREPARATION
- TYPES OF MANUSCRIPTS
- COPYRIGHT, LICENSING, AND ARCHIVING POLICY
- ARTICLE PROCESSING CHARGE
- OFFPRINTS AND CHARGES
- CONTACT

**INSTRUCTION**

All manuscripts should be submitted online (<http://www.jpatholm.org>), and should meet the Recommendations for the Conduct, Reporting, Editing, and Publication of Scholarly Work in Medical Journals (<http://www.icmje.org/>).

Manuscripts should be written in English. Authors from non-English speaking countries are encouraged to have their manuscripts proofread by professional English editors. The medical terms of Korean authors should be in accordance with the glossary published by the Korean Medical Association. The Editors may return the manuscript to the authors before the review process when the content, format, and grammar of the manuscript do not conform to the guidelines or when a breach of publication ethics is present.

*Journal of Pathology Translational Medicine* (J Pathol Transl Med, JPTM) is published bimonthly on the 15th of January, March, May, July, September, and November.

**ETHICS**

The journal adheres to the ethical guidelines for research and publication described in Good Publication Practice Guidelines for Medical Journals ([https://www.kamje.or.kr/board/view?b\\_name=bo\\_publication&bo\\_id=13&per\\_page=](https://www.kamje.or.kr/board/view?b_name=bo_publication&bo_id=13&per_page=)) and Guidelines on Good Publication (<http://publicationethics.org/resources/guidelines>).

**1. Ethical Approval**

All studies on human subjects should follow the World Medical Association Declaration of Helsinki (1964) and the authors should provide an affirmation that the studies have been ap-

proved by the appropriate institutional review board (IRB) and/or national research ethics committee with relevant reference numbers and dates. The following statement should be included in the text at the end of the Materials and Methods section: "All procedures performed in the current study were approved by IRB and/or national research ethics committee (reference number and date) in accordance with the 1964 Helsinki declaration and its later amendments." Clinical studies that do not meet the Helsinki Declaration will not be considered for publication. Animal studies also need to be approved by the institutional Animal Ethics Committee (AEC) or its equivalent. Research on animals should be performed based on the National or Institutional Guide for the Care and Use of Laboratory Animals, and the ethical treatment of all experimental animals should be maintained.

**2. Informed Consent**

Authors should have obtained written informed consent from all participants prior to inclusion in the study, and the following statement should be included at the end of the Materials and Methods section after the IRB approval statement: "Informed consent was obtained from all individual participants included in the study." Identifying details of the participants (e.g. names, dates of birth, and unit numbers) should not be published in written descriptions, photographs, and genetic profiles. In cases where identifying details are essential for scientific purposes, the participant should have given written informed consent for the identifying information to be published and it should be stated separately as following: "Additional informed consent was obtained from all individual participants for whom identifying information is included in this article."

Waiver of the informed consent can only be granted by the appropriate IRB and/or national research ethics committee in compliance with the current laws of the country in which the study was performed, and this should be separately stated as following: "Formal written informed consent was not required with a waiver by the appropriate IRB and/or national research ethics committee." It should be noted that manuscripts that do not contain statements on IRB approval and patient informed consent can be returned to the authors before the review process.

For autopsy case reports, an informed consent is not required

under the premises that consent was previously obtained for the autopsy to be conducted and that the strict anonymity of the patient has been respected.

### 3. Disclosure of Potential Conflicts of Interest

A statement disclosing all relationships or interests that could have direct or potential influence on the work should be included in a separate section before the reference list.

The authors will be held responsible for any false statements or failure to follow the ethical guidelines.

Each author should have participated in the research and/or article preparation. All authors are responsible for disclosing any conflict of interest that could influence the content of papers.

### 4. Redundant Publication and Plagiarism

Redundant publication is defined as “reporting (publishing or attempting to publish) substantially the same work more than once, without attribution of the original source(s).” Characteristics of reports that are substantially similar include the following: (a) “at least one of the authors must be common to all reports (if there are no common authors, it is more likely plagiarism than redundant publication),” (b) “subjects or study populations are the same or overlapped,” (c) “methodology is typically identical or nearly so,” and (d) “results and their interpretation generally vary little, if at all.”

When submitting a manuscript, authors should include a letter informing the editor of any potential overlap with other already published material or material being evaluated for publication, and should also state how the manuscript submitted to JPTM substantially differs from other materials. If all or part of your patient population was previously reported, this should be mentioned in the Methods section, with citation of appropriate reference(s).

## REVIEW PROCESS

### 1. Peer-Review Process

All papers, including those invited by the Editor, are subject to peer review. Manuscripts is reviewed by at least 2 external experts and editors. Received manuscripts will be peer-reviewed and a primary editorial decision will be sent to the authors within 2 weeks after submission. The Editor is responsible for the final decision whether the manuscript is accepted or rejected. All articles will be published within 2 months after final

acceptance by the Editorial Office.

- The journal uses a single-blind peer review process: the reviewers know the identity of the authors, but not vice versa.
- Decision letter will be sent to corresponding author via registered e-mail. Reviewers can request authors to revise the content. The corresponding author must indicate the modifications made in their item-by-item response to the reviewers’ comments. Failure to resubmit the revised manuscript within 4 weeks of the editorial decision is regarded as a withdrawal.
- The editorial committee has the right to revise the manuscript without the authors’ consent, unless the revision substantially affects the original content.
- After review, the editorial board determines whether the manuscript is accepted for publication or not. Once rejected, the manuscript does not undergo another round of review. If manuscripts from Editor-in-Chief or Associate Editors are submitted, it is also treated through same process with other manuscripts. However, those authors are not involved in the peer reviewer selection, review process, or final decision.
- AI use by peer reviewers: Generative AI tools can lack up-to-date knowledge and may produce nonsensical, biased or false information. Manuscripts may also include sensitive or proprietary information that should not be shared outside the peer review process. For these reasons we ask that, while the journal explores providing our peer reviewers with access to safe AI tools, peer reviewers do not upload manuscripts into generative AI tools. If any part of the evaluation of the claims made in the manuscript was in any way supported by an AI tool, we ask peer reviewers to declare the use of such tools transparently in the peer review report.

### 2. How the Journal Handles Complaints and Appeals

Authors who wish to appeal a decision should contact the Editor-in-Chief, explaining in detail the reasons for the appeal. Appeals will only be considered when a reviewer or editor is thought to have made a significant factual error or when his/her objectivity is compromised by a documented competing interest, and when a reversal based on either of these grounds would change the original decision. The journal staff will ask for confirmation of the reason(s) in the first instance.

If the authors proceed, the original editor(s) will usually be asked to consider the appeal. Additional editorial board members may also be consulted. The editors will try to handle an appeal expeditiously; however, each appeal is unique and the journal cannot guarantee the turnaround time or the outcome.

The process of handling complaints and appeals follows the guidelines of COPE available from (<https://publicationethics.org/appeals>). JPTM does not consider second appeals.

### 3. Roles of Editors and Editorial Board Members

#### 1) Editors-in-Chief

- Responsible for the whole journal content
- Select, appoint and manage associate editors and editorial board members
- Make the final decision to accept or reject the manuscript for publication.
- Attract high-quality manuscripts
- Responsible for handling allegations on scientific misbehaviors and misconducts
- Provide guidelines to the authors for submission of manuscript and journal policies.

#### 2) Senior Editors

- A group of respected scholars in the field of pathology and translational medicine who had served as Editors-in-Chief for the journal
- Advise on policy and scope of the journal

#### 3) Associate Editors

- Assist EICs in getting manuscripts reviewed and published
- Handle articles by subject areas
- Initial screening of manuscripts
- Check for plagiarism and similarity

#### 4) Consulting Editors

Advise on journal policy, editing, and publication when consulted

#### 5) Ethics Editor

- Advise on ethical issues of the journal

#### 6) Statistics Editor

- Verify and advise on the statistics results described in the manuscripts

#### 7) Manuscript Editor

- Assist EICs and AEs
- Handle day-to-day paperwork
- Perform technical check on all submitted manuscripts

#### 8) Layout Editors

- Responsible for the final layout and printing of the manuscripts

#### 9) Editorial Board

- A group of respected scholars in the field of pathology and translational medicine
- Assist with peer review
- Suggest ideas for special issues
- Recommend review articles with an impact

## COVER LETTER

A cover letter must be included with each manuscript submission. It must be confirmed that neither the manuscript nor any parts of its content are currently under consideration or published in another journal. It must also be verified that each author approves of the submitted version of the manuscript. Optional: The authors may explain in the cover letter why the content of the paper is significant, placing the findings in the context of existing work and why it fits the scope of JPTM, and add anything else that the editors may find useful.

## MANUSCRIPT PREPARATION

### 1. General Guidelines

Manuscripts should be submitted as Microsoft Word files (doc, docx).

Abbreviations should be fully described in parentheses at first appearance in the text. After that the abbreviation can be used instead of the full term. The first letter of a name, place and a proper noun should be typed in capital letters. Numbers should be in Arabic numerals. Weight and other measurements should be written in the CGS (centimeter-gram-second) system of units. Other units need to be in the International System of Units. Species name and name of a gene should be typed in italic characters. The word of a Latin origin such as *et al.*, *in vivo*, etc. needs not to be typed in italic characters. The spelled-out abbreviation followed by the abbreviation in parentheses should be used on the first mention unless the abbreviation is a standard one.

Text and spacing requirements are: font size of 10 points, double-spaced and blank space of at least 2.5 cm from every margin of A4 paper size. The preferred font is Arial or Times New Roman. Page numbers should be at the bottom center of

the page. Please do not number the subsections. Please do not embed any tables or figures in the main manuscript file. Please do not include any supplemental material in the manuscript file.

## 2. Reporting Guidelines for Specific Study Designs

For the specific study design, such as randomized control studies, studies of diagnostic accuracy, meta-analyses, observational studies, and non-randomized studies, it is recommended that the authors follow the reporting guidelines. A good source of reporting guidelines is the EQUATOR Network (<http://www.equator-network.org/home/>) and the United States National Institutes of Health/National Library of Medicine ([http://www.nlm.nih.gov/services/research\\_report\\_guide.html](http://www.nlm.nih.gov/services/research_report_guide.html)).

## TYPES OF MANUSCRIPTS

### 1. Original Articles

The arrangement of an original article is as follows: Title Page, Abstract and Keywords, Introduction, Materials and Methods, Results, Discussion, Conflict of Interest, Acknowledgments, References, and Legend for figures. Tables and Graphic files are included separately.

#### 1) Title Page

The title page must include the title of manuscript, the full name of all the authors and their affiliations, running title of not more than 40 characters, contact information of the corresponding author (postal address, e-mail address, telephone number, fax number), and ORCID (Open Researcher and Contributor ID) of all authors.

Avoid abbreviations in the title of the manuscript. Names of authors should be described fully without abbreviation. Any title of degree or professions such as MD or PhD should not be added in the author name listing. If the manuscript has more than one author and more than one affiliation, superscripted numbers should be used to match individual authors with their corresponding affiliations. Address of affiliation should comprise at least the institute, city, and country.

All authors are recommended to provide an ORCID identifier. To obtain an ORCID identifier, authors should register on the ORCID web site: <http://orcid.org>. Registration is free. An example of an ORCID description is as follows: Chan Kwon Jung: <https://orcid.org/0000-0001-6843-3708>.

#### 2) Abstract/Key Words

An abstract must not exceed 250 words. A structured format is preferred with subheadings of 'Background', 'Methods', 'Results', and 'Conclusions'.

List three to five key words, selected from the Medical Subject Headings (MeSH) of Index Medicus (<http://www.ncbi.nlm.nih.gov/mesh>), if possible.

#### 3) Introduction

The introduction should begin on separate pages. It should provide a research background and specific purpose or objectives for the research. The hypothesis tested can be stated. The references should be exactly pertinent to the subject presented and they should be provided a reference number.

#### 4) Materials and Methods

If the authors' work contains human or animal studies, it must be stated that the studies have been approved by institutional review committees in the Materials and Methods section. If there is no IRB number, it should be discussed with the editor during the review process.

Clearly describe the selection of observational or experimental participants (healthy individuals or patients, including controls), including eligibility and exclusion criteria and a description of the source population. Because the relevance of such variables as age, sex, or ethnicity is not always known at the time of study design, researchers should aim for inclusion of representative populations into all study types and at a minimum provide descriptive data for these and other relevant demographic variables.

Ensure correct use of the terms sex (when reporting biological factors) and gender (identity, psychosocial or cultural factors). Unless inappropriate, report the sex and/or gender of study participants, the sex of animals or cells, and describe the methods used to determine sex or gender. If the study involved an exclusive population (only one sex, for example), authors should justify why, except in obvious cases (e.g., prostate cancer). Authors should define how they determined race or ethnicity, and justify their relevance.

Statistical methods should be described meticulously. Authors may be requested to provide raw data to the Editorial Office, if the reviewer wish to analyze the data. Softwares used for the statistical analysis should be stated with the name, manufacturer and version. Statistical results are encouraged to provide measurement error or uncertainty such as confidence

Contributor Role	Role Definition
Conceptualization	Ideas; formulation or evolution of overarching research goals and aims.
Data Curation	Management activities to annotate (produce metadata), scrub data and maintain research data (including software code, where it is necessary for interpreting the data itself) for initial use and later reuse.
Formal Analysis	Application of statistical, mathematical, computational, or other formal techniques to analyze or synthesize study data.
Funding Acquisition	Acquisition of the financial support for the project leading to this publication.
Investigation	Conducting a research and investigation process, specifically performing the experiments, or data/evidence collection.
Methodology	Development or design of methodology; creation of models
Project Administration	Management and coordination responsibility for the research activity planning and execution.
Resources	Provision of study materials, reagents, materials, patients, laboratory samples, animals, instrumentation, computing resources, or other analysis tools.
Software	Programming, software development; designing computer programs; implementation of the computer code and supporting algorithms; testing of existing code components.
Supervision	Oversight and leadership responsibility for the research activity planning and execution, including mentorship external to the core team.
Validation	Verification, whether as a part of the activity or separate, of the overall replication/reproducibility of results/experiments and other research outputs.
Visualization	Preparation, creation and/or presentation of the published work, specifically visualization/data presentation.
Writing – Original Draft Preparation	Creation and/or presentation of the published work, specifically writing the initial draft (including substantive translation).
Writing – Review & Editing	Preparation, creation and/or presentation of the published work by those from the original research group, specifically critical review, commentary or revision – including pre- or post-publication stages.

intervals besides providing p-values.

## 5) Results

Authors should briefly describe the core results related to the conclusion in the text when data are provided in tables or in figures. Contents of tables and/or figures should not be duplicated in the Results section.

## 6) Discussion

It is important to deduce the conclusion from the results while avoiding statements not described in other sections. Emphasize the core findings and the conclusions drawn from them with the best available evidence.

## 7) Author Contributions

JPTM participates in the CRediT standard for author contributions (<https://casrai.org/credit/>). The contributions of all authors must be described using the CRediT Taxonomy of author roles. For each of the categories below, please enter the initials of the authors who contributed in that category. If listing more than one author in a category, separate each set of initials with a coma. If no one contributed in a category, you may leave that box blank.

The corresponding author is responsible for completing this information at submission, and it is expected that all authors would have reviewed, discussed, and agreed to their individual contributions ahead of this time.

Examples of authors' contributions are as followings:

- Conceptualization: CKJ
- Data curation: YMJ
- Formal analysis: SJ, CKJ
- Funding acquisition: CKJ
- Investigation: CKJ
- Methodology: SJ, YMJ, YK, CKJ
- Project administration: SJ
- Resources: CKJ
- Software:
- Supervision: CKJ
- Validation: SJ, CKJ
- Visualization: SJ, YK, CKJ
- Writing—original draft: SJ, CKJ.
- Writing— review & editing: SJ, YMJ, YK, CKJ.
- Approval of final manuscript: all authors.

## 8) Conflict of Interest

For potential conflict of interest, a specific disclosure must be

stated as following: “Author A has received a research grant from Company X.”; “Author A owns stock in Company X.”; or “Author A is a member of the Committee X.” If there is no potential conflict of interest, the following should be stated: “The authors declare that they have no potential conflicts of interest to disclose.”

### 9) Funding statement

Funding to the research should be provided here. Providing a FundRef ID is recommended including the name of the funding agency, country and the number of the grant provided by the funding agency.

### 10) Acknowledgments (optional)

Any individual and/or organization that contributed to the study or the manuscript, but not meeting the requirements of an authorship could be mentioned here. For mentioning any individuals or organizations in this section, there should be a written permission from them.

### 11) References

References are numbered in the order of citation within the article. Citations in the main text must appear in square bracket at the end of the sentence or immediately after the authors' name. References with up to six authors must list all names; for more than six authors, list the names of the first three authors followed by et al. Periodical abbreviations should follow those used by Index Medicus.

When citing references, journal articles are the most preferable. Nowadays, website material is also used frequently. The problem with website materials is the frequent change of the URL address or sudden disappearance of data. Therefore, it is recommended to cite open access or free access book archived in a public web site such as Bookshelf (<http://www.ncbi.nlm.nih.gov/books>) or ScienceCentral Books (<http://www.e-sciencecentral.org/books/>). Materials equipped with a DOI are also recommended as references.

Individual references should be formatted in Vancouver style as follows:



#### *Journal articles*

1. Slebos RJ, Hruban RH, Dalesio O, Mooi WJ, Offerhaus GJ,

Rodenhuis S. Relationship between K-ras oncogene activation and smoking in adenocarcinoma of the human lung. *J Natl Cancer Inst* 1991; 83: 1024-7.

#### *Books*

2. Kumar V, Abbas AK, Fausto N, Aster JC. Robbins pathologic basis of disease. 8th ed. Philadelphia: Saunders-Elsevier, 2010; 79-86.

#### *Book chapters*

3. Frosch MP, Anthony DC, De Girolami U. The central nervous system. In: Kumar V, Abbas AK, Fausto N, Aster JC, eds. Robbins pathologic basis of disease. 8th ed. Philadelphia: Saunders-Elsevier, 2010; 1279-344.

#### *Internet resources*

4. Medicare now covers HIV tests [Internet]. Chicago: American Medical Association, c1995-2010 [cited 2010 Jan 28]. Available from: <http://www.ama-assn.org/amednews/2009/12/21/gvsf1223.htm>.

### 12) Legend for Figures

All figures should have a short explanatory title and caption. Define any abbreviations used in the figures.

### 13) Tables

Each table should appear on a separate page and must be uploaded as a separate file. Remove internal horizontal or vertical lines. The horizontal line is only used for the title field and the bottom line. The line should be single. Explanatory words should be placed in footnotes including explanation of nonstandard abbreviation. To indicate the specific content in the table, use the superscript a, b, c, d consequently and explain them at the footnote.

### 14) Figures

Authors must submit illustrations as electronic files. Acceptable figure file formats are TIFF, BMP, JPEG, and PPT/PPTX. Figures are loaded as separate files during the submission process. Each figure needs to be prepared in a resolution higher than 300 dpi with good contrast and sharpness. The file size of each submitted figure should not exceed 10 MB per figure.

If any tables or figures are replicated or modified from other papers, authors should obtain permission through the Copyright Clearance Center <https://www.copyright.com/> or from

the individual publisher if the materials are not included in an open access journal published according to the Creative Commons license. If figures are from an open access journal, simply verify the source of the journal precisely in the footnote. Please note that a free access journal is different from that of open access; therefore, it is necessary to obtain permission from the publisher of the free access journal for using figures from these sources.

### 15) Supplementary Materials

Authors can submit supplementary materials for online-only publication when there is insufficient space to include the materials in the main article. Supplementary materials should be original and important to the understanding and interpretation of the report. As supplementary materials will not be edited or formatted after publication, authors are responsible for the accuracy and presentation of this material.

Supplementary materials should be submitted in a single Word document, a single Excel file, or a single PDF file which should include all materials (information, tables, figures, and references). Each element included as supplementary material should be cited in the text of the main manuscript (e.g., Supplementary Table S1, Supplementary Fig. S1, Supplementary Methods). The first page of the online-only document should list the number and title of each element included in the document.

### 2. Reviews and Editorials

Reviews and Editorials are normally by invitation only. Unsolicited articles are rarely considered, but if you wish to enquire further about the suitability of your article, you can email the Editorial office of J Pathol Transl Med at [office@jpatholtm.org](mailto:office@jpatholtm.org). Manuscripts should include the following: (1) title page, (2) abstract (not more than 250 words) and keywords, (3) introduction, (4) main text, (5) conclusion, (6) author contributions, (7) conflict of interest, (8) acknowledgments (optional), (9) references, and (10) legend for figures. Tables and Graphic files are included separately. There are no restrictions to the number and size of the figures. Ethics statement: If your manuscript does not report on or involve the use of any animal or human data or tissue, please state “Not applicable” in this section.

### 3. Case Studies

A small series or a single case with unique pathological aspect and in-depth scientific content including genetic analysis or

literature review can be reported as Case Studies. The manuscripts must include the following: (1) abstract (one paragraph, not more than 150 words), (2) introduction, (3) case description, (4) discussion, (5) author contributions, and (6) references.

For Case Studies with human subjects, there should be a certificate of waiver, an agreement, or the approval by the Institutional Review Board (IRB) of the author’s affiliated institution. Personal information of the patient(s) must be de-identified or the patient’s written authorization to allow information on their case to be published should be supplied.

### 4. Letters to the Editors

The Editors welcome brief letters (not more than two A4 pages in length) commenting on articles appearing in recent issues, on general interests for pathologists, and personal opinions on specific topics. Those letters selected for publication will first be referred to the author of the paper in question, whose response may also be published.

## COPYRIGHT, LICENSING, AND ARCHIVING POLICY

All published papers become the permanent property of the Korean Society of Pathologists and the Korean Society for Cytopathology. Copyrights of all published materials are owned by the Korean Society of Pathologists and the Korean Society for Cytopathology. Permission must be obtained from the Korean Society of Pathologists and the Korean Society for Cytopathology for any commercial use of materials. Every author should agree to the copyright transfer during the publication process and sign the copyright transfer agreement forms via online submission system. Articles cannot be published until a signed copyright transfer agreement form has been received.

JPTM is an open access journal. Articles are distributed under the terms of the Creative Commons Attribution Non-Commercial License (<http://creativecommons.org/licenses/by-nc/4.0>), which permits unrestricted use, distribution, and reproduction in any medium, provided the original work is properly cited.

To use the tables or figures of JPTM in other journals, books or media for scholarly, educational purposes, the process of permission request to the publisher of JPTM is not necessary. All contents of the journal are available immediately upon publication without embargo period.

Full text of JPTM has been archived in PubMed Central

(PMC). According to the deposit policy (self-archiving policy) of Sherpa/Romeo (<http://www.sherpa.ac.uk/>), authors cannot archive pre-print (i.e., pre-refereeing), but they can archive postprint (i.e., final draft post-refereeing). Authors can archive publisher's version/PDF. JPTM provides the electronic backup and preservation of access to the journal content in the event the journal is no longer published by archiving in PubMed Central. Authors can archive publisher's version/PDF.

## ARTICLE PROCESSING CHARGE

JPTM publishes all contents Open Access and makes the content freely available online.

Original articles and reviews are exempt from author submission fees or other publication-related charges.

For others (case studies and letters), authors are required to pay publication fees. Page charges are \$150 USD per 4 printed pages or less and \$25 USD per additional page. The surcharge for color figures is \$100 USD per page.

## OFFPRINTS AND CHARGES

The charge for print copies of each article is \$50 USD per 50 printed copies and the surcharge is \$10 USD per additional copy.

## CONTACT

All manuscripts should be submitted through the web site of the Journal of Pathology and Translational Medicine ([www.jpatholm.org](http://www.jpatholm.org)).

Inquiries about the manuscript submission and processing can be sent to Editorial Office:

Journal of Pathology and Translational Medicine Room 1209  
Gwanghwamun Officia, 92 Saemunan-ro, Jongnogu, Seoul  
03186, Korea /

#1508 Renaissancetower, 14, Mallijae-ro, Mapo-gu, Seoul 04195,  
Korea

Tel: +82-2-795-3094 / +82-2-593-6943,

Fax: +82-2-790-6635 / +82-2-593-6944,

E-mail: [office@jpatholm.org](mailto:office@jpatholm.org)